Constraints on subleading interactions in beta decay Lagrangian

Adam Falkowski [ID],[a] **Martín González-Alonso** [ID],[b] **Ajdin Palavrić** [ID][c] **and Antonio Rodríguez-Sánchez** [ID][a]

[a]*Université Paris-Saclay, CNRS/IN2P3, IJCLab,*
91405 Orsay, France
[b]*Departament de Física Teòrica, IFIC, Universitat de València - CSIC,*
Apt. Correus 22085, E-46071 València, Spain
[c]*Albert Einstein Center for Fundamental Physics, Institute for Theoretical Physics,*
University of Bern,
CH-3012 Bern, Switzerland

E-mail: adam.falkowski@ijclab.in2p3.fr, martin.gonzalez@ific.uv.es,
ajdin.palavric@unibe.ch, arodriguez@ijclab.in2p3.fr

Abstract: We discuss the effective field theory (EFT) for nuclear beta decay. The general quark-level EFT describing charged-current interactions between quarks and leptons is matched to the nucleon-level non-relativistic EFT at the $\mathcal{O}(\text{MeV})$ momentum scale characteristic for beta transitions. The matching takes into account, for the first time, the effect of all possible beyond-the-Standard-Model interactions at the subleading order in the recoil momentum. We calculate the impact of all the Wilson coefficients of the leading and subleading EFT Lagrangian on the differential decay width in allowed beta transitions. As an example application, we show how the existing experimental data constrain the subleading Wilson coefficients corresponding to pseudoscalar, weak magnetism, and induced tensor interactions. The data display a 3.5 sigma evidence for nucleon weak magnetism, in agreement with the theory prediction based on isospin symmetry.

https://doi.org/10.1007/JHEP02(2024)091

Contents

1 Introduction

Nuclear beta transitions have been at the center of the particle physics research program since over a hundred years. Historically they have been essential for understanding various ingredients of the Standard Model (SM), such as the existence of neutrinos, non-conservation of parity, or the Lorentz structure of weak interactions [1–6]. From the vantage point of a particle physicist today, their main role is twofold. On one hand they offer an opportunity for precision measurements of fundamental constants of the SM, notably of the V_{ud} CKM matrix element [7–11]. They also provide insight into the complex non-perturbative dynamics emerging from the SM, for instance through phenomenological determinations of the axial nucleon charge g_A [7, 10, 11]. On the other hand, they yield important constraints on physics beyond the SM (BSM), such as leptoquarks and other hypothetical particles contributing to scalar and tensor currents in weak interactions [8, 11, 12]. On a more theoretical side, because of a wide range of scales and physical processes involved, beta transitions are a perfect laboratory to research and develop the concepts of Effective Field Theory (EFT).

The main ingredients of the theory of beta transitions were worked out by the end of 1950s, see in particular refs. [4, 13, 14]. The flip side is that the habitual language in the literature may sometimes be unfamiliar to contemporary QFT practitioners. One of the goals of this paper is to reformulate beta transitions in the modern EFT language. The advantage, apart from the conceptual side, is that the theory can be smoothly incorporated into the ladder of EFTs spanning various energy scales, from the TeV scale down to MeV. In particular, the EFT for beta transitions can be matched to the so-called WEFT (the general EFT of SM degrees of freedom *below* the electroweak scale), and via this intermediary to the SMEFT (the general EFT of SM degrees of freedom *above* the electroweak scale). This way, the general effects of heavy non-SM particles can be naturally incorporated, along with the more studied SM effects, into the low-energy effective theory of beta decay.

An appropriate EFT framework to describe beta decay is the pionless EFT [15]. The relevant degrees of freedom are the nucleons (protons and neutrons) and leptons (electrons and electron neutrinos). Most of the details of the pionless EFT Lagrangian, such as the nucleon self-interactions describing the nuclear forces, are not relevant for our discussion. For the sake of this paper we will focus instead on the interactions mediating beta transitions, which are quartic terms connecting the proton, neutron, electron, and neutrino fields and their derivatives. Amplitudes for the neutron decay can be directly calculated starting from this Lagrangian. As for the beta decay of nuclei with the mass number $A > 1$, the amplitudes involve matrix elements of the nucleon bilinears between the nuclear states. This is analogous to the usual treatment of hadrons in QCD, where the amplitudes involve matrix elements of quark operators between hadronic states.

The important difference between the present EFT approach and hadrons in QCD is in power counting. Since the 3-momentum transfer in beta transitions is much smaller than the nucleon mass m_N, the EFT Lagrangian can be organized in a non-relativistic expansion in powers of $\boldsymbol{\nabla}/m_N$.[1] Focusing on the part of the Lagrangian mediating beta transitions, the leading $\mathcal{O}(\boldsymbol{\nabla}^0)$ term in this expansion encodes the usual Fermi and Gamow-Teller

---

[1]In this paper we use the notation where 3-vectors are represented by **bold-font** symbols.

contributions to the allowed beta decays. This includes the SM-like contributions from the vector and axial currents, as well as the non-SM ones from the scalar and tensor currents. The resulting beta decay observables, such as the lifetime or angular correlations, are described exactly by the formulas obtained by Jackson, Treiman, and Wyld in the seminal ref. [13].[2]

The subleading corrections to these leading order expressions are the main focus of this paper. They vanish in the limit where 3-momenta of the parent and daughter nuclei are zero, hence in the literature they are referred to as the *recoil corrections*. We restrict to discussing the effects linear in 3-momenta of the nuclei. These originate from two sources. One is the $\mathcal{O}(\boldsymbol{\nabla}^1)$ terms in the EFT Lagrangian, which gives a complete description of recoil effects in neutron decay. For nuclei with $A > 1$ the other source is the $\mathcal{O}(\boldsymbol{\nabla}^0)$ Lagrangian with the nuclear matrix elements expanded to linear order in the 3-momenta. We give the full expressions for the amplitudes at the linear recoil level, as well as the corresponding differential decay width in a convenient parametrization. In the limit where non-standard currents are absent, our results can be matched to those in ref. [16]. The novelty of this paper is that we also present a complete treatment on non-standard corrections at the linear recoil level. We describe how the quark-level scalar and pseudoscalar interactions enter the beta decay observables. Moreover, we give a complete description of the effects of quark-level tensor interactions, which lead a number of distinct terms in the leading and subleading Lagrangian of our low-energy EFT.

Parameters of the leading-order EFT interactions have been fit from data for more than 70 years. The existing experimental data on beta transitions [7–10, 17] are nowadays precise enough to be sensitive to recoil corrections. Our formalism can be employed to place meaningful constraints on Wilson coefficients of leading and subleading EFT operators. We construct a global likelihood function for the Wilson coefficients based on the state-of-the art measurements of superallowed $0^+ \to 0^+$ transitions, neutron decay, mirror decay, and other allowed transitions. This likelihood encodes confidence intervals for all the Wilson coefficients. In addition to constraints on the leading Wilson coefficients, already obtained in ref. [11], we derive constraints on certain Wilson coefficients of subleading EFT operators generated by BSM physics. In particular, we analyse the effects of pseudoscalar interactions on beta transitions, and obtain simultaneous constraints on non-standard pseudoscalar, scalar, tensor, and right-handed currents. Next, we discuss the Wilson coefficient of the EFT operator describing the nucleon-level weak magnetism. Usually, its magnitude is determined by theory using isospin symmetry, which in this context is referred to as the conserved vector current (CVC) hypothesis. We show that this Wilson coefficient is now efficiently constrained by the global data, which provides the first evidence for the nucleon-level weak magnetism. Finally, we also discuss a subleading EFT operator describing the so-called induced tensor interactions (one of the second class currents in the classification of [14]). While isospin symmetry predicts that this Wilson coefficient should be negligibly small, the data show a 1.8 sigma preference for its non-zero value.

This paper is organized as follows. In section 2 we lay out the formalism connecting the general quark-level EFT below the electroweak scale to the low-energy EFT describing weak

---

[2]In the present EFT we assume the SM degrees of freedom, thus right-handed neutrinos are absent. More precisely, the leading order EFT interactions lead to the formulas of ref. [13] in the limit where their couplings to right-handed neutrinos are set to zero. It is trivial to generalize our EFT to include right-handed neutrinos as well.

charged-current interactions of nucleons. Based on the latter EFT, in section 3 we calculate the recoil corrections to the beta transition amplitudes and observables (the lifetime and correlation coefficients). Global fits to the Wilson coefficients are presented in section 4. Our conclusions are contained in section 5. Appendix A.1 contains some useful mathematical details about spin representations, while the contributions of all one-derivative EFT operators to the beta decay correlations coefficients are summarized in appendix B.

2 Effective Lagrangian for beta decay

2.1 WEFT

The starting point is the so-called weak EFT (WEFT) Lagrangian, which is defined at the scale $\mu \simeq 2\,\text{GeV}$ and organized in an expansion in ∂/m_W, where the W boson mass m_W plays the role of the cutoff scale. The leading order term describing charged-current interactions between quarks and leptons is [18]

$$
\mathcal{L}_{\text{WEFT}} \supset -\frac{V_{ud}}{v^2}\Big\{ (1+\epsilon_L)\ \bar{e}\gamma_\mu\nu_L \cdot \bar{u}\gamma^\mu(1-\gamma_5)d + \epsilon_R\,\bar{e}\gamma_\mu\nu_L \cdot \bar{u}\gamma^\mu(1+\gamma_5)d
$$
$$
+ \frac{1}{2}\epsilon_T\ \bar{e}\sigma_{\mu\nu}\nu_L \cdot \bar{u}\sigma^{\mu\nu}d + \epsilon_S\,\bar{e}\nu_L \cdot \bar{u}d - \epsilon_P\,\bar{e}\nu_L \cdot \bar{u}\gamma_5 d \Big\} + \text{h.c.} \tag{2.1}
$$

where u, d, e, and $\nu_L \equiv (1-\gamma_5)\nu/2$ are the up quark, down quark, electron, and left-handed electron neutrino fields, $\sigma_{\mu\nu} \equiv \frac{i}{2}[\gamma_\mu,\gamma_\nu]$, V_{ud} is the CKM matrix element, and $v \equiv (\sqrt{2}G_F)^{-1/2} \approx 246.22\,\text{GeV}$. The central assumption is that, below $2\,\text{GeV}$, there are no other light degrees of freedom except for those of the SM. We treat the neutrino as massless, its tiny mass having no discernible effects on the observables studied in this paper. The Wilson coefficients ϵ_X, $X = L, R, S, P, T$, parametrize possible effects of non-SM particles heavier than $2\,\text{GeV}$. In the SM limit, $\epsilon_X = 0$ for all X.

The Lagrangian in eq. (2.1) is convenient to connect to new physics at *high* scales. For example, integrating out the so-called S_1 leptoquark [19, 20] with mass M and Yukawa couplings y can be approximated by the Wilson coefficients $\epsilon_S \approx -\epsilon_P \approx -\epsilon_T = \frac{|y|^2}{4V_{ud}M^2}$, up to loop and RG corrections. More generally, ϵ_X can be matched at the scale $\mu \simeq m_W$ to the Wilson coefficients of the SMEFT (see e.g. [21]), which captures a broad range of new physics scenarios with heavy particles [22]. In this paper, however, we are interested in *low-energy* physics of beta transitions. In these processes, the relevant degrees of freedom are not quarks but *nucleons* (protons and neutrons) or composite states thereof. In the following we connect the EFT in eq. (2.1) to another EFT describing charged-current interactions of nucleons and leptons.

2.2 Nucleon matrix elements

As a first step toward this end, we define the matrix elements of quark currents between nucleon states [14, 16, 18]:[3]

$$
\langle p(k)|\,\bar{u}\gamma_\mu d\,|n(p)\rangle = \bar{u}_p\bigg[g_V(q^2)\gamma_\mu + \frac{g_{IS}(q^2)}{2m_N}q_\mu - i\frac{g_M(q^2)-g_V(q^2)}{2m_N}\sigma_{\mu\nu}q^\nu\bigg]u_n,
$$

---

[3]For the vector and axial matrix elements our notation is close to that of ref. [16], except that we trade $g_{II} \to g_{IT}$, and $g_{S,P} \to g_{IS,IP}$ (to remove the conflict with the $g_{S,P}$ form factors in the scalar and pseudoscalar currents). The notation for the scalar, pseudoscalar, and tensor matrix elements follows that of ref. [18], up to i and m_N factors to make the $g_T^{(i)}$ form factors real and dimensionless. Compared to [18] we also omit the $g_T^{(2)}$ form factor because its effect is equivalent to that of $g_T^{(1)}$ up to $\mathcal{O}(\boldsymbol{q}^2/m_N^2)$.

$$\langle p(k)| \, \bar{u}\gamma_\mu\gamma_5 d \, |n(p)\rangle = \bar{u}_p \Big[g_A(q^2)\gamma_\mu\gamma_5 + \frac{g_{IP}(q^2)}{2m_N}\gamma_5 q_\mu - i\frac{g_{IT}(q^2)}{2m_N}\sigma_{\mu\nu}\gamma_5 q^\nu \Big] u_n,$$

$$\langle p(k)| \, \bar{u}d \, |n(p)\rangle = g_S(q^2)\bar{u}_p u_n,$$

$$\langle p(k)| \, \bar{u}\gamma_5 d \, |n(p)\rangle = g_P(q^2)\bar{u}_p \gamma_5 u_n,$$

$$\langle p(k)| \, \bar{u}\sigma_{\mu\nu} d \, |n(p)\rangle = \bar{u}_p \Big[g_T(q^2)\sigma_{\mu\nu} + \frac{ig_T^{(1)}(q^2)}{m_N}(q_\mu\gamma_\nu - q_\nu\gamma_\mu)$$

$$+ \frac{ig_T^{(3)}(q^2)}{m_N}(\gamma_\mu\gamma_\rho\gamma_\nu - \gamma_\nu\gamma_\rho\gamma_\mu)q^\rho \Big] u_n. \tag{2.2}$$

Above p and k are the momenta of an incoming neutron and an outgoing proton, and $q = p - k$ is the momentum transfer. Next, $m_N \equiv (m_n + m_p)/2$ is the nucleon mass, and u_N is the Dirac spinor wave function of the neutron or proton, which implicitly depends on the respective momentum and polarization. The matrix elements take the most general form allowed by the Lorentz symmetry and the discrete P and T symmetries of QCD. The dependence on the momentum transfer is encoded in the form factors $g_X(q^2)$, which must be real by T invariance. We also define nucleon charges $g_X \equiv g_X(0)$, which are the relevant parameters for beta transitions, where $q^2 \ll m_N^2$. Symmetries impose important restrictions on the possible values of the charges coming from the different quark currents:

- *Vector current.* The Ademollo-Gatto theorem implies that, up to second order in isospin breaking, $g_V = 1$ [23, 24]. The induced scalar coupling, g_{IS}, vanishes in the isospin limit and then an $\mathcal{O}(10^{-2} - 10^{-3})$ value is expected for it. Finally, g_M can be related, through an isospin rotation (CVC), to the response of the nucleons to an external magnetic field and can be fixed, up to relative $\mathcal{O}(10^{-2})$ isospin breaking corrections, from the experimentally known difference of the magnetic moment of the nucleons [16, 25, 26],

$$g_M = \frac{\mu_p - \mu_n}{\mu_N} = 4.706, \tag{2.3}$$

  where μ_N is the nuclear magneton $\frac{e}{2m_p}$.

- *Axial current.* The axial charge g_A is not known from symmetry considerations alone and in practice is fixed from experimental data or by lattice calculations. As for the latter, the FLAG'21 average quotes $g_A = 1.246(28)$ [27–30]. The induced pseudoscalar charge, g_{IP}, only enters into the observables at second order in the recoil expansion and then, in principle, it is beyond the scope of this analysis. Notice however that g_{IP} is enhanced by the pion pole. Indeed, using partial conservation of axial current one has [31]

$$-\frac{q^2 g_{IP}(q^2)}{4m_N^2} = \frac{\overline{m}_q}{m_N}g_P(q^2) - g_A(q^2), \tag{2.4}$$

  where $\overline{m}_q$ is the average of the light quark masses. Using that $g_A(q^2)$ is a very smooth function of q^2 for $q^2 \lesssim m_\pi^2$ and that $g_P(q^2)$ is dominated by the pion pole contribution (e.g. see [32, 33]), one obtains, up to a few per-cent level correction,

$$g_{IP} = -\frac{4m_N^2}{m_\pi^2}g_A \approx -226(5), \tag{2.5}$$

where the displayed uncertainty is due to the error on the lattice determination of g_A. Finally the induced tensor, g_{IT}, which by itself enters suppressed by one power in the recoil expansion, vanishes in the isospin limit, and then its expected size is $\mathcal{O}(10^{-2} - 10^{-3})$.

- *Non-standard currents.* The $q^2 \to 0$ limit of eq. (2.4) fixes the pseudoscalar charge in terms of the axial one [31]:

$$g_P = \frac{m_N}{\overline{m}_q} g_A = 346(9), \tag{2.6}$$

where we use $\overline{m}_q = 3.381(40)\,\mathrm{MeV}$ from the lattice [27, 34–40], and the error is again dominated by the lattice uncertainty of g_A. For the scalar and tensor charges we use the lattice values $g_S = 1.022(100)$ and $g_T = 0.989(34)$ [27, 28] (see also ref. [31]). Concerning the recoil level tensor charges, $g_T^{(1)}$ is expected to be $\mathcal{O}(1)$, while $g_T^{(3)}$ vanishes in the isospin limit and then its expected size is $\mathcal{O}(10^{-2} - 10^{-3})$.

2.3 Pionless EFT

Beta transitions are characterized by a 3-momentum transfer much smaller than the nucleon mass, typically $|\boldsymbol{q}| \sim$ 1–10 MeV. Therefore, the nucleon degrees of freedom are non-relativistic (in an appropriate reference frame), and can be described by non-relativistic quantum fields ψ_N, $N = p, n$, which are 2-component spinors. On the other hand, we continue describing leptons by the relativistic fields ν_L and e. The effective Lagrangian is constructed as the most general function of ψ_N, e, and ν_L and their derivatives, respecting the rotational symmetry and Galilean boosts. It is organized in an expansion in $\boldsymbol{\nabla}/m_N$, where $\boldsymbol{\nabla}$ denotes spatial derivatives.[4] This framework is known as the *pionless EFT* [15]. In this paper we are interested in the subset of the pionless EFT Lagrangian relevant for beta transitions, that is in the quartic interactions between a proton, a neutron, an electron, and a neutrino.[5] We organize these interactions as

$$\mathcal{L}_{\not\pi\mathrm{EFT}} \supset \mathcal{L}^{(0)} + \mathcal{L}^{(1)} + \mathcal{O}(\boldsymbol{\nabla}^2/m_N^2) + \mathrm{h.c.}, \tag{2.7}$$

where $\mathcal{L}^{(n)}$ refers to $\mathcal{O}(\boldsymbol{\nabla}^n/m_N^n)$ terms. At the zero-derivative level, the most general Lagrangian respecting the rules mentioned above is[6]

$$\mathcal{L}^{(0)} = -(\psi_p^\dagger \psi_n)\left[C_V^+ \bar{e}_L \gamma^0 \nu_L + C_S^+ \bar{e}_R \nu_L\right] + (\psi_p^\dagger \sigma^k \psi_n)\left[C_A^+ \bar{e}_L \gamma^k \nu_L + C_T^+ \bar{e}_R \gamma^0 \gamma^k \nu_L\right], \tag{2.8}$$

---

[4]Notice that all hadronic degrees of freedom, including pions, have been integrated out and, as a consequence, certain Wilson Coefficients can get enhanced by the large m_N/m_π ratio. In particular, the coefficient of pseudo-scalar interactions C_P^+ is enhanced by m_N^2/m_π^2, cf. eq. (2.6). This enhancement is however significantly smaller than the recoil suppression of C_P^+ effects in nuclear beta transitions, and therefore it is consistent to treat the pseudo-scalar interactions as subleading.

[5]Interactions with more than two nucleon fields also contribute to nuclear beta transitions (A>1), in particular the ones with four nucleons and two leptons are referred to as two-body currents in the literature. We comment on this issue in appendix D.

[6]For brevity, we do not display the overall $e^{\pm i(m_p - m_n)t}$ factors multiplying the Lagrangian terms away from the isospin limit.

where σ^k are the Pauli matrices, $\gamma^\mu = \begin{pmatrix} 0 & \sigma^\mu \\ \bar{\sigma}^\mu & 0 \end{pmatrix}$, $\sigma^\mu = (\sigma^0, \sigma^k)$, $\bar{\sigma}^\mu = (\sigma^0, -\sigma^k)$. At this level we have only two distinct nucleon bilinears, $\psi_p^\dagger \psi_n$ and $\psi_p^\dagger \sigma^k \psi_n$, which, up to two-body current effects, mediate the so-called allowed Fermi and Gamow-Teller (GT) transitions, respectively. The labels and normalization of the Wilson coefficients C_X^+ are chosen such that they simply relate to the familiar parameters of the Lee-Yang Lagrangian [4]: $C_X^+ \equiv C_X + C_X'$ for $X = V, A, S, T$. In order to match C_X^+ to the parameters of the quark-level Lagrangian we calculate the $n \to p e^- \bar{\nu}$ amplitude in two ways: using eq. (2.8), and using eq. (2.1) together with eq. (2.2). We then demand that both calculations give the same result in the limit $\boldsymbol{q} \to 0$. This procedure leads to the matching equations

$$C_V^+ = \frac{V_{ud}}{v^2}\left\{ g_V\left(1 + \epsilon_L + \epsilon_R\right)\sqrt{1 + \Delta_R^V} - \frac{m_e}{m_N}g_T^{(1)}\epsilon_T \right\},$$

$$C_A^+ = -\frac{V_{ud}}{v^2}\left\{ g_A\left(1 + \epsilon_L - \epsilon_R\right)\sqrt{1 + \Delta_R^A} + 2\frac{m_e}{m_N}g_T^{(3)}\epsilon_T \right\},$$

$$C_S^+ = \frac{V_{ud}}{v^2}\left\{ g_S\epsilon_S + \frac{m_e}{2m_N}g_{IS}\left(1 + \epsilon_L + \epsilon_R\right) \right\},$$

$$C_T^+ = \frac{V_{ud}}{v^2}g_T\epsilon_T, \tag{2.9}$$

up to $\mathcal{O}(\boldsymbol{q}^2/m_N^2)$ effects which are consistently neglected in our analysis. On the other hand, we keep track of $\mathcal{O}(\boldsymbol{q}/m_N)$ effects, which appear in this matching as the terms suppressed by m_e/m_N. One important thing to notice is that the quark-level pseudoscalar interactions, parametrized by ϵ_P in eq. (2.1), do not affect the leading order Lagrangian of pionless EFT. The matching in eq. (2.9) is essentially tree-level, but for the vector and axial Wilson coefficients we also included the short-distance (inner) radiative corrections, where we use the numerical values $\Delta_R^V = 0.02467(22)$ [41] and $\Delta_R^A - \Delta_R^V = 0.00026(26)$ [42] (see also [26]). Other radiative corrections in this matching are not relevant from the phenomenological point of view and are omitted.

At the next-to-leading (one-derivative) order we consider the following interactions:

$$\mathcal{L}^{(1)} = \frac{1}{2m_N}\left\{ iC_P^+(\psi_p^\dagger \sigma^k \psi_n)\nabla_k\left(\bar{e}_R \nu_L\right) - C_M^+ \epsilon^{ijk}(\psi_p^\dagger \sigma^j \psi_n)\nabla_i\left(\bar{e}_L \gamma^k \nu_L\right) \right.$$

$$- iC_E^+(\psi_p^\dagger \sigma^k \psi_n)\nabla_k\left(\bar{e}_L \gamma^0 \nu_L\right) - iC_{E'}^+(\psi_p^\dagger \sigma^k \psi_n)\partial_t\left(\bar{e}_L \gamma^k \nu_L\right)$$

$$- iC_{T1}^+(\psi_p^\dagger \psi_n)\nabla_k\left(\bar{e}_R \gamma^0 \gamma^k \nu_L\right) + iC_{T2}^+(\psi_p^\dagger \psi_n)(\bar{e}_R \overleftrightarrow{\partial_t} \nu_L) + 2iC_{T3}^+(\psi_p^\dagger \sigma^k \psi_n)(\bar{e}_R \overleftrightarrow{\nabla}_k \nu_L)$$

$$\left. - iC_{FV}^+(\psi_p^\dagger \overleftrightarrow{\nabla}_k \psi_n)(\bar{e}_L \gamma^k \nu_L) + iC_{FA}^+(\psi_p^\dagger \sigma^k \overleftrightarrow{\nabla}_k \psi_n)(\bar{e}_L \gamma^0 \nu_L) + C_{FT}^+ \epsilon^{ijk}(\psi_p^\dagger \sigma^i \overleftrightarrow{\nabla}_j \psi_n)(\bar{e}_R \gamma^0 \gamma^k \nu_L) \right\},$$

$$\tag{2.10}$$

where $f_1\Gamma\overleftrightarrow{\nabla}f_2 \equiv f_1\Gamma\nabla f_2 - \nabla f_1\Gamma f_2$. Again, we calculate the $n \to p e^- \bar{\nu}$ amplitude in two ways: using eq. (2.10) and using eq. (2.1) together with eq. (2.2), but now we concentrate on linear terms in $\boldsymbol{q}$ in the limit $|\boldsymbol{q}|/m_N \ll 1$. Matching these linear terms requires the following identification of the nucleon-level and quark-level Wilson coefficients:

$$C_P^+ = \frac{V_{ud}}{v^2}g_P\epsilon_P,$$

$$C_M^+ = \frac{V_{ud}}{v^2}g_M\left(1 + \epsilon_L + \epsilon_R\right) = \frac{g_M}{g_V}C_V^+,$$

$$C_E^+ = C_{E'}^+ = \frac{V_{ud}}{v^2}g_{IT}(1 + \epsilon_L - \epsilon_R) = -\frac{g_{IT}}{g_A}C_A^+,$$

$$C_{T1}^+ = \frac{V_{ud}}{v^2}g_T\epsilon_T = C_T^+,$$

$$C_{T2}^+ = -\frac{2V_{ud}}{v^2}g_T^{(1)}\epsilon_T = -2\frac{g_T^{(1)}}{g_T}C_T^+,$$

$$C_{T3}^+ = -\frac{2V_{ud}}{v^2}g_T^{(3)}\epsilon_T = -2\frac{g_T^{(3)}}{g_T}C_T^+,$$

$$C_{FV}^+ = \frac{V_{ud}}{v^2}g_V(1 + \epsilon_L + \epsilon_R) = C_V^+,$$

$$C_{FA}^+ = -\frac{V_{ud}}{v^2}g_A(1 + \epsilon_L - \epsilon_R) = C_A^+,$$

$$C_{FT}^+ = \frac{V_{ud}}{v^2}g_T\epsilon_T = C_T^+, \tag{2.11}$$

where all the equalities are true up to $\mathcal{O}(\boldsymbol{q}/m_N)$ corrections, i.e up to terms suppressed by m_e/m_N or $(m_n - m_p)/m_N$. Note that we should not keep such terms in the matching of the Wilson coefficients of the *subleading* Lagrangian, as they correspond to $\mathcal{O}(\boldsymbol{q}^2/m_N^2)$ effects in our EFT counting. We can see that quark-level pseudoscalar interactions, which arise only beyond the SM, induce the interaction term proportional to C_P^+ in eq. (2.10).[7] The interaction term proportional to C_M^+ is known as the *weak magnetism*, while that proportional to C_E^+ is referred to as the induced tensor term.[8] The Wilson coefficients C_{T1}^+-C_{T3}^+ are all proportional to ϵ_T parametrizing tensor interactions at the quark-level. They are less important phenomenologically, as we expect to first observe effects of ϵ_T through its contributions to the leading order Lagrangian in eq. (2.8). The interactions in the first two lines of eq. (2.10) depend on the same nucleon bilinears $\psi_p^\dagger\psi_n$ and $\psi_p^\dagger\sigma^k\psi_n$ as the leading Lagrangian in eq. (2.8). On the other hand, the last line contains bilinears where the derivative acts on the nucleon field. They appear in the subleading Lagrangian for the first time, and lead to three new nuclear matrix elements entering the decay amplitude at the linear level in recoil.

From the matching in eq. (2.11) it follows that the subleading Wilson coefficients C_E^+, $C_{E'}^+$, and C_{T3}^+ vanish in the isospin limit. Since the beta decay kinematics relates the maximum value of the 3-momentum transfer $\boldsymbol{q}$ to the isospin-breaking nuclear mass difference $\Delta \equiv m_{\mathcal{N}} - m_{\mathcal{N}'}$, in principle one could consider the corresponding terms as $\mathcal{O}(\boldsymbol{q}^2/m_N^2)$ and relegate them to the $\mathcal{O}(\boldsymbol{\nabla}^2/m_N^2)$ Lagrangian. In this paper we keep them in eq. (2.10) for completeness, however, in practice, recoil and isospin suppression together results in $\mathcal{O}(10^{-5})$ effects at most, which are unobservable in current experiments.

3 Recoil corrections to beta decay observables

Starting from the EFT Lagrangian in eq. (2.7) one can calculate the associated amplitude and differential distributions for the nuclear beta transitions $\mathcal{N} \to \mathcal{N}'e\nu$. Here, $\mathcal{N}(\mathcal{N}')$ denotes

---

[7]Within the SM one has the contribution to C_P^+ through the induced pseudoscalar coupling, $\Delta C_P^+ = \frac{V_{ud}}{v^2}\frac{m_e}{2m_N}g_{IP}$. This is however suppressed by an additional factor of $\boldsymbol{q}/m_N$, and thus is neglected here as an $\mathcal{O}(\boldsymbol{q}^2/m_N^2)$ effect.

[8]This is a misnomer because it has nothing to do with the bona fide tensor interactions at the quark level, which contribute to completely different structures in the non-relativistic EFT Lagrangian. We will however use this name, to conform with the bulk of the beta decay literature.

the parent (daughter) nucleus, e denotes the beta particle ($e^\mp$ for $\beta^\mp$ transitions), and ν denotes the antineutrino (for β^-) or the neutrino (for β^+). In this paper we focus on the allowed beta transitions where $\mathcal{N}$ and $\mathcal{N}'$ have the same spin, $J' = J$; the discussion of the allowed decays with $J' = J \pm 1$ is analogous. We first introduce the general structure of the amplitude including the recoil effects, and then move to discussing differential distributions.

3.1 Structure of the decay amplitude

For concreteness, we present the formulas for the β^- decay amplitude, $\mathcal{M}_{\beta^-} \equiv \mathcal{M}(\mathcal{N} \to \mathcal{N}' e^- \bar{\nu})$. The amplitude can be expanded in powers of recoil momenta: $\mathcal{M}_{\beta^-} \equiv \mathcal{M}^{(0)}_{\beta^-} + \mathcal{M}^{(1)}_{\beta^-} + \ldots$. In this expansion, all 3-momenta involved ($\boldsymbol{p}_\mathcal{N}$, $\boldsymbol{k}_{\mathcal{N}'}$, $\boldsymbol{k}_e$, $\boldsymbol{k}_\nu$), the lepton energies and electron mass (E_e, m_e, $E_\nu \equiv E_e^{\max} - E_e$) as well as the nuclear mass difference Δ count as one order in recoil, and we denote these collectively as $\mathcal{O}(\boldsymbol{q}/m_N)$.

Only the leading order Lagrangian in eq. (2.8) contributes to the leading part of the amplitude $\mathcal{M}^{(0)}_{\beta^-}$. One finds

$$\mathcal{M}^{(0)}_{\beta^-} = -\langle \psi_p^\dagger \psi_n \rangle [C_V^+ L^0 + C_S^+ L] + \langle \psi_p^\dagger \sigma^k \psi_n \rangle [C_A^+ L^k + C_T^+ L^{0k}]. \tag{3.1}$$

Above, C_X^+ are the Wilson coefficients in the Lagrangian of eq. (2.8). The leptonic currents are defined as $L^\mu \equiv \bar{u}_L(k_e)\gamma^\mu v_L(k_\nu)$, $L \equiv \bar{u}_R(k_e)v_L(k_\nu)$, $L^{0k} \equiv \bar{u}_R(k_e)\gamma^0\gamma^k v_L(k_\nu)$, where $k = 1\ldots3$, and u and v are the spinor wave functions of the outgoing electron and antineutrino (the L/R subindex denote the chirality projection). Finally, $\langle \cdot \rangle \equiv \langle \mathcal{N}'(\boldsymbol{k}_{\mathcal{N}'})| \cdot |\mathcal{N}(\boldsymbol{p}_\mathcal{N})\rangle$ denotes matrix elements of the non-relativistic nucleon fields sandwiched between the daughter and parent nuclear states in relativistic normalization $\langle \mathcal{N}(\boldsymbol{p}')|\mathcal{N}(\boldsymbol{p})\rangle = 2E_\mathcal{N}(2\pi)^3\delta^3(\boldsymbol{p} - \boldsymbol{p}')$. The matrix elements entering into eq. (3.1) are labeled as Fermi and GT, respectively. We will write them down in the limit of unbroken isospin symmetry.[9] As we discuss in great detail in appendix A, rotational and Galilean symmetry, parity, time-reversal, and isospin invariance constrain the Fermi and GT matrix elements to take the most general form:

$$\langle \psi_p^\dagger \psi_n \rangle = \kappa\, M_F \delta_{J_z' J_z} + \mathcal{O}(\boldsymbol{q}^2/m_N^2),$$
$$\langle \psi_p^\dagger \sigma^k \psi_n \rangle = r\, \kappa\, M_F \frac{[\mathcal{T}_{(J)}^k]_{J_z'}^{J_z}}{\sqrt{J(J+1)}} + \mathcal{O}(\boldsymbol{q}^2/m_N^2), \tag{3.2}$$

where $\kappa \equiv 2\sqrt{E_\mathcal{N} E_{\mathcal{N}'}}$, and $\mathcal{T}_{(J)}^k$ are the spin-J generators of the rotation group defined in eq. (A.2). For $J = 0$ one should take the limit $r \to 0$ while ignoring all apparent $1/J$ singularities. Terms linear in $\boldsymbol{p}$ or $\boldsymbol{p}'$ cannot appear in eq. (3.2) due to parity conservation. The common normalization factor M_F can be calculated when parent and daughter nuclei are members of the same isospin multiplet. For $\beta^\mp$ transitions one has $M_F = \delta_{j'j}\delta_{j_3',j_3\pm1}\sqrt{j(j+1) - j_3(j_3\pm1)}$, where (j, j_3) and (j', j_3') are the isospin quantum numbers of the parent and daughter nuclei. The parameter r, which is real by time-reversal

---

[9]Isospin breaking should be included separately, whenever it is phenomenologically relevant. Given the current precision of the beta decay experiments, isospin breaking effects must be taken into account in the case of the Fermi matrix element. In our analysis, these will be included in the δ_R correction in eq. (3.6). For the GT one, since the matrix element is proportional to the unknown parameter r which has to be anyway fixed from experiment, the isospin breaking corrections do not play an important role.

invariance, is referred to as the ratio of GT and Fermi matrix elements in the literature. For the neutron decay $r = \sqrt{3}$. For decays with $A > 1$, it cannot currently be calculated from first principles with high accuracy, and instead has to be extracted from experiment or estimated in nuclear models. In this notation the so-called mixing ratio is given by $\rho = r\, C_A^+/C_V^+$, up to radiative corrections. Finally, $\mathcal{O}(\boldsymbol{q^2}/m_N^2)$ refers to corrections of the second order in recoil, which are consistently neglected in this paper.

The subleading Lagrangian in eq. (2.10) contributes at the next-to-leading order in the recoil expansion. The amplitude at this order takes the form

$$
\begin{aligned}
\mathcal{M}_{\beta^-}^{(1)} = \frac{1}{2m_N}\bigg\{ & \langle \psi_p^\dagger \psi_n \rangle \Big[-C_{T1}^+ q^k L^{0k} - C_{T2}^+(E_\nu - E_e)L \Big] \\
& + \langle \psi_p^\dagger \sigma^k \psi_n \rangle \Big[C_P^+ q^k L - C_E^+ q^k L^0 + C_{E'}^+(E_\nu + E_e)L^k - iC_M^+ \epsilon^{ijk}q^i L^j + 2C_{T3}^+(k_\nu^k - k_e^k)L \Big] \\
& - i\langle \psi_p^\dagger \overleftrightarrow{\nabla}_k \psi_n \rangle C_{FV}^+ L^k + i\langle \psi_p^\dagger \sigma^k \overleftrightarrow{\nabla}_k \psi_n \rangle C_{FA}^+ L^0 + \epsilon^{ijk}\langle \psi_p^\dagger \sigma^i \overleftrightarrow{\nabla}_j \psi_n \rangle C_{FT}^+ L^{0k} \bigg\}. \quad (3.3)
\end{aligned}
$$

The matrix elements in the first two lines are the Fermi and GT ones, already discussed around eq. (3.2). In the last line, three new nuclear matrix elements enter at the next-to-leading order in recoil. Lorentz symmetry, parity, time-reversal, and isospin invariance constrain their form as

$$
\begin{aligned}
i\langle \psi_p^\dagger \overleftrightarrow{\nabla}_k \psi_n \rangle &= \kappa\, M_F \bigg\{ -\frac{1}{A}P^k \delta_{J_z' J_z} - i\beta_{FV}\frac{r}{\sqrt{J(J+1)}}\epsilon^{klm}q^l[\mathcal{T}_{(J)}^m]_{J_z'}^{J_z} \bigg\} + \mathcal{O}(\boldsymbol{q^2}/m_N^2), \\
i\langle \psi_p^\dagger \sigma^k \overleftrightarrow{\nabla}_k \psi_n \rangle &= r\,\kappa\, M_F \bigg\{ -\frac{1}{A\sqrt{J(J+1)}}P^k[\mathcal{T}_{(J)}^k]_{J_z'}^{J_z} \bigg\} + \mathcal{O}(\boldsymbol{q^2}/m_N^2), \\
\epsilon^{ijk}\langle \psi_p^\dagger \sigma^i \overleftrightarrow{\nabla}_j \psi_n \rangle &= \kappa\, M_F \bigg\{ i\frac{r}{A\sqrt{J(J+1)}}\epsilon^{klm}P^l[\mathcal{T}_{(J)}^m]_{J_z'}^{J_z} + \alpha_{FT}q^k\delta_{J_z'}^{J_z} + \gamma_{FT}\frac{r}{J\sqrt{J(J+1)}}q^l[\mathcal{T}_{(J)}^{kl}]_{J_z'}^{J_z} \bigg\} \\
&\quad + \mathcal{O}(\boldsymbol{q^2}/m_N^2), \quad (3.4)
\end{aligned}
$$

where $\boldsymbol{P} \equiv \boldsymbol{p}_\mathcal{N} + \boldsymbol{k}_{\mathcal{N}'}$, $A = \frac{m_\mathcal{N}}{m_N}$ is approximately the mass number of the parent nucleus, and the matrix $\mathcal{T}_{(J)}^{jk}$ is defined in eq. (A.4). For the subleading matrix elements, the isospin breaking corrections are not phenomenologically relevant, given the current experimental sensitivity. The coefficients of the terms proportional to $\boldsymbol{P}$ are related by Lorentz invariance to those in eq. (3.2) [16], as we also derive in appendix A. On the other hand, the form factors β_{FV}, α_{FT}, and γ_{FT} are transition-dependent and are determined by strong dynamics. Time-reversal invariance implies they are real, while isospin symmetry (CVC) relates β_{FV} to the magnetic moments of the parent and daughter nuclei [16]:

$$
\frac{\mu_+ - \mu_-}{\mu_N} = (g_M + \beta_{FV})r\sqrt{\frac{J}{J+1}}, \quad (3.5)
$$

where μ_+ and μ_- denote the magnetic moments of the nuclei with larger and smaller j_3 quantum number, respectively. The form factors α_{FT}, β_{FV} and γ_{FT} vanish for neutron decay. For nuclear transitions α_{FT} and γ_{FT} can be non-zero, and they are not fixed by isospin symmetry unlike β_{FV}. In order to analyze the effects of tensor interactions at the recoil level, α_{FT} and γ_{FT} have to be estimated for each transition using lattice or nuclear models.

Given the leading and subleading amplitudes in eq. (3.1) and eq. (3.3) it is straightforward if tedious to calculate the differential decay width. In the next subsection we discuss the general parametrization of the differential width appropriate to incorporate the subleading corrections in the recoil expansion.

3.2 Parametrization of the differential width

We focus on observables summed over the daughter and β particle polarizations. We are interested in the differential decay width at the leading and subleading order in recoil momenta. In this observable, the effects of the Wilson coefficients in the EFT Lagrangian fit into the following template:[10]

$$
\begin{aligned}
\frac{d\Gamma}{dE_e d\Omega_e d\Omega_\nu} = M_F^2 F(Z, E_e)(1+\delta_R) & \frac{p_e E_e (E_e^{\max} - E_e)^2}{64\pi^5} \hat{\xi} \Bigg\{ 1 + b\frac{m_e}{E_e} + \xi_b(E_e) \\
& + a(E_e)\frac{\boldsymbol{k}_e \cdot \boldsymbol{k}_\nu}{E_e E_\nu} + a'(E_e)\left[\left(\frac{\boldsymbol{k}_e \cdot \boldsymbol{k}_\nu}{E_e E_\nu}\right)^2 - \frac{p_e^2}{3E_e^2}\right] \\
& + \frac{\boldsymbol{J} \cdot \boldsymbol{k}_e}{JE_e}\left[A(E_e) + A'(E_e)\frac{\boldsymbol{k}_e \cdot \boldsymbol{k}_\nu}{E_e E_\nu} - \frac{B'(E_e)}{3}\right] + \frac{\boldsymbol{J} \cdot \boldsymbol{k}_\nu}{JE_\nu}\left[B(E_e) + B'(E_e)\frac{\boldsymbol{k}_e \cdot \boldsymbol{k}_\nu}{E_e E_\nu} - \frac{A'(E_e)}{3}\frac{p_e^2}{E_e^2}\right] \\
& + \frac{\boldsymbol{J} \cdot (\boldsymbol{k}_e \times \boldsymbol{k}_\nu)}{JE_e E_\nu}\left[D(E_e) + D'(E_e)\frac{\boldsymbol{k}_e \cdot \boldsymbol{k}_\nu}{E_e E_\nu}\right] \\
& + \frac{J(J+1) - 3(\boldsymbol{J} \cdot \boldsymbol{j})^2}{J(J+1)}\Bigg[\left(\hat{c}(E_e) + c'(E_e)\frac{\boldsymbol{k}_e \cdot \boldsymbol{k}_\nu}{E_e E_\nu}\right)\frac{(\boldsymbol{k}_e \cdot \boldsymbol{k}_\nu) - 3(\boldsymbol{k}_e \cdot \boldsymbol{j})(\boldsymbol{k}_\nu \cdot \boldsymbol{j})}{3E_e E_\nu} \\
& + c_1(E_e)\frac{\boldsymbol{k}_\nu^2 - 3(\boldsymbol{k}_\nu \cdot \boldsymbol{j})^2}{E_\nu^2} + c_2(E_e)\frac{\boldsymbol{k}_e^2 - 3(\boldsymbol{k}_e \cdot \boldsymbol{j})^2}{E_e^2} \\
& + c_3(E_e)\frac{((\boldsymbol{k}_e \times \boldsymbol{k}_\nu) \cdot \boldsymbol{j})(\boldsymbol{k}_\nu \cdot \boldsymbol{j})}{E_e E_\nu^2} + c_4(E_e)\frac{((\boldsymbol{k}_e \times \boldsymbol{k}_\nu) \cdot \boldsymbol{j})(\boldsymbol{k}_e \cdot \boldsymbol{j})}{E_e E_\nu^2}\Bigg]\Bigg\},
\end{aligned}
\tag{3.6}
$$

where F is the Fermi function:

$$
F(Z, E_e) \equiv 2(1+\gamma)(2p_e R)^{-2(1-\gamma)}\frac{e^{\pi\eta}\Gamma(\gamma + i\eta)\Gamma(\gamma - i\eta)}{\Gamma(1+2\gamma)^2}, \quad \gamma \equiv \sqrt{1 - \alpha^2 Z^2}, \quad \eta \equiv \pm\frac{\alpha Z E_e}{p_e},
\tag{3.7}
$$

R is the nuclear radius, α is the fine structure constant, δ_R stands for radiative corrections,[11] Z is the daughter nucleus charge, $p_e \equiv \sqrt{E_e^2 - m_e^2}$, m_e is the electron mass, E_e is the electron energy in the range $E_e \in [m_e, E_e^{\max}]$, the endpoint electron energy is $E_e^{\max} = \Delta + \frac{m_e^2 - \Delta^2}{2m_\mathcal{N}}$ with $\Delta = m_\mathcal{N} - m_{\mathcal{N}'}$. In eq. (3.7) and hereinafter, the upper (lower) sign applies to $\beta^-(\beta^+)$ transitions. Finally, $\boldsymbol{k}_e$ and $\boldsymbol{k}_\nu$ denote the 3-momenta of the beta particle and neutrino, $\boldsymbol{J}$ is the polarization vector of the parent nucleus, and $\boldsymbol{j}$ is the unit vector in the polarization direction (if $J = 0$ then all terms proportional to $1/J$ should be set to zero).

The bullets below offer some comments and rationale regarding our parametrization.

- Only the first line in eq. (3.6) contributes to the total beta decay width (or lifetime/half-life) of the nucleus. The overall normalization $\hat{\xi}$ and the Fierz term b are related to the

---

[10]The contributions proportional to γ_{FT} entering via the tensor matrix element in eq. (3.4) generate additional correlations not included in the template of eq. (3.6). These are treated separately later, cf. eq. (B.21).

[11]Customarily, one splits $1 + \delta_R = (1 + \delta'_R)(1 + \delta^V_{NS} - \delta^V_C)$, where δ'_R is the long-distance (outer) radiative correction, δ_{NS} is the nuclear-structure dependent correction, and δ_C is the isospin breaking correction.

parameters of the leading order Lagrangian in eq. (2.8) as [13]

$$\hat{\xi} = |C_V^+|^2 + |C_S^+|^2 + r^2\Big[|C_A^+|^2 + |C_T^+|^2\Big],$$

$$b\hat{\xi} = \pm 2\,\mathrm{Re}\left[C_V^+\bar{C}_S^+ + r^2 C_A^+\bar{C}_T^+\right],\tag{3.8}$$

and by definition do not receive any recoil-order corrections. The latter are encoded in $\xi_b(E_e)$. At the linear order in recoil $\xi_b(E_e) = b_{-1}\frac{m_e}{E_e} + b_0 + b_1\frac{E_e}{m_e}$, with $b_{-1,0,1}$ independent of E_e. Above and hereafter we use a bar to denote complex conjugation. The relation with the traditional notation of ref. [13] is simply $\xi = M_F^2\,\hat{\xi}/2$.

- For unpolarized decays, the differential distribution should be averaged over the possible quantized values of $\boldsymbol{J}$ in the range $\boldsymbol{J} \in [-J, J]$. Only the first two lines of eq. (3.6) survive the averaging. In addition to the parameters affecting the total width, the relevant parameters for unpolarized decays include the β-ν correlation $a(E_e)$, and $a'(E_e)$ parametrizing recoil effects quadratic in $\cos(\boldsymbol{k}_\beta, \boldsymbol{k}_\nu)$. The former can be represented as $a(E_e) = a_0 + \Delta a(E_e)$, where a_0 is generated by the leading order Lagrangian in eq. (2.8) and is independent of E_e [13]:

$$a_0\hat{\xi} = |C_V^+|^2 - |C_S^+|^2 - \frac{r^2}{3}\Big[|C_A^+|^2 - |C_T^+|^2\Big],\tag{3.9}$$

while $\Delta a(E_e)$ arises at the recoil level and in general does depend on the energy of the beta particle. As for $a'(E_e)$, at the linear order in recoil we have $a'(E_e) = b_a\frac{E_e}{m_e}$ with b_a independent of E_e.

- Effects linear in the polarization vector $\boldsymbol{J}$ are described by the third and fourth lines of eq. (3.6). Only $A(E_e)$, $B(E_e)$, $D(E_e)$ arise at the leading order in recoil. We again split $A(E_e) = A_0 + \Delta A(E_e)$, $B(E_e) = B_0 + b_B\frac{m_e}{E_e} + \Delta B(E_e)$, $D(E_e) = D_0 + \Delta D(E_e)$ where A_0, B_0, b_B, D_0 generated by the leading order Lagrangian in eq. (2.8) and are independent of E_e [13]:

$$A_0\hat{\xi} = -2\frac{r\sqrt{J}}{\sqrt{J+1}}\mathrm{Re}\left[C_V^+\bar{C}_A^+ - C_S^+\bar{C}_T^+\right] \mp \frac{r^2}{J+1}\Big[|C_A^+|^2 - |C_T^+|^2\Big],$$

$$B_0\hat{\xi} = -2\frac{r\sqrt{J}}{\sqrt{J+1}}\mathrm{Re}\left[C_V^+\bar{C}_A^+ + C_S^+\bar{C}_T^+\right] \pm \frac{r^2}{J+1}\Big[|C_A^+|^2 + |C_T^+|^2\Big],$$

$$b_B\hat{\xi} = \mp 2\frac{r\sqrt{J}}{\sqrt{J+1}}\mathrm{Re}\left[C_V^+\bar{C}_T^+ + C_S^+\bar{C}_A^+\right] + 2\frac{r^2}{J+1}\mathrm{Re}\left[C_A^+\bar{C}_T^+\right],$$

$$D_0\hat{\xi} = -2\frac{r\sqrt{J}}{\sqrt{J+1}}\mathrm{Im}\left[C_V^+\bar{C}_A^+ - C_S^+\bar{C}_T^+\right],\tag{3.10}$$

while $\Delta A(E_e)$, $\Delta B(E_e)$, $\Delta D(E_e)$, and also $A'(E_e)$, $B'(E_e)$, $D'(E_e)$ arise only at the recoil level. Note that the latter group of coefficients also depends on the beta particle energy in general, but we do not stress this fact in our notation.

- Out of the terms linear in $\boldsymbol{J}$, only $A(E_e)$ survives when the distribution is integrated over the neutrino direction $d\Omega_\nu$. Thus, the remaining coefficients will not affect experiments

measuring the β-asymmetry, where the neutrino momentum is not reconstructed. Similarly, only $B(E_e)$ survives when these terms are integrated over the electron direction $d\Omega_e$, and the remaining coefficients will not affect experiments measuring the β-asymmetry once the information about $e^\pm$ kinematics is integrated out. These features make our parametrization more convenient in practice than e.g. the (equivalent) one used in refs. [16, 18, 43].

- The last three lines in eq. (3.6) describe effects relevant only for polarized decays with $J \geq 1$ (thus in particular they are absent in neutron decay). We have $\hat{c}(E_e) = \hat{c}_0 + \Delta c(E_e)$ where $\hat{c}_0$ generated by the leading order Lagrangian [13]:[12]

$$\hat{c}_0 \hat{\xi} = r^2 \Big[|C_A^+|^2 - |C_T^+|^2 \Big], \qquad (3.11)$$

  while $\Delta c(E_e)$, $c'(E_e)$, and $c_{1,2,3,4}$ arise at the recoil level. To our knowledge these correlations have never been experimentally measured, even the leading order $\hat{c}_0$, and thus their phenomenological role is currently null. We nevertheless quote them here for completeness.

- The coefficients $a'(E_e)$, $c'(E_e)$ and $D'(E_e)$ are actually not generated by the interactions in eq. (2.10). They are however generated via kinematic recoil corrections to the 3-body decay phase space, which we treat on the same footing.

- The leading electromagnetic corrections are included in eq. (3.6) via the Fermi function $F(Z, E_e)$ and via δ_R. The correlation coefficients receive other $\mathcal{O}(\alpha)$ corrections ("outer radiative corrections"), see e.g. [43]. In this paper we do not discuss these explicitly, but they are taken into account in the experimental analyses that we use as input of our phenomenological analysis in the next section, whenever they are required for the theory predictions to match the experimental accuracy.

The complete dependence of all the correlation coefficients in eq. (3.6) on the Wilson coefficients in the subleading EFT Lagrangian in eq. (2.10) is summarized in appendix B. Compared to earlier works [16, 18, 43, 44] our results include complete BSM effects arising at the subleading order in the EFT, that is at the linear order in recoil. Let us note that our results include terms that are quadratic in BSM couplings. These results will be employed in the next section to perform global fits constraining the EFT Wilson coefficients. We will focus on the effects of the pseudoscalar interactions (C_P^+), nucleon-level weak magnetism (C_M^+), and induced tensor interactions (C_E^+), but our results allow one to constrain any pattern of the Wilson coefficient entering the leading and subleading EFT Lagrangian in eq. (2.10).

3.3 Observables

Before embarking on that analysis, let us first discuss how common experimental observables are related to the correlation coefficients in eq. (3.6). The total width is given by the expression[13]

$$\Gamma = \frac{M_F^2(1 + \delta_R)m_e^5 f}{4\pi^3} \hat{\xi} \left(1 + b \left\langle \frac{m_e}{E_e} \right\rangle + \langle \xi_b(E_e) \rangle \right), \qquad (3.12)$$

---

[12]Compared to ref. [13], we have rescaled the c coefficient by $(2J-1)/(J+1)$ and renamed $c \to \hat{c}$.

[13]In the formulas presented here we omit the Coulomb corrections to non-standard terms, see ref. [45].

where

$$f \equiv \frac{1}{m_e^5} \int_{m_e}^{E_e^{\max}} dE_e p_e E_e (E_e^{\max} - E_e)^2 F\,, \tag{3.13}$$

and

$$\langle X \rangle \equiv \frac{\int_{m_e}^{E_e^{\max}} dE_e p_e E_e (E_e^{\max} - E_e)^2 F\, X}{\int_{m_e}^{E_e^{\max}} dE_e p_e E_e (E_e^{\max} - E_e)^2 F}. \tag{3.14}$$

Concerning the β-asymmetry, experiments typically measure the number of events $N_\uparrow$ and $N_\downarrow$ with the beta particle emitted, respectively, into the northern and southern hemisphere in reference to the parent polarization direction $\boldsymbol{j}$. The corresponding up-down asymmetry is given by

$$\frac{N_\uparrow - N_\downarrow}{N_\uparrow + N_\downarrow} = P \frac{\int_{m_e}^{E_e^{\max}} dE_e p_e^2 (E_e^{\max} - E_e)^2 A(E_e) F}{2 \int_{m_e}^{E_e^{\max}} dE_e p_e E_e (E_e^{\max} - E_e)^2 \left[1 + b\frac{m_e}{E_e} + \xi_b(E_e)\right] F}, \tag{3.15}$$

where P the parent polarization fraction. We substitute $A(E_e) = A_0 + \Delta A(E_e)$ and expand the above to linear order in recoil:

$$\frac{N_\uparrow - N_\downarrow}{N_\uparrow + N_\downarrow} = P \frac{\int_{m_e}^{E_e^{\max}} dE_e p_e^2 (E_e^{\max} - E_e)^2 F}{2 \int_{m_e}^{E_e^{\max}} dE_e p_e E_e (E_e^{\max} - E_e)^2 F \left[1 + b\frac{m_e}{E_e}\right]} \left\{ \right.$$
$$\left. A_0 + \frac{\int_{m_e}^{E_e^{\max}} dE_e p_e^2 (E_e^{\max} - E_e)^2 F \Delta A(E_e)}{\int_{m_e}^{E_e^{\max}} dE_e p_e^2 (E_e^{\max} - E_e)^2 F} - A_0 \frac{\int_{m_e}^{E_e^{\max}} dE_e p_e E_e (E_e^{\max} - E_e)^2 F \xi_b(E_e)}{\int_{m_e}^{E_e^{\max}} dE_e p_e E_e (E_e^{\max} - E_e)^2 F \left[1 + b\frac{m_e}{E_e}\right]} \right\}. \tag{3.16}$$

Experimental collaborations often translate the observable asymmetry into a measurement of A_0, assuming vanishing Fierz term and the recoil corrections calculated in the absence of new physics beyond the SM. BSM physics can contribute as an E_e-independent shift of A_0 and b, or as an E_e-dependent shift of $\Delta A(E_e)$ and $\xi_b(E_e)$. We split the SM and BSM contributions at the recoil level as $\Delta A(E_e) = \Delta A^{\mathrm{SM}} + \Delta A^{\mathrm{BSM}}$, $\xi_i = \xi_i^{\mathrm{SM}} + \xi_i^{\mathrm{BSM}}$. With this notation, we reinterpret the experimental extraction of A_0 as a measurement of $\tilde{A}$, defined as[14]

$$\tilde{A} = \frac{1}{1 + b\langle \frac{m_e}{E_e} \rangle} \left\{ A_0 + \langle \Delta A^{\mathrm{BSM}} \rangle_p - b \langle \frac{m_e}{E_e} \rangle \langle \Delta A^{\mathrm{SM}} \rangle_p - A_0 \frac{\langle \xi_b^{\mathrm{BSM}} \rangle - 2b \langle \frac{m_e}{E_e} \rangle \langle \xi_b^{\mathrm{SM}} \rangle - b^2 \langle \frac{m_e}{E_e} \rangle^2 \langle \xi_b^{\mathrm{SM}} \rangle}{1 + b\langle \frac{m_e}{E_e} \rangle} \right\}, \tag{3.17}$$

where

$$\langle X \rangle_p \equiv \frac{\int_{m_e}^{E_e^{\max}} dE_e p_e^2 (E_e^{\max} - E_e)^2 F\, X}{\int_{m_e}^{E_e^{\max}} dE_e p_e^2 (E_e^{\max} - E_e)^2 F}. \tag{3.18}$$

At the leading order in recoil this reduces to the usual tilde prescription: $\tilde{A} = \frac{A_0}{1 + b\langle m_e/E_e \rangle}$ [11, 46]. Eq. (3.17) generalizes this prescription to the subleading order in recoil.

---

[14]We neglect the small SM contribution to b, which enters at the linear level in recoil and is in addition suppressed by isospin breaking.

By the same logic one can define the tilde prescription for the neutrino asymmetry and for the β-ν asymmetry:

$$
\begin{aligned}
\tilde{B} = {} & \frac{1}{1+b\langle\frac{m_e}{E_e}\rangle}\bigg\{ B_0 + b_B\Big\langle\frac{m_e}{E_e}\Big\rangle + \langle\Delta B^{\mathrm{BSM}}\rangle - b\Big\langle\frac{m_e}{E_e}\Big\rangle\langle\Delta B^{\mathrm{SM}}\rangle \\
& - B_0\frac{\langle\xi_b^{\mathrm{BSM}}\rangle - 2b\langle\frac{m_e}{E_e}\rangle\langle\xi_b^{\mathrm{SM}}\rangle - b^2\langle\frac{m_e}{E_e}\rangle^2\langle\xi_b^{\mathrm{SM}}\rangle}{1+b\langle\frac{m_e}{E_e}\rangle} - b_B\Big\langle\frac{m_e}{E_e}\Big\rangle\frac{\langle\xi_b\rangle}{1+b\langle\frac{m_e}{E_e}\rangle}\bigg\}, \\
\tilde{a} = {} & \frac{1}{1+b\langle\frac{m_e}{E_e}\rangle}\bigg\{ a_0 + \langle\Delta a^{\mathrm{BSM}}\rangle_p - b\Big\langle\frac{m_e}{E_e}\Big\rangle\langle\Delta a^{\mathrm{SM}}\rangle_p - a_0\frac{\langle\xi_b^{\mathrm{BSM}}\rangle - 2b\langle\frac{m_e}{E_e}\rangle\langle\xi_b^{\mathrm{SM}}\rangle - b^2\langle\frac{m_e}{E_e}\rangle^2\langle\xi_b^{\mathrm{SM}}\rangle}{1+b\langle\frac{m_e}{E_e}\rangle}\bigg\}.
\end{aligned}
\tag{3.19}
$$

If the correlations are measured as a function of energy of the beta particle, we can likewise define $\tilde{X}(E_e)$ with the dE_e integration restricted to a given energy bin. Note also that experimental conditions often imply that only a part of the phase space is effectively detected, and that should be taken into account when the $\langle\cdot\rangle$ averages are calculated [46].

4 Global fit to recoil effects

In our phenomenological analysis we use the experimental data summarized in appendix C. The differences of this dataset with the one used in the recent analysis of leading-order effects [11] are the following:

1. An older measurement of the β-ν correlation of the neutron [47] by the aCORN collaboration is superseded by the new result $\tilde{a}_n = -0.1078(18)$ [48].

2. The latest UCNτ measurement of the neutron lifetime [49] leads to the improved combined result $\tau_n = 878.64(59)$, where we include both bottle and beam measurements and average the errors *à la* PDG with the scale factor $S = 2.2$.

3. We update the lattice value of the axial coupling of the nucleon to the FLAG'21 average $g_A = 1.246(28)$ [27–30].

4. We do not use the pure GT transitions and beta polarization ratios P_F/P_{GT}, because the recoil corrections to these observables are not calculated in this paper. Currently, these observables (calculated at leading-order) have a negligible impact on the global fit.

For the sake of these fits we assume all Wilson coefficients are real, since the sensitivity to the imaginary parts of the considered observables is limited.[15]

---

[15]Constraints on the imaginary parts can be improved by including in the analysis experimental measurements of CP-violating beta decay observables, such as the D [50] or R [51] parameter of the neutron [8]. This is left for future work. In addition, in specific new physics scenarios the imaginary parts will be correlated with the strongly constrained Wilson coefficients of CP-violating neutral current operators contributing to EDMs [52–54].

	n	^{17}F	^{19}Ne	^{21}Na	^{29}P	^{35}Ar	^{37}K
$\langle \xi_b(E_e) \rangle$	-0.9	-0.9	-1.1	-0.5	-0.4	-0.1	-0.5
$\Delta a(E_e)$	-1.2	-0.9	-1.0	-0.5	-0.3	-0.1	-0.4
$\Delta A(E_e)$	-0.9	-1.8	1.1	-1.6	-1.0	-0.9	1.5
$\langle \Delta B(E_e) \rangle$	-0.7	1.7	1.2	-1.8	-1.3	-1.1	1.9

Table 1. Sensitivity of the correlation coefficients in neutron and mirror decays to pseudoscalar interactions parametrized by the Wilson coefficient C_P^+. The entries are in units of 10^{-4} and correspond to the averaged function multiplying C_P^+ in eq. (4.2) for different parent nuclei. For the sake of this table, C_V^+, C_A^+, and r are set to their minimum values in the SM fit (although they are kept as free parameters in the fits of this section). For $\xi_b(E_e)$ and $\Delta B(E_e)$ the average is defined in eq. (3.14), while in the case of $\Delta a(E_e)$ and $\Delta A(E_e)$ the pseudoscalar contribution is independent of the β particle energy and thus no average is needed.

4.1 Pseudoscalar

This subsection is focused on the pseudo-scalar interactions:

$$\mathcal{L}^{(1)} \supset C_P^+ \frac{i}{2m_N} (\psi_p^\dagger \sigma^k \psi_n) \nabla_k (\bar{e}_R \nu_L) + \text{h.c.} \tag{4.1}$$

entering into the subleading EFT Lagrangian of eq. (2.10). The complete effect of this interaction term on the correlation coefficients of eq. (3.6) is given in appendix B.1.

It is instructive to first discuss a simpler setting where, with the exception of C_P^+, only the leading order Wilson coefficients C_V^+ and C_A^+ are present.[16] In particular, we assume $C_S^+ = C_T^+ = 0$ in the leading order Lagrangian in eq. (2.8). In this limit the pseudoscalar contributions to the correlations simplify:

$$\xi_b(E_e) = \frac{m_e}{3m_N}\left[\frac{E_e^{\text{max}}}{E_e} - 1\right]\frac{r^2 C_A^+ C_P^+}{(C_V^+)^2 + r^2(C_A^+)^2},$$

$$\Delta a(E_e) = \frac{m_e}{3m_N}\frac{r^2 C_A^+ C_P^+}{(C_V^+)^2 + r^2(C_A^+)^2},$$

$$\Delta A(E_e) = -\frac{m_e}{m_N}\sqrt{\frac{J}{J+1}}\frac{r C_V^+ C_P^+}{(C_V^+)^2 + r^2(C_A^+)^2},$$

$$\Delta B(E_e) = -\frac{m_e}{m_N}\left[\frac{E_e^{\text{max}}}{E_e} - 1\right]\sqrt{\frac{J}{J+1}}\frac{r C_V^+ C_P^+}{(C_V^+)^2 + r^2(C_A^+)^2}. \tag{4.2}$$

There are also contributions to $\Delta c(E_e)$ and $c_1(E_e)$, which are not relevant for our analysis. One can observe that, in each case, the pseudoscalar contribution is multiplied by $m_e/m_N \sim 10^{-3}$, which is a typical suppression factor for recoil corrections in beta transitions. For this reason one expects much weaker constraints on C_P^+ compared to those on C_V^+ and C_A^+. Furthermore, the pseudoscalar corrections vanish in the limit $r \to 0$, that is they are zero for pure Fermi transitions. In particular, they do not affect the superallowed $0^+ \to 0^+$ transitions, currently the most accurate nuclear measurement, which further diminishes the experimental sensitivity

---

[16]We note that SM recoil corrections are included, since they have been taken into account in the experimental analyses that we use as inputs.
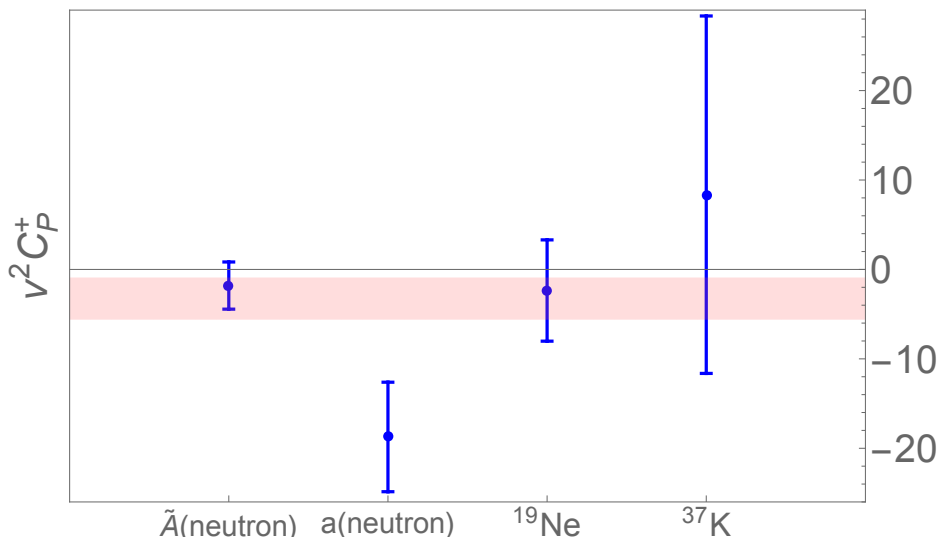
Figure 1. Constraints on the pseudo-scalar coefficient C_P^+ from a subset of most sensitive observables. We show the fit to C_P^+ marginalized over C_V^+ and C_A^+, assuming other Wilson coefficients vanish. The error bars show the 68% CL intervals obtained using $\mathcal{F}t(0^+ \to 0^+)$, neutron's lifetime, and one of the following: neutron's beta asymmetry, neutron's β-ν correlation, $\mathcal{F}t$ and beta asymmetry of ^{19}Ne, or $\mathcal{F}t$, beta asymmetry, and neutrino asymmetry of ^{37}K. The pink band corresponds to the global fit in eq. (4.3).

to C_P^+. Let us note that the $\xi_b(E_e)$ expression given above agrees with the result of ref. [31] for the neutron decay case. Finally, let us stress that linear C_P^+ effects appear not only in the beta spectrum (as with scalar and tensor interactions) but also in the angular correlations.

Comparing eq. (4.2) with the leading contributions to correlations, cf. section 3, one can see clearly that the pattern of the pseudoscalar contributions to the correlation is distinct than that of C_V^+ or C_A^+. Therefore, a global fit with enough different observables can discriminate C_P^+ from other Wilson coefficient. Indeed we obtain the following simultaneous constraints on all three Wilson coefficients:

$$v^2 \begin{pmatrix} C_V^+ \\ C_A^+ \\ C_P^+ \end{pmatrix} = \begin{pmatrix} 0.98559(26) \\ -1.25778(42) \\ -3.3(2.4) \end{pmatrix}, \qquad \rho = \begin{pmatrix} 1 & -0.02 & 0.49 \\ & 1 & 0.41 \\ & & 1 \end{pmatrix}. \tag{4.3}$$

As expected, the uncertainty of C_P^+ is $\mathcal{O}(10^4)$ larger than that of C_V^+ of C_A^+. The relative sensitivity of various observables contributing to this result is visualized in figure 1.

We can relax our assumptions by allowing new physics to enter also via scalar and tensor interactions at the quark level, which leads to C_S^+ and C_T^+ being non-zero in the leading order Lagrangian in eq. (2.8). The existing experimental data allows for a simultaneous fit of all five Wilson coefficients:

$$v^2 \begin{pmatrix} C_V^+ \\ C_A^+ \\ C_S^+ \\ C_T^+ \\ C_P^+ \end{pmatrix} = \begin{pmatrix} 0.98544(49) \\ -1.25818(82) \\ -0.0005(12) \\ 0.0008(16) \\ -5.9(4.4) \end{pmatrix}, \qquad \rho = \begin{pmatrix} 1 & -0.07 & 0.85 & 0.22 & 0.45 \\ & 1 & -0.06 & -0.84 & 0.73 \\ & & 1 & 0.24 & 0.38 \\ & & & 1 & -0.64 \\ & & & & 1 \end{pmatrix}. \tag{4.4}$$

Introduction of C_S^+ and C_T^+ increases the degeneracy of the parameter space, leading to the constraints on C_V^+, C_A^+ and C_P^+ being relaxed by approximately a factor of two compared to the simplified scenario in eq. (4.3). This is enough to disentangle the five independent WEFT couplings present in eq. (2.1). At linear order in new physics, they can be identified with the new physics parameters $\epsilon_{R,S,P,T}$ and the "polluted" CKM element corresponding to the combination $\hat{V}_{ud} \equiv V_{ud}(1 + \epsilon_L + \epsilon_R)$ [11].[17] Indeed, using the matching in eqs. (2.9) and (2.11), we can translate the fit above into constraints on the parameters of the quark-level Lagrangian in eq. (2.1), in such a way that all the new physics parameters except for ϵ_L can be disentangled. We obtain

$$
\begin{pmatrix} \hat{V}_{ud} \\ \epsilon_S \\ \epsilon_T \\ \epsilon_R \\ \epsilon_P \end{pmatrix} = \begin{pmatrix} 0.97353(49) \\ -0.0004(12) \\ 0.0008(17) \\ -0.010(11) \\ -0.017(13) \end{pmatrix}, \qquad \rho = \begin{pmatrix} 1 & 0.83 & 0.21 & 0.02 & 0.44 \\ & 1 & 0.24 & 0.02 & 0.38 \\ & & 1 & -0.02 & -0.64 \\ & & & 1 & 0.03 \\ & & & & 1 \end{pmatrix}. \tag{4.5}
$$

This is the first time such general constraints, including those on the pseudoscalar parameter ϵ_P, are extracted from nuclear data. Inclusion of ϵ_P in the fit does not increase substantially the uncertainty on the remaining new physics parameters (see the fit without ϵ_P in ref. [11]), as also indicated by moderate off-diagonal entries in the last row/column of the correlation matrix. Curiously, the uncertainty on ϵ_P is only percent-level, which is even slightly smaller than that on ϵ_R. The lower sensitivity to the latter is in part a consequence of the relatively large uncertainty of the lattice input for g_A when we match to eq. (2.9), but it also shows that beta transitions have decent sensitivity to pseudoscalar interactions, even though their effects are suppressed by $\mathcal{O}(m_e/m_N) \sim 10^{-3}$, thanks to the large value of the pseudoscalar charge g_P [31]. All in all, the magnitudes of ϵ_X effectively probed by beta transitions is well within the validity range of the quark-level EFT. However, the sensitivity of beta transitions to ϵ_P is well inferior to that of pion decays. Very recently, ref. [55] obtained the constraint $\epsilon_P = 3.9(4.3) \times 10^{-6}$ in the combined fit to beta and pion decay data. This is more than three orders of magnitude better than the result in eq. (4.5) based nuclear beta transitions alone.[18]

4.2 Weak magnetism

Recoil corrections generated by scalar and tensor interactions have a negligible impact in the previous fit, because we are not yet sensitive to much larger leading BSM contributions. Recoil effects in the SM vector and axial currents are, however, relevant and automatically incorporated in the experimental data used for the previous fit. Here we study the sensitivity to the dominant recoil effect, the weak magnetism. The name *weak magnetism* refers to a sum of two distinct effects entering at the subleading order in recoil. One is the contribution to the decay amplitude due to the operator

$$
\mathcal{L}^{(1)} \supset -C_M^+ \frac{1}{2m_N} \epsilon^{ijk} (\psi_p^\dagger \sigma^j \psi_n) \nabla_i (\bar{e}_L \gamma^k \nu_L) \tag{4.6}
$$

---

[17]Let us stress that one cannot simultaneously extract V_{ud} and ϵ_L from any set of observables associated to the Lagrangian of eq. (2.1). Beyond the linear order, one may take $\{\hat{V}_{ud}, \hat{\epsilon}_{R,S,P,T} \equiv \frac{\epsilon_{R,S,P,T}}{1+\epsilon_L+\epsilon_R}\}$ as a basis of WEFT couplings.

[18]If one allows for cancellations between the linear and quadratic pseudoscalar contributions to pion decays, then the bound is relaxed to $|\epsilon_P| \sim 4 \times 10^{-4}$ [8].

in the subleading EFT Lagrangian in eq. (2.10). We will refer to this effect as the *universal* weak magnetism, because it is common for all nuclear transitions. It turns out that a part of the contribution of another operator in eq. (2.10),

$$\mathcal{L}^{(1)} \supset -C_{FV}^+ \frac{i}{2m_N}(\psi_p^\dagger \overleftrightarrow{\nabla}_k \psi_n)(\bar{e}_L \gamma^k \nu_L), \tag{4.7}$$

has the same tensor structure as that originating from eq. (4.6). Namely, using the parametrization of the $\langle \psi_p^\dagger \overleftrightarrow{\nabla}_k \psi_n \rangle$ matrix element in eq. (3.4) and retaining only the part proportional to β_{FV}, the subleading decay amplitude is affected by the operators in eq. (4.6) and eq. (4.7) as

$$\mathcal{M}_{\beta^-}^{(1)} \supset i(C_M^+ + \beta_{FV}C_{FV}^+)rM_F A\epsilon^{ijk}\boldsymbol{q}^i \frac{[\mathcal{T}_{(J)}^j]_{J_z' J_z}}{\sqrt{J(J+1)}} L^k. \tag{4.8}$$

We will refer to the contribution entering via the operator in eq. (4.7) as the nucleus-dependent contribution to weak-magnetism (because the form factor β_{FV} depends on the nuclei participating in the transition) or, in short, *nuclear* weak magnetism. Once again, it is instructive to first display the correlations in a simplified setting where we only take into account the interference between weak magnetism and the leading SM effects proportional to C_V^+ and C_A^+. Defining $C_{WM}^+ \equiv C_M^+ + \beta_{FV}C_{FV}^+$, at the linear order in recoil the total (universal+nuclear) weak magnetism enters the relevant correlations as:

$$
\begin{aligned}
\xi_b(E_e) &= \pm r^2 \frac{2(E_e^{\max} - 2E_e + m_e^2/E_e)}{3m_N} \frac{C_A^+ C_{WM}^+}{(C_V^+)^2 + r^2(C_A^+)^2}, \\
\Delta a(E_e) &= \pm r^2 \frac{2(2E_e - E_e^{\max})}{3m_N} \frac{C_A^+ C_{WM}^+}{(C_V^+)^2 + r^2(C_A^+)^2}, \\
\Delta A(E_e) &= \mp r\sqrt{\frac{J}{J+1}} \frac{2(E_e^{\max} - E_e)}{3m_N} \frac{C_V^+ C_{WM}^+}{(C_V^+)^2 + r^2(C_A^+)^2} + \frac{r^2}{J+1} \frac{5E_e - 2E_e^{\max}}{3m_N} \frac{C_A^+ C_{WM}^+}{(C_V^+)^2 + r^2(C_A^+)^2}, \\
\Delta B(E_e) &= \pm r\sqrt{\frac{J}{J+1}} \frac{2p_e^2}{3m_N E_e} \frac{C_V^+ C_{WM}^+}{(C_V^+)^2 + r^2(C_A^+)^2} + \frac{r^2}{J+1} \frac{3E_e E_e^{\max} - 5E_e^2 + 2m_e^2}{3m_N E_e} \frac{C_A^+ C_{WM}^+}{(C_V^+)^2 + r^2(C_A^+)^2}.
\end{aligned}
\tag{4.9}
$$

See appendix B.2 for the complete expressions including the interference with scalar and tensor currents and for the remaining correlations. Much as the pseudoscalar interactions in the previous subsections, weak magnetism is zero for pure Fermi transitions, in particular it does not affect the superallowed $0^+ \to 0^+$ transitions. Unlike pseudoscalar, weak magnetism leads to all correlation coefficients picking up a dependence on the beta particle energy E_e.

As discussed in section 2, the numerical value of C_{WM}^+ for each transition is fixed by isospin symmetry (CVC), assuming the absence of large contributions to C_M^+ from higher-dimensional operators in the quark-level Lagrangian. More precisely, $C_{WM}^{+,\mathrm{CVC}} \approx (g_M^{\mathrm{CVC}} + \beta_{FV}^{\mathrm{CVC}})C_V^+$ up to small isospin breaking effects, where $g_M^{\mathrm{CVC}} = (\mu_p - \mu_n)/\mu_N \approx 4.7$, and $\beta_{FV}^{\mathrm{CVC}}$ is transition-dependent and can be related to nuclear magnetic moments via eq. (3.5). The goal of this subsection is to show that the existing experimental data is powerful enough to pinpoint universal weak magnetism parametrized by C_M^+, *without* a theoretical input from isospin symmetry.

	n	$^{17}\mathrm{F}$	$^{19}\mathrm{Ne}$	$^{21}\mathrm{Na}$	$^{29}\mathrm{P}$	$^{35}\mathrm{Ar}$	$^{37}\mathrm{K}$
$\langle \xi_b(E_e) \rangle$	-0.1	-0.1	-0.1	-0.1	0.0	0.0	-0.1
$\langle \Delta a(E_e) \rangle_p$	-1.8	1.1	1.2	0.5	0.3	0.1	0.3
$\langle \Delta A(E_e) \rangle_p$	-3.1	1.3	-4.6	2.0	1.7	2.7	-6.1
$\langle \Delta B(E_e) \rangle$	-0.3	-2.8	0.2	-3.5	-3.8	-3.3	4.5

Table 2. Sensitivity of the correlation coefficients in neutron and mirror decays to the nucleon-level weak magnetism parametrized by the Wilson coefficient C_M^+. The entries are in units of 10^{-4} and correspond to the averaged function multiplying C_M^+ in eq. (4.9) for different parent nuclei. For the sake of this table, C_V^+, C_A^+, and r are set to their minimum values in the SM fit (although they are kept as free parameters in the fits of this section). The averages $\langle \cdot \rangle_{(p)}$ over the β particle energy E_e are defined in eqs. (3.14) and (3.18).

Notice first that $\beta_{FV} = 0$ for the neutron decay. Therefore, restricting to the subset of data that includes only the $0^+ \to 0^+$ transitions and the neutron decay, we can directly determine C_M^+ (treated as a free parameter) along with other Wilson coefficients in the EFT Lagrangian. In the restricted framework where only C_V^+, C_A^+, and C_M^+ are non-zero, we obtain the simultaneous constraint on the remaining three Wilson coefficients:

$$v^2 \begin{pmatrix} C_V^+ \\ C_A^+ \\ C_M^+ \end{pmatrix} = \begin{pmatrix} 0.98563(26) \\ -1.25785(52) \\ 3.6(1.1) \end{pmatrix}, \qquad \rho = \begin{pmatrix} 1 & 0.13 & 0.47 \\ & 1 & 0.66 \\ & & 1 \end{pmatrix}. \tag{4.10}$$

The fit is dominated by the measurements of $\mathcal{F}t(0^+ \to 0^+)$ (which fixes C_V^+), neutron's lifetime (which then fixes C_A^+), and the neutron's beta asymmetry (which then fixes C_M^+). We observe that the result is consistent with the CVC prediction $C_M^{+,\mathrm{CVC}} \approx 4.6/v^2$, and that $C_M^+ = 0$ is excluded at more than 3 sigma. To our knowledge this is the first experimental evidence for the universal (nucleon-level) weak magnetism.

We can sharpen this evidence somewhat by including data from mirror transitions studied in ref. [11]. In those cases β_{FV} is non-zero, therefore those transitions do not give us an unobstructed access to the C_M^+ Wilson coefficient. Ideally for this argument, β_{FV} would be determined by first principle calculations, for example by ab initio nuclear computations. In absence of such, for the sake of the fits below we fix β_{FV} from the CVC relation in eq. (3.5). Following this procedure we obtain

$$v^2 \begin{pmatrix} C_V^+ \\ C_A^+ \\ C_M^+ \end{pmatrix} = \begin{pmatrix} 0.98570(24) \\ -1.25778(48) \\ 3.86(87) \end{pmatrix}, \qquad \rho = \begin{pmatrix} 1 & 0.02 & 0.36 \\ & 1 & 0.60 \\ & & 1 \end{pmatrix}, \tag{4.11}$$

where the uncertainty on C_M^+ is improved by $\sim 20\%$ and the experimental evidence for universal weak magnetism is strengthened above 4σ. The relative sensitivity of various observables contributing to this result is visualized in figure 2. Admittedly, our assumption that $\beta_{FV} = \beta_{FV}^{\mathrm{CVC}}$ makes the above argument a bit circular. Note however that the constraining power of the mirror data is currently dominated by the $^{19}\mathrm{Ne}$ decay [56, 57]. Indeed, discarding all other mirror data except for $^{19}\mathrm{Ne}$ leads to $C_M^+ = 3.86(90)$, a negligible difference compared to eq. (4.11). Furthermore, this result is very weakly sensitive to the precise value of $\beta_{FV}(^{19}\mathrm{Ne})$
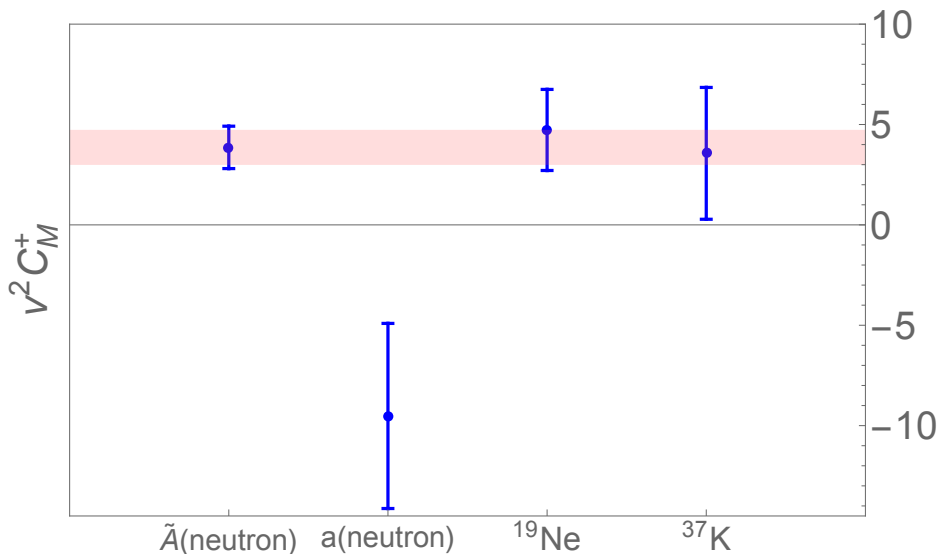
Figure 2. Constraints on the universal weak-magnetism C_M^+ from a subset of most sensitive observables. We show the fit to C_M^+ marginalized over C_V^+ and C_A^+, assuming other Wilson coefficients vanish. The error bars show the 68% CL intervals obtained using $\mathcal{F}t(0^+ \to 0^+)$, neutron's lifetime, and one of the following: neutron's beta asymmetry, neutron's β-ν correlation, $\mathcal{F}t$ and beta asymmetry of ^{19}Ne, or $\mathcal{F}t$, beta asymmetry, and neutrino asymmetry of ^{37}K. The pink band corresponds to the global fit in eq. (4.11) and the dashed line marks the prediction of isospin symmetry.

used in the fit. Using a much weaker assumption, $\beta_{FV}(^{19}\text{Ne}) = (1 \pm 1)\beta_{FV}^{\text{CVC}}(^{19}\text{Ne})$, where $\beta_{FV}^{\text{CVC}}(^{19}\text{Ne}) = 1.5$, leads to $C_M^+ = 3.80(94)$, which is still 4σ away from zero. We conclude that the further evidence for fundamental weak magnetism provided by the mirror data is robust.

Finally, we can also make a more general fit by allowing for new physics entering as scalar and tensor current at the leading order:

$$v^2 \begin{pmatrix} C_V^+ \\ C_A^+ \\ C_S^+ \\ C_T^+ \\ C_M^+ \end{pmatrix} = \begin{pmatrix} 0.98576(44) \\ -1.2578(13) \\ 0.0002(11) \\ 0.0000(23) \\ 4.0(1.9) \end{pmatrix}, \qquad \rho = \begin{pmatrix} 1 & -0.41 & 0.83 & 0.53 & -0.16 \\ & 1 & -0.36 & -0.93 & 0.91 \\ & & 1 & 0.5 & -0.16 \\ & & & 1 & -0.84 \\ & & & & 1 \end{pmatrix}. \qquad (4.12)$$

Even in this more general framework the preference for non-zero C_M^+ is still at the $\sim 2\sigma$ level.

We remark that all our fits in this section use only observables integrated over the energy spectrum of the beta particle, because only that information is provided by experimental collaborations in the readily usable form. On the other hand, as is clear from eq. (4.9), weak magnetism predicts specific dependence of the correlations on E_e. Exploring this energy dependence will allow one to further tighten the theory-independent bounds on C_M^+, possibly pushing the evidence for weak magnetism beyond the 5σ threshold.

4.3 Induced tensor

As the final example of application of our formalism, we present the fit to the Wilson coefficient parametrizing the so-called induced tensor interactions in the subleading EFT

	n	^{17}F	^{19}Ne	^{21}Na	^{29}P	^{35}Ar	^{37}K
$\langle \xi_b(E_e) \rangle$	-6.9	8.4	11.5	5.9	5.7	2.3	8.1
$\Delta a(E_e)$	5.2	-7.5	-10.7	-5.6	-5.5	-2.3	-7.9
$\langle \Delta A(E_e) \rangle_p$	4.8	5.1	7.6	5.8	7.6	4.2	-1.1
$\langle \Delta B(E_e) \rangle$	-6.6	0.3	-11.7	0.6	-1.5	2.1	-9.6

Table 3. Sensitivity of the correlation coefficients in neutron and mirror decays to the induced tensor interactions parametrized by the Wilson coefficients $C_{E'}^+ = C_E^+$. The entries are in units of 10^{-4} and correspond to the averaged function multiplying C_E^+ in eq. (4.14) for different parent nuclei. For the sake of this table, C_V^+, C_A^+, and r are set to their minimum values in the SM fit (although they are kept as free parameters in the fits of this section). The averages $\langle \cdot \rangle_{(p)}$ over the β particle energy E_e are defined in eqs. (3.14) and (3.18); for $\Delta a(E_e)$ the induced tensor contribution is independent of E_e.

Lagrangian in eq. (2.10):

$$\mathcal{L}^{(1)} \supset -C_E^+ \frac{i}{2m_N} (\psi_p^\dagger \sigma^k \psi_n) \nabla_k (\bar{e}_L \gamma^0 \nu_L) - C_{E'}^+ \frac{i}{2m_N} (\psi_p^\dagger \sigma^k \psi_n) \partial_t (\bar{e}_L \gamma^k \nu_L). \tag{4.13}$$

As discussed in section 2, the UV matching relations for these Wilson coefficients imply $C_E^+ = C_{E'}^+ = -C_A^+ g_{IT}/g_A$, thus in the following we set $C_{E'}^+ = C_E^+$ and assume C_E^+ is real. We expect the nucleon-level parameter g_{IT} to be suppressed by small isospin breaking effects, hence $v^2|C_E^+|$ is $\mathcal{O}(10^{-2} - 10^{-3})$. But, as in the preceding subsection, we can ask the question what does experiment tell about C_E^+ *without* any theoretical input from isospin symmetry. At the level of interference with C_V^+ and C_A^+, the operators in eq. (4.13) affect the correlations as

$$\xi_b(E_e) = \pm r^2 \frac{2E_e^{\max} + m_e^2/E_e}{3m_N} \frac{C_A^+ C_E^+}{(C_V^+)^2 + r^2(C_A^+)^2},$$

$$\Delta a(E_e) = \mp r^2 \frac{2E_e^{\max}}{3m_N} \frac{C_A^+ C_E^+}{(C_V^+)^2 + r^2(C_A^+)^2},$$

$$\Delta A(E_e) = \mp r \sqrt{\frac{J}{J+1}} \frac{2(E_e^{\max} - E_e)}{3m_N} \frac{C_V^+ C_E^+}{(C_V^+)^2 + r^2(C_A^+)^2} - \frac{r^2}{J+1} \frac{2E_e^{\max} + E_e}{3m_N} \frac{C_A^+ C_E^+}{(C_V^+)^2 + r^2(C_A^+)^2},$$

$$\Delta B(E_e) = \mp r \sqrt{\frac{J}{J+1}} \frac{2E_e + m_e^2/E_e}{3m_N} \frac{C_V^+ C_E^+}{(C_V^+)^2 + r^2(C_A^+)^2}$$
$$+ \frac{r^2}{J+1} \frac{3E_e^{\max} - E_e + m_e^2/E_e}{3m_N} \frac{C_A^+ C_E^+}{(C_V^+)^2 + r^2(C_A^+)^2}. \tag{4.14}$$

See appendices B.3 and B.4 for the complete expressions including the interference with scalar and tensor currents and for the remaining correlations. Note that, in principle, isospin breaking contributions to the $\langle \psi_p^\dagger \sigma^k \overleftrightarrow{\nabla}_k \psi_n \rangle$ matrix element in eq. (3.4) would lead to additional transition-dependent contributions to the correlations with the same functional form as eq. (4.14). In this analysis we assume that such contributions are absent.

Assuming that C_E^+ is the only free parameter in the fit in addition to the SM Wilson coefficients C_V^+ and C_A^+, we obtain

$$v^2 \begin{pmatrix} C_V^+ \\ C_A^+ \\ C_E^+ \end{pmatrix} = \begin{pmatrix} 0.98566(23) \\ -1.25881(90) \\ 1.7(1.1) \end{pmatrix}, \qquad \rho = \begin{pmatrix} 1 & 0.16 & -0.30 \\ & 1 & -0.90 \\ & & 1 \end{pmatrix}. \tag{4.15}$$

Clearly, the existing data are sensitive only to $|C_E^+| \sim 1/v^2$ (similarly as for the other recoil-level Wilson coefficients, e.g. C_P^+ or C_M^+). This is 3 orders of magnitude larger than the theoretically expected magnitude and hence experimental detection of C_E^+ is unlikely in the envisagable future. Furthermore, the current data show a mild 1.6σ preference for a non-zero C_E^+, driven largely by the measurement of neutron's β-ν correlation in the aSPECT experiment [58]. It will be interesting to see if this preference goes away, as experiments acquire more precise data.

5   Conclusions

In this paper we discussed the EFT for beta transitions. Working in the framework of the pionless EFT, with nucleons as degrees of freedom, the effective interactions between nucleons and leptons were organized in a non-relativistic expansion in powers of $\boldsymbol{\nabla}/m_N$. The novelty of this paper is that the low-energy EFT was matched to the general quark-level EFT at higher energy. The latter, which we refer to as the WEFT, describes the effects of the SM weak interactions, as well as possible effects of new heavy particles from beyond the SM. We worked out the matching between the WEFT and the low-energy EFT up to the subleading order in $\boldsymbol{\nabla}/m_N$, that is including the linear recoil effects. The results in eq. (2.9) and eq. (2.11) describe the matching conditions for the Wilson coefficients of the leading and subleading Lagrangian in eq. (2.8) and eq. (2.10). In particular, the matching of the non-standard tensor interactions in the WEFT to the recoil-level non-relativistic interactions at low energy was worked out for the first time.

The EFT framework allows us to systematically describe how the standard and non-standard weak interactions affect beta decay observables, such as the lifetime, beta energy spectrum, and various angular correlations. We calculated the impact of all the terms in the leading and subleading Lagrangian on the differential decay width in allowed beta transitions summed over the beta particle and daughter nucleus polarizations. In eqs. (3.6) and (B.21) we list all correlation coefficients that appear at the leading and subleading orders in recoil; the ones in eq. (B.21) receive recoil-level contributions only in the presence of tensor interactions. We express the correlation coefficients in terms of the Wilson coefficients of the effective Lagrangian and matrix elements of non-relativistic nucleon currents. Partial results, most relevant for our numerical analysis, were displayed in section 4, while the complete results are collected in appendix B.

With the expressions for the observables at hand, we can use the existing experimental data on beta transitions to determine confidence intervals for the Wilson coefficients in the EFT Lagrangian. For the leading Lagrangian this exercise was already completed in ref. [11], where $\mathcal{O}(10^{-4})$ relative precision was found for the standard Wilson coefficients corresponding to the vector and axial currents, and stringent constraints were established on the non-standard scalar and tensor interactions. In this paper we extended this analysis to recoil-level Wilson coefficients. In particular, we performed the first ever comprehensive analysis of the pseudoscalar interactions in allowed beta decay. We find that nuclear decays set a robust constraint on the Wilson coefficient descending from the pseudoscalar interactions in the WEFT, even though it enters the observables only at the linear order in recoil. This translates into a percent-level constraint on the pseudoscalar WEFT parameter (ϵ_P in eq. (2.1)), which

is comparable to the sensitivity to the right-handed WEFT current (ϵ_R), and one order of magnitude weaker than the sensitivity to the scalar and tensor currents (ϵ_S and ϵ_T). One should note, however, that within the WEFT framework, constraints on ϵ_P from pion decays are 4 orders of magnitude stronger. It would be interesting to extend this analysis to the recoil-level effects of tensor interactions. In particular, at this order, tensor interactions contribute to the very precisely measured $0^+ \to 0^+$ transitions. However, a quantitative analysis of this kind would require (at least approximate) knowledge of the subleading tensor charges $g_T^{(1,3)}$, cf. eq. (2.2), as well as of the nuclear form factors α_{FT} and γ_{FT}, cf. eq. (3.4).

Weak magnetism is another recoil-level effect to which experiment is sensitive. Our global analysis of the allowed beta decay data showed a 3 sigma evidence for a non-zero value of the EFT Wilson coefficient corresponding to the universal (nucleon-level) weak magnetism. The evidence is dominated by the neutron decay measurements (lifetime and beta asymmetry), and is further strengthened by mirror decay data. We also discussed the recoil-level EFT operator describing the so-called induced tensor interactions. The isospin symmetry of QCD predicts that this Wilson coefficient should be suppressed so as to give negligible contributions to observables. Instead, our global analysis showed a small 1.8 σ preference for non-zero induced tensor interactions. Future measurements and better theoretical calculations will improve the understanding of the effects of these Wilson coefficients.

Acknowledgments

A Symmetry constraints on nuclear matrix elements

In this appendix we discuss the nuclear matrix elements of the form

$$\langle \mathcal{N}' | \, \bar{p} \Gamma n \, | \mathcal{N} \rangle \,. \tag{A.1}$$

Here, $|\mathcal{N}\rangle$ and $|\mathcal{N}'\rangle$ are nuclear states with spin J, J_z and J'_z projection of the spin on the z-axis, and momenta p and p'. They both belong to the same isospin multiplet with the isospin quantum number j and the isospin projections related by $j'_3 - j_3 = 1$. The operator sandwiched between the states is made of relativistic neutron and proton fields n and p evaluated at $x = 0$. Below we will consider the vector, axial, and tensor matrix elements, that is $\Gamma = \gamma^\mu, \gamma^\mu \gamma^5, \sigma^{\mu\nu}$. We do not consider the (pseudo)scalar cases because, as we will see, they are not needed to extract the non-relativistic matrix elements that we are interested in.

The aim of this appendix is to write down the most general expression for the matrix element in eq. (A.1) consistent with Lorentz invariance and the discrete symmetries of the strong interactions: parity and time reversal invariance. We will work in the isospin limit where $\mathcal{N}$ and $\mathcal{N}'$ (and also p and n) have the same mass, thus $p^2 = p'^2 = m_\mathcal{N}^2$. In this limit, the matrix element is also invariant under another discrete symmetry called G-parity, which can be defined as a product of P, T, and a 180 degrees isospin rotation. Given the relativistic matrix elements, it will be straightforward to take the non-relativistic limit where $\boldsymbol{p}$ and $\boldsymbol{p}'$ are much smaller than the nucleon mass, and by this means to determine the most general form of the non-relativistic matrix elements used in our analysis.

A.1 Spin-J representation matrices

We first introduce the spin-J representation matrices $\mathcal{T}_{(J)}^k$, which appear in nuclear matrix elements at the leading and subleading order of recoil expansion. It is convenient to define them in terms of the Clebsch-Gordan coefficients. The latter are denoted by $C(J_1, m_1; J_2, m_2; J, m)$ and defined by $|J, m\rangle = \sum_{m_i=-J_i}^{J_i} C(J_1, m_1; J_2, m_2; J, m) |J_1, m_1\rangle \otimes |J_2, m_2\rangle$ with the Condon-Shortley phase conventions. We can define the $(2J+1) \times (2J+1)$-dimensional matrices $\mathcal{T}_{(J)}^k$ as follows

$$
\begin{aligned}
[\mathcal{T}_{(J)}^1]_{J_z'}^{J_z} &\equiv -\sqrt{\frac{J(J+1)}{2}} \Big[C(J, J_z; 1, 1; J, J_z') - C(J, J_z; 1, -1; J, J_z') \Big], \\
[\mathcal{T}_{(J)}^2]_{J_z'}^{J_z} &\equiv i\sqrt{\frac{J(J+1)}{2}} \Big[C(J, J_z; 1, 1; J, J_z') + C(J, J_z; 1, -1; J, J_z') \Big], \\
[\mathcal{T}_{(J)}^3]_{J_z'}^{J_z} &\equiv \sqrt{J(J+1)}\, C(J, J_z; 1, 0; J, J_z').
\end{aligned}
\tag{A.2}
$$

These are the familiar spin-J generators of the SO(3) Lie algebra, normalized such that $\mathcal{T}_{(J)}^3 = \mathrm{diag}(J, J-1, \ldots, -J)$.[19] In particular $\mathcal{T}_{(0)}^k = 0$, $\mathcal{T}_{(1/2)}^k = \sigma^k/2$, and

$$
\mathcal{T}_{(1)}^1 = \begin{pmatrix} 0 & \frac{1}{\sqrt{2}} & 0 \\ \frac{1}{\sqrt{2}} & 0 & \frac{1}{\sqrt{2}} \\ 0 & \frac{1}{\sqrt{2}} & 0 \end{pmatrix}, \quad \mathcal{T}_{(1)}^2 = \begin{pmatrix} 0 & -\frac{i}{\sqrt{2}} & 0 \\ \frac{i}{\sqrt{2}} & 0 & -\frac{i}{\sqrt{2}} \\ 0 & \frac{i}{\sqrt{2}} & 0 \end{pmatrix}, \quad \mathcal{T}_{(1)}^3 = \begin{pmatrix} 1 & 0 & 0 \\ 0 & 0 & 0 \\ 0 & 0 & -1 \end{pmatrix}.
\tag{A.3}
$$

One property of the $\mathcal{T}_{(J)}^{1,2}$ matrices is that, for any J, the only non-zero entries are those with $|J_z - J_z'| = 1$. For $J \geq 1$ we can also define the 2-index Hermitian and traceless matrices:

$$
\mathcal{T}_{(J)}^{kl} \equiv \mathcal{T}_{(J)}^k \mathcal{T}_{(J)}^l + \mathcal{T}_{(J)}^l \mathcal{T}_{(J)}^k - \frac{2}{2J+1} \mathrm{Tr}[\mathcal{T}_{(J)}^k \mathcal{T}_{(J)}^l] \mathbf{1}_{2J+1}.
\tag{A.4}
$$

These can appear in nuclear matrix elements at the subleading order in recoil expansion, and have non-zero entries for $|J_z - J_z'| \leq 2$. The matrices $\mathcal{T}_{(J)}^k$ and $\mathcal{T}_{(J)}^{kl}$ satisfy the useful

---

[19]In our conventions the rows (columns) of $\mathcal{T}_{(J)}$ correspond to J_z' (J_z) going from $+J$ to $-J$.

sum rules (for any value of J_z):

$$\sum_{J'_z=-J}^{J} [\mathcal{T}^{k}_{(J)}]^{J_z}_{J'_z}\delta_{J'_z J_z} = J^k,$$

$$\sum_{J'_z=-J}^{J} [\mathcal{T}^{k}_{(J)}]^{J_z}_{J'_z}[\mathcal{T}^{l*}_{(J)}]^{J_z}_{J'_z} = \frac{J(J+1)}{3}\delta^{kl} + \frac{J(J+1)-3(\boldsymbol{Jj})^2}{6}(\delta^{kl}-3j^k j^l) - \frac{i}{2}\epsilon^{klr}J^r,$$

$$\sum_{J'_z=-J}^{J} [\mathcal{T}^{kl}_{(J)}]^{J_z}_{J'_z}\delta_{J'_z J_z} = \frac{J(J+1)-3(\boldsymbol{Jj})^2}{3}(\delta^{kl}-3j^k j^l),$$

$$\sum_{J'_z=-J}^{J} [\mathcal{T}^{kl}_{(J)}]^{J_z}_{J'_z}[\mathcal{T}^{j*}_{(J)}]^{J_z}_{J'_z} = \frac{(2J+3)(2J-1)}{6}(\delta^{jk}J^l+\delta^{jl}J^k) - J^j(4J^k J^l - j^k j^l)$$

$$+ \frac{J(J+1)-3(\boldsymbol{Jj})^2}{3}\Big[(\delta^{kl}-3j^k j^l)J^j + (\delta^{kj}-3j^k j^j)J^l + (\delta^{lj}-3j^j j^l)J^k\Big]$$

$$+ i\frac{3}{2}\Big[\epsilon^{jkn}J^l+\epsilon^{jln}J^k\Big]J^n - i\frac{J(J+1)}{2}\Big[\epsilon^{jkn}j^l+\epsilon^{jln}j^k\Big]j^n. \tag{A.5}$$

A.2 Spinor conventions

We will express relativistic nuclear matrix elements in terms of commuting spinor variables using the formalism introduced in ref. [59]. Here we provide a lightning review of this formalism.

Let us first define our conventions for the 2-component spinor algebra. We work in four dimensions with the mostly-minus metric $\eta_{\mu\nu} = \mathrm{diag}(1,-1,-1,-1)$. The Lorentz algebra can be decomposed into $\mathrm{SL}(2,\mathbb{C})\times\mathrm{SL}(2,\mathbb{C})$. Holomorphic and anti-holomorphic spinors χ_α and $\tilde{\chi}_{\dot\alpha}$, $\alpha=1,2$, transform under the respective $\mathrm{SL}(2,\mathbb{C})$ factors with indices being raised and lowered by the antisymmetric epsilon tensor:

$$\chi^\alpha = \epsilon^{\alpha\beta}\chi_\beta, \quad \chi_\alpha = \epsilon_{\alpha\beta}\chi^\beta, \qquad \tilde{\chi}^{\dot\alpha} = \epsilon^{\dot\alpha\dot\beta}\tilde{\chi}_{\dot\beta}, \quad \tilde{\chi}_{\dot\alpha} = \epsilon_{\dot\alpha\dot\beta}\tilde{\chi}^{\dot\beta}, \tag{A.6}$$

where summing over repeated spinor indices is implicit, and we use the convention $\epsilon^{12}=1$, $\epsilon_{12}=-1$. One can construct Lorentz invariants from two holomorphic or two anti-holomorphic spinors: $\chi\psi \equiv \chi^\alpha\psi_\alpha$, $\tilde{\chi}\tilde{\psi} \equiv \tilde{\chi}_{\dot\alpha}\tilde{\psi}^{\dot\alpha}$. Furthermore, spinor indices can be traded for the vector ones with the help of the sigma matrices: $[\sigma^\mu]_{\alpha\dot\beta} = (\mathbb{I},\boldsymbol{\sigma})$ and $[\bar{\sigma}^\mu]^{\dot\alpha\beta} = (\mathbb{I},-\boldsymbol{\sigma})$, where $\boldsymbol{\sigma}$ are the usual Pauli matrices. For example, $\chi\sigma^\mu\tilde{\psi} \equiv \chi^\alpha[\sigma^\mu]_{\alpha\dot\beta}\tilde{\psi}^{\dot\beta}$ and $\tilde{\chi}\bar{\sigma}^\mu\psi \equiv \tilde{\chi}_{\dot\alpha}[\bar{\sigma}^\mu]^{\dot\alpha\beta}\psi_\beta$ both transform as Lorentz vectors. In the 2-component context we also define $\sigma^{\mu\nu} \equiv \frac{i}{2}(\sigma^\mu\bar{\sigma}^\nu - \sigma^\nu\bar{\sigma}^\mu)$ and $\bar{\sigma}^{\mu\nu} \equiv \frac{i}{2}(\bar{\sigma}^\mu\sigma^\nu - \bar{\sigma}^\nu\sigma^\mu)$, using which one can construct Lorentz tensors $\chi\sigma^{\mu\nu}\psi$ and $\tilde{\chi}\bar{\sigma}^{\mu\nu}\tilde{\psi}$.

Consider now a massive particle whose (four-)momentum p satisfies the on-shell condition $p^2 = m^2$. We treat p as incoming momentum, thus $p^0 > 0$ for initial state particles, and $p^0 < 0$ for final state particles. The momentum can be equivalently represented by four *commuting* two-component spinors χ^K and $\tilde{\chi}_K$, where $K = 1,2$:

$$[p_\mu\sigma^\mu]_{\alpha\dot\beta} = \sum_{K=1}^{2} \chi^K_\alpha\tilde{\chi}_{\dot\beta K}, \qquad (p\bar{\sigma})^{\dot\alpha\beta} = \sum_{K=1}^{2} \tilde{\chi}^{\dot\alpha}_K\chi^{\beta K}. \tag{A.7}$$

In our conventions the spinors are normalized as

$$(\chi^K\chi_L) = \delta^K_L m, \qquad (\tilde{\chi}_K\tilde{\chi}^L) = \delta^L_K m. \tag{A.8}$$

It follows that they satisfy the Dirac equation:

$$(p_\mu \sigma^\mu)\tilde{\chi}^K = m\chi^K\,, \quad (p_\mu \bar{\sigma}^\mu)\chi^K = m\tilde{\chi}^K\,, \quad \chi^K(p_\mu \sigma^\mu) = -m\tilde{\chi}^K\,, \quad \tilde{\chi}^K(p_\mu \bar{\sigma}^\mu) = -m\chi^K\,. \tag{A.9}$$

eqs. (A.7) and (A.8) are invariant under the SU(2) little group rotation of the spinors: $\chi^K \to [U]^K_L \chi^L$, $\chi_K \to \chi_L [U^\dagger]^L_K$, $\chi_K \to [U^*]^L_K \chi_L$. where from now on summation over repeated little group indices is implicit. In complete analogy to spinor indices, the little group indices can be raised and lowered by the epsilon tensor: $\chi_K = \epsilon_{KL}\chi^L$, etc. For a real momentum p the spinors χ and $\tilde{\chi}$ are related by complex conjugation. For an initial-state particle (positive p^0) we have

$$(\chi^K_\alpha)^* = \tilde{\chi}_{\dot{\alpha}\,K}\,, \quad (\tilde{\chi}_{\dot{\alpha}\,K})^* = \chi^K_\alpha\,, \quad (\tilde{\chi}^K_{\dot{\alpha}})^* = -\chi_{\alpha\,K}\,, \quad (\chi_{\alpha\,K})^* = -\tilde{\chi}^K_{\dot{\alpha}}\,, \tag{A.10}$$

while for a final-state particle (negative p^0) the signs on the right-hand sides of eq. (A.10) are reversed.

Let us parametrize particle's 3-momentum as $\boldsymbol{p} = |p|\boldsymbol{n}$, where $\boldsymbol{n} \equiv (\sin\theta\cos\phi, \sin\theta\sin\phi, \cos\theta)$ is the unit 3-vector in the direction of motion. A convenient representation of the corresponding spinors is

$$\chi^K = \frac{\sqrt{E_p + |p|} + \sqrt{E_p - |p|}}{2}\eta^K + \frac{\sqrt{E_p + |p|} - \sqrt{E_p - |p|}}{2}\zeta^K\,,$$

$$\tilde{\chi}^K = \pm\frac{\sqrt{E_p + |p|} + \sqrt{E_p - |p|}}{2}\tilde{\eta}^K \pm \frac{\sqrt{E_p + |p|} - \sqrt{E_p - |p|}}{2}\tilde{\zeta}^K\,, \tag{A.11}$$

where $E_p = \sqrt{|p|^2 + m^2}$, the upper (lower) sign refers to an initial- (final-) state particle, and we introduced

$$\eta^K_\alpha \equiv \delta^K_\alpha\,, \qquad \zeta^{K=1}_\alpha \equiv \begin{pmatrix} -\cos\theta \\ -e^{i\phi}\sin\theta \end{pmatrix}\,, \quad \zeta^{K=2}_\alpha \equiv \begin{pmatrix} -e^{-i\phi}\sin\theta \\ \cos\theta \end{pmatrix}\,. \tag{A.12}$$

The representation of eq. (A.11) is particularly useful in the non-relativistic limit, because the small-velocity expansion is the same as the expansion in powers of ζ's.

Lorentz invariance implies that an amplitude describing scattering of n massive particles with spins J_i, $i = 1\ldots n$ must be a scalar function of the relevant momenta p^μ_i and spinors χ_i, $\tilde{\chi}_i$. Moreover, little group covariance requires that the amplitude contains exactly $2J_i$ of the spinors χ_i or $\tilde{\chi}_i$ with uncontracted little group indices (spinors with contracted little group indices can be traded for momenta using eq. (A.7)). Initial-state particles will be represented by spinors with raised little group indices, $\chi^{K_j}_i$ or $\tilde{\chi}^{K_j}_i$, $j = 1\ldots 2J_i$, while final-state particles will be represented by spinors with lowered little group indices, $\chi_{i\,L_j}$, $\tilde{\chi}_{i\,L_j}$. The little group indices corresponding to the same particle are always implicitly symmetrized. To reduce clutter, the little group indices are often omitted whenever it does not lead to ambiguities.

In the representation of eq. (A.11), the little group index of a spinor or a twiddle spinor corresponds to the projection of particle's polarization J_z on the z-axis. For example, an initial-state spin 1/2 particle with polarization $J_z = +1/2$ is represented by $\chi^{K=1}$, and $J_z = -1/2$ is represented by $\chi^{K=2}$. Likewise, for a final-state particle we use $\chi_{L=1}$ for $J_z = +1/2$, and $\chi_{L=2}$ for $J_z = -1/2$. For an initial-state spin-1, a pair $(\chi^{K=1}, \chi^{K=1})$

	$\bar{p}\gamma^\mu n$	$\bar{p}\gamma^\mu\gamma_5 n$	$\bar{p}\sigma^{\mu\nu} n$
η_Γ^P	$(-)^\mu$	$-(-)^\mu$	$(-)^\mu(-1)^\nu$
η_Γ^T	$(-)^\mu$	$(-)^\mu$	$-(-)^\mu(-)^\nu$
η_Γ^{PT}	$+1$	-1	-1

Table 4. Transformation properties of the nucleon currents under parity and time reversal. We define $(-)^{\mu=0} \equiv 1$ and $(-)^{\mu=1,2,3} \equiv -1$.

represents $J_z = +1$, a pair $(\chi^{K=1}, \chi^{K=2})$ represents $J_z = 0$ (after symmetrizing the little group index), and $(\chi^{K=2}, \chi^{K=2})$ represents $J_z = -1$. And so on. Other spin quantization axes can be obtained from eq. (A.11) by appropriate little group rotations, e.g. the helicity representation is obtained using the SU(2) rotation matrix $U = \begin{pmatrix} \cos\frac{\theta}{2} & e^{i\phi}\sin\frac{\theta}{2} \\ -e^{-i\phi}\sin\frac{\theta}{2} & \cos\frac{\theta}{2} \end{pmatrix}$.

A.3 Discrete symmetries

The spinor formalism allows for a transparent description of the discrete symmetries corresponding to the parity ($\boldsymbol{x} \to -\boldsymbol{x}$) and time reversal ($t \to -t$) invariance of the strong interactions. The matrix element in eq. (A.1) can be expressed as a functional F of the momenta p^μ, p'^μ and of the spinor variables χ_1, χ_2 associated with these momenta. Parity and time reversal invariance can be re-formulated as constraints on the functional F. In the discussion below, we will always assume that $\mathcal{N}$ and $\mathcal{N}'$ transform in the same way under parity and time reversal (in particular, they are both parity-even, or both parity-odd).

The relevant nucleon bi-linears transform under the unitary Hilbert space parity operator $\mathcal{P}$ as $\mathcal{P}[\bar{p}\Gamma n(t, \boldsymbol{x})]\mathcal{P}^{-1} = \eta_\Gamma^P \bar{p}\Gamma n(t, -\boldsymbol{x})$, where the values of η_Γ^P are collected in table 4. Then, parity conservation implies that $F \xrightarrow{P} \eta_\Gamma^P F$ under the following transformation P of the spinors and momenta:

$$\chi_{1\alpha} \overset{P}{\leftrightarrow} \tilde{\chi}_1^{\dot\alpha}, \qquad \chi_1^\alpha \overset{P}{\leftrightarrow} -\tilde{\chi}_{1\dot\alpha}, \qquad \chi_{2\alpha} \overset{P}{\leftrightarrow} -\tilde{\chi}_2^{\dot\alpha}, \qquad \chi_2^\alpha \overset{P}{\leftrightarrow} \tilde{\chi}_{2\dot\alpha},$$
$$P^\mu \xrightarrow{P} (-)^\mu P^\mu, \qquad q^\mu \xrightarrow{P} (-)^\mu q^\mu, \tag{A.13}$$

where $P^\mu = p^\mu + p'^\mu$, $q^\mu = p^\mu - p'^\mu$, $(-)^{\mu=0} \equiv 1$, $(-)^{\mu=1,2,3} \equiv -1$, and the sign difference between χ_1 and χ_2 transformations is due to the former (latter) corresponding to an initial- (final-) state particle. Little group indices are not displayed in eq. (A.13), but implicitly they always match, that is $\chi^K \overset{P}{\leftrightarrow} \tilde{\chi}^K$, and $\chi_K \overset{P}{\leftrightarrow} \tilde{\chi}_K$. It follows for example that $\chi_1\chi_2 \pm \tilde{\chi}_1\tilde{\chi}_2$ transforms under P into $\pm$ itself, while $\chi_1\sigma^\mu\tilde{\chi}_2 \xrightarrow{P} (-)^\mu\chi_2\sigma^\mu\tilde{\chi}_1$.

For the anti-unitary Hilbert space time-reversal operator $\mathcal{T}$, the action on the nucleon bi-linears is $\mathcal{T}[\bar{p}\Gamma n(t, \boldsymbol{x})]\mathcal{T}^{-1} = \eta_\Gamma^T \bar{p}\Gamma n(-t, \boldsymbol{x})$, see table 4. Time reversal implies that $F \xrightarrow{T} \eta_\Gamma^T F^*$ under the following transformation T of the spinors and momenta:

$$\chi_{i\alpha} \xrightarrow{T} [\chi_i^\alpha]^*, \quad \chi_i^\alpha \xrightarrow{T} -[\chi_{i\alpha}]^*, \qquad \tilde{\chi}_{i\dot\alpha} \xrightarrow{T} [\tilde{\chi}_i^{\dot\alpha}]^*, \quad \tilde{\chi}_i^{\dot\alpha} \xrightarrow{T} -[\tilde{\chi}_{i\dot\alpha}]^*,$$
$$P^\mu \xrightarrow{T} (-)^\mu P^\mu, \qquad q^\mu \xrightarrow{T} (-)^\mu q^\mu, \tag{A.14}$$

for $i = 1, 2$, and again the matching little group indices are implicit. It follows for example that both $[\chi_1\chi_2]^*$ and $[\tilde{\chi}_1\tilde{\chi}_2]^*$ transform into their complex conjugates under T, while $[\chi_1\sigma^\mu\tilde{\chi}_2]^* \xrightarrow{T} (-)^\mu\chi_1\sigma^\mu\tilde{\chi}_2$.

Finally, we define G-parity as $\mathcal{G} = e^{i\pi\tau^2}\mathcal{T}\mathcal{P}$, where $e^{i\pi\tau^2}$ is the 180 degrees isospin rotation transforming $(p,n) \to (-n,p)$ and $(\mathcal{N}, \mathcal{N}') \to (\mp\mathcal{N}', \pm\mathcal{N})$. Isospin invariance implies that $F \overset{G}{\to} \eta_\Gamma^{PT} F$ under the following transformation G of the spinors and momenta:

$$\begin{pmatrix} \chi_1^K \\ \chi_{2L} \\ \tilde{\chi}_1^K \\ \tilde{\chi}_{2L} \end{pmatrix} \overset{G}{\to} \begin{pmatrix} -\chi_{2L} \\ \chi_1^K \\ \tilde{\chi}_{2L} \\ -\tilde{\chi}_1^K \end{pmatrix}, \qquad P^\mu \overset{G}{\to} P^\mu, \quad q^\mu \overset{G}{\to} -q^\mu. \tag{A.15}$$

It follows for example that both $\chi_1\chi_2$ and $\tilde{\chi}_1\tilde{\chi}_2$ transform into itself under G, while $\chi_1\sigma^\mu\tilde{\chi}_2 \overset{G}{\to} \chi_2\sigma^\mu\tilde{\chi}_1$.

A.4 Relativistic matrix elements

Using the spinor formalism, the most general form of the relativistic nuclear matrix elements in eq. (A.1) consistent with Lorentz, parity, time reversal, and G-parity invariance is

$$\langle\mathcal{N}'|\bar{p}\gamma^\mu n|\mathcal{N}\rangle = \frac{\alpha_V}{(2m_\mathcal{N})^{2J}}\big(\chi_1\chi_2 + \tilde{\chi}_1\tilde{\chi}_2\big)^{2J}P^\mu + \frac{\beta_V}{(2m_\mathcal{N})^{2J-1}}\big(\chi_1\chi_2 + \tilde{\chi}_1\tilde{\chi}_2\big)^{2J-1}\big(\chi_1\sigma^\mu\tilde{\chi}_2 + \chi_2\sigma^\mu\tilde{\chi}_1\big) + \dots$$

$$\langle\mathcal{N}'|\bar{p}\gamma^\mu\gamma_5 n|\mathcal{N}\rangle = \frac{\beta_A}{(2m_\mathcal{N})^{2J-1}}\big(\chi_1\chi_2 + \tilde{\chi}_1\tilde{\chi}_2\big)^{2J-1}\big(\chi_1\sigma^\mu\tilde{\chi}_2 - \chi_2\sigma^\mu\tilde{\chi}_1\big) + \dots$$

$$\langle\mathcal{N}'|\bar{p}\sigma^{\mu\nu} n|\mathcal{N}\rangle = i\frac{\alpha_T}{(2m_\mathcal{N})^{2J+1}}\big(\chi_1\chi_2 + \tilde{\chi}_1\tilde{\chi}_2\big)^{2J}(P^\mu q^\nu - P^\nu q^\mu)$$
$$+ \frac{\beta_T}{(2m_\mathcal{N})^{2J-1}}\big(\chi_1\chi_2 + \tilde{\chi}_1\tilde{\chi}_2\big)^{2J-1}\big(\chi_1\sigma^{\mu\nu}\chi_2 + \tilde{\chi}_1\bar{\sigma}^{\mu\nu}\tilde{\chi}_2\big)$$
$$+ i\frac{\gamma_T}{(2m_\mathcal{N})^{2J}}\big(\chi_1\chi_2 + \tilde{\chi}_1\tilde{\chi}_2\big)^{2J-2}\big(\chi_1\chi_2 - \tilde{\chi}_1\tilde{\chi}_2\big)\bigg[\big(\chi_1\sigma^\mu\tilde{\chi}_2 - \chi_2\sigma^\mu\tilde{\chi}_1\big)P^\nu - (\mu\leftrightarrow\nu)\bigg]$$
$$+ \dots \tag{A.16}$$

Above, the dots stand for terms leading to effects that are quadratic or higher order in recoil; e.g. in the axial matrix element we have $\big(\chi_1\chi_2 + \tilde{\chi}_1\tilde{\chi}_2\big)^{2J-3}\big(\chi_1\chi_2 - \tilde{\chi}_1\tilde{\chi}_2\big)^2\big(\chi_1\sigma^\mu\tilde{\chi}_2 - \chi_2\sigma^\mu\tilde{\chi}_1\big)$, $\big(\chi_1\chi_2 + \tilde{\chi}_1\tilde{\chi}_2\big)^{2J-5}\big(\chi_1\chi_2 - \tilde{\chi}_1\tilde{\chi}_2\big)^4\big(\chi_1\sigma^\mu\tilde{\chi}_2 - \chi_2\sigma^\mu\tilde{\chi}_1\big)$, and so on. Other similar terms in the axial matrix element, e.g. $\big(\chi_1\chi_2 + \tilde{\chi}_1\tilde{\chi}_2\big)^{2J-2}\big(\chi_1\chi_2 - \tilde{\chi}_1\tilde{\chi}_2\big)\big(\chi_1\sigma^\mu\tilde{\chi}_2 - \chi_2\sigma^\mu\tilde{\chi}_1\big)$ or $\big(\chi_1\chi_2 + \tilde{\chi}_1\tilde{\chi}_2\big)^{2J-1}\big(\chi_1\sigma^\mu\tilde{\chi}_2 + \chi_2\sigma^\mu\tilde{\chi}_1\big)$ are forbidden by parity invariance. The form factors $\alpha_{V,T}$, $\beta_{V,A,T}$, γ_T are in principle functions of q^2, but for our purpose they can be treated as constants. Time reversal invariance dictates that these form factors are all real. Eq. (A.16) is valid for any integer $2J \geq 0$ with the convention that whenever a naive evaluation of some term leads to spinors in a denominator then this term should be set to zero. In particular, for $J = 0$ only the $\alpha_{V,T}$ structures survive, while for $J = 1/2$ the γ_T term should be set to zero.

As we discussed, eq. (A.16) is obtained in the isospin limit, and in particular it does not contain G-parity-odd terms. These "second-class currents" in the nomenclature of Weinberg [14] are often considered in the literature, and searched for in many experiments. For completeness, we list here the G-parity-odd contributions to the relativistic vector, axial, and tensor matrix elements that lead to effects of linear order in recoil:

$$\Delta\langle\mathcal{N}'|\bar{p}\gamma^\mu n|\mathcal{N}\rangle = \frac{\alpha_V'}{(2m_\mathcal{N})^{2J}}\big(\chi_1\chi_2 + \tilde{\chi}_1\tilde{\chi}_2\big)^{2J}q^\mu$$
$$+ \frac{\beta_V'}{(2m_\mathcal{N})^{2J-1}}\big(\chi_1\chi_2 + \tilde{\chi}_1\tilde{\chi}_2\big)^{2J-2}\big(\chi_1\chi_2 - \tilde{\chi}_1\tilde{\chi}_2\big)\big(\chi_1\sigma^\mu\tilde{\chi}_2 - \chi_2\sigma^\mu\tilde{\chi}_1\big),$$

$$\Delta \langle \mathcal{N}'| \bar{p}\gamma^\mu \gamma_5 n |\mathcal{N}\rangle = \frac{\alpha'_A}{(2m_\mathcal{N})^{2J}}(\chi_1\chi_2 + \tilde{\chi}_1\tilde{\chi}_2)^{2J-1}(\chi_1\chi_2 - \tilde{\chi}_1\tilde{\chi}_2)P^\mu,$$

$$\Delta \langle \mathcal{N}'| \bar{p}\sigma^{\mu\nu} n |\mathcal{N}\rangle = i\frac{\alpha'_T}{(2m_\mathcal{N})^{2J}}(\chi_1\chi_2 + \tilde{\chi}_1\tilde{\chi}_2)^{2J-1}\left[(\chi_1\sigma^\mu\tilde{\chi}_2 + \chi_2\sigma^\mu\tilde{\chi}_1)P^\nu - (\mu \leftrightarrow \nu)\right].$$
$$(A.17)$$

A.5 Non-relativistic limit

We now take the non-relativistic limit of eq. (A.16). On the right-hand side, using the $|p| \to 0$ limit of the representation in eq. (A.11), we find the following approximations:

$$\big(\chi_1\chi_2 + \tilde{\chi}_1\tilde{\chi}_2\big)^{2J} \approx (2m_\mathcal{N})^{2J}\delta^{J_z}_{J'_z},$$

$$\big(\chi_1\chi_2 + \tilde{\chi}_1\tilde{\chi}_2\big)^{2J-1}\big(\chi_1\chi_2 - \tilde{\chi}_1\tilde{\chi}_2\big) \approx -\frac{(2m_\mathcal{N})^{2J-1}}{J}q^m[\mathcal{T}^m_{(J)}]^{J_z}_{J'_z}, \tag{A.18}$$

$$\big(\chi_1\chi_2 + \tilde{\chi}_1\tilde{\chi}_2\big)^{2J-1}\big(\chi_1\sigma^0\tilde{\chi}_2 + \chi_2\sigma^0\tilde{\chi}_1\big) \approx -(2m_\mathcal{N})^{2J}\delta^{J_z}_{J'_z},$$

$$\big(\chi_1\chi_2 + \tilde{\chi}_1\tilde{\chi}_2\big)^{2J-1}\big(\chi_1\sigma^k\tilde{\chi}_2 + \chi_2\sigma^k\tilde{\chi}_1\big) \approx -(2m_\mathcal{N})^{2J-1}\left(P^k\delta^{J_z}_{J'_z} + \frac{i}{J}\epsilon^{klm}q^l[\mathcal{T}^m_{(J)}]^{J_z}_{J'_z}\right), \tag{A.19}$$

$$\big(\chi_1\chi_2 + \tilde{\chi}_1\tilde{\chi}_2\big)^{2J-1}\big(\chi_1\sigma^0\tilde{\chi}_2 - \chi_2\sigma^0\tilde{\chi}_1\big) \approx \frac{(2m_\mathcal{N})^{2J-1}}{J}P^l[\mathcal{T}^l_{(J)}]^{J_z}_{J'_z},$$

$$\big(\chi_1\chi_2 + \tilde{\chi}_1\tilde{\chi}_2\big)^{2J-1}\big(\chi_1\sigma^k\tilde{\chi}_2 - \chi_2\sigma^k\tilde{\chi}_1\big) \approx \frac{(2m_\mathcal{N})^{2J}}{J}[\mathcal{T}^k_{(J)}]^{J_z}_{J'_z}, \tag{A.20}$$

$$\big(\chi_1\chi_2 + \tilde{\chi}_1\tilde{\chi}_2\big)^{2J-1}\big(\chi_1\sigma^{0k}\chi_2 + \tilde{\chi}_1\bar{\sigma}^{0k}\tilde{\chi}_2\big) \approx (2m_\mathcal{N})^{2J-1}\left[-iq^k\delta^{J_z}_{J'_z} + \frac{1}{J}\epsilon^{klm}P^l[\mathcal{T}^m_{(J)}]^{J_z}_{J'_z}\right],$$

$$\big(\chi_1\chi_2 + \tilde{\chi}_1\tilde{\chi}_2\big)^{2J-1}\big(\chi_1\sigma^{ij}\chi_2 + \tilde{\chi}_1\bar{\sigma}^{ij}\tilde{\chi}_2\big) \approx -\frac{(2m_\mathcal{N})^{2J}}{J}\epsilon^{ijm}[\mathcal{T}^m_{(J)}]^{J_z}_{J'_z}, \tag{A.21}$$

$$\big(\chi_1\chi_2 + \tilde{\chi}_1\tilde{\chi}_2\big)^{2J-2}\big(\chi_1\chi_2 - \tilde{\chi}_1\tilde{\chi}_2\big)\big(\chi_1\sigma^0\tilde{\chi}_2 - \chi_2\sigma^0\tilde{\chi}_1\big) \approx 0,$$

$$\big(\chi_1\chi_2 + \tilde{\chi}_1\tilde{\chi}_2\big)^{2J-2}\big(\chi_1\chi_2 - \tilde{\chi}_1\tilde{\chi}_2\big)\big(\chi_1\sigma^k\tilde{\chi}_2 - \chi_2\sigma^k\tilde{\chi}_1\big) \approx -(2m_\mathcal{N})^{2J-1}\left[\frac{1}{3}q^k\delta^{J_z}_{J'_z} + \frac{1}{J(2J-1)}q^l[\mathcal{T}^{kl}_{(J)}]^{J_z}_{J'_z}\right], \tag{A.22}$$

up to quadratic terms in recoil. On the left-hand side of eq. (A.16) we trade the relativistic nucleon fields N for their non-relativistic counterparts ψ_N. To this end, working in the isospin limit, we make the following replacement of the left- and right-handed components of N:

$$N = \begin{pmatrix} N_{L\,\alpha} \\ N_R^{\dot{\alpha}} \end{pmatrix} \to \frac{1}{\sqrt{2}}\begin{pmatrix} \left[1 + i\frac{\boldsymbol{\sigma}\cdot\boldsymbol{\nabla}}{2m_N}\right]_{\alpha\beta}\psi_{N\,\beta} \\ \left[1 - i\frac{\boldsymbol{\sigma}\cdot\boldsymbol{\nabla}}{2m_N}\right]_{\alpha\beta}\psi_{N\,\beta} \end{pmatrix}, \tag{A.23}$$

where $\alpha = 1, 2$ is the spinor index. Here, ψ_N are 2-component anti-commuting spinor fields containing only particle (and no anti-particle) modes. The rationale for this substitution is that, up to quadratic terms in $\boldsymbol{\nabla}/m_N$, the equation of motion for ψ_N is the Schrödinger equation, and the kinetic terms of particle and anti-particle modes are decoupled. Up to $\mathcal{O}(\boldsymbol{\nabla}^2/m_N^2)$ corrections, one can derive the following non-relativistic approximations for the relativistic nucleon bi-linear currents:

$$\bar{p}\gamma^0 n = \psi_p^\dagger \psi_n,$$

$$\bar{p}\gamma^k n = -\frac{i}{2m_N}\left[\psi_p^\dagger \overset{\leftrightarrow}{\nabla}_k \psi_n + i\epsilon^{klm}\nabla_l[\psi_p^\dagger \sigma^m \psi_n]\right], \tag{A.24}$$

$$\bar{p}\gamma^0\gamma_5 n = -\frac{i}{2m_N}[\psi_p^\dagger\boldsymbol{\sigma}\cdot\overleftrightarrow{\boldsymbol{\nabla}}\psi_n],$$
$$\bar{p}\gamma^k\gamma_5 n = \psi_p^\dagger\sigma^k\psi_n, \tag{A.25}$$

$$\bar{p}\sigma^{0k}n = \frac{1}{2m_N}\Big[\nabla_k[\psi_p^\dagger\psi_n] + i\epsilon^{klm}\psi_p^\dagger\sigma^m\overleftrightarrow{\nabla}_l\psi_n\Big],$$
$$\bar{p}\sigma^{ij}n = \epsilon^{ijk}\psi_p^\dagger\sigma^k\psi_n, \tag{A.26}$$

where $\psi^\dagger\Gamma\overleftrightarrow{\boldsymbol{\nabla}}\psi \equiv \psi^\dagger\Gamma\nabla\psi - \nabla\psi^\dagger\Gamma\psi$. Plugging this on the left-hand side of eq. (A.16) and disentagling the non-relativistic matrix elements, we obtain

$$\langle\psi_p^\dagger\psi_n\rangle = 2m_{\mathcal{N}}\delta_{J_z'}^{J_z}M_F,$$
$$\langle\psi_p^\dagger\sigma^k\psi_n\rangle = \frac{r}{\sqrt{J(J+1)}}2m_{\mathcal{N}}[\mathcal{T}_{(J)}^k]_{J_z'}^{J_z}M_F,$$
$$\frac{i}{2m_N}\langle\psi_p^\dagger\overleftrightarrow{\nabla}_k\psi_n\rangle = \Big\{-P^k\delta_{J_z'}^{J_z} - i\beta_{FV}\frac{rA}{\sqrt{J(J+1)}}\epsilon^{klm}q^l[\mathcal{T}_{(J)}^m]_{J_z'}^{J_z}\Big\}M_F,$$
$$\frac{i}{2m_N}\langle\psi_p^\dagger\boldsymbol{\sigma}\cdot\overleftrightarrow{\boldsymbol{\nabla}}\psi_n\rangle = -\frac{r}{\sqrt{J(J+1)}}P^k[\mathcal{T}_{(J)}^k]_{J_z'}^{J_z}M_F,$$
$$\frac{1}{2m_N}\epsilon^{klm}\langle\psi_p^\dagger\sigma^m\overleftrightarrow{\nabla}_l\psi_n\rangle = \Big\{i\frac{r}{\sqrt{J(J+1)}}\epsilon^{klm}P^l[\mathcal{T}_{(J)}^m]_{J_z'}^{J_z} + A\alpha_{FT}q^k\delta_{J_z'}^{J_z} + \gamma_{FT}\frac{Ar}{J\sqrt{J(J+1)}}q^l[\mathcal{T}_{(J)}^{kl}]_{J_z'}^{J_z}\Big\}M_F, \tag{A.27}$$

where the parameters M_F, β_{FV}, α_{FT}, γ_{FT} are related to the form factors in eq. (A.16) as

$$\alpha_V - \beta_V = M_F, \quad \beta_V = -rA\sqrt{\frac{J}{J+1}}\Big[\beta_{FV}+1\Big]M_F,$$
$$\beta_A = r\sqrt{\frac{J}{J+1}}M_F,$$
$$\alpha_T - \beta_T + \frac{\gamma_T}{3} = A(\alpha_{FT}+1)M_F, \quad \beta_T = -r\sqrt{\frac{J}{J+1}}M_F, \quad \gamma_T = r\frac{2J-1}{\sqrt{J(J+1)}}A\gamma_{FT}M_F. \tag{A.28}$$

B Subleading corrections to correlations

In this appendix we present the dependence of the correlations in the mixed Fermi-GT beta decay $(J'=J)$ on the Wilson coefficients of the subleading effective Lagrangian in eq. (2.10). To organize the presentation, each subsection below deals with the contribution of a single Wilson coefficient. The left-hand-sides refer to the correlation coefficients defined by eq. (3.6), and we recall the definition $\hat{\xi} \equiv |C_V^+|^2 + |C_S^+|^2 + r^2(|C_A^+|^2 + |C_T^+|^2)$. We are interested in $\mathcal{O}(\boldsymbol{q}/m_N)$ effects, that is linear order in recoil, which are suppressed by one power of the nucleon mass m_N or the nuclear mass $m_{\mathcal{N}}$. We neglect $\mathcal{O}(\boldsymbol{q}^2/m_N^2)$ and higher order effects, in particular we neglect the contributions quadratic in the Wilson coefficients of eq. (2.10). In expression containing $\pm$ or $\mp$, the upper (lower) sign refers to β^- (β^+) transitions. These results are new because they include the effects of subleading non-SM Wilson coefficients (C_P^+, C_{T1}^+, C_{T2}^+, C_{T3}^+, C_{FT}^+) at the linear order in recoil, as well as interference of the subleading Wilson coefficients with the non-SM leading order Wilson coefficients (C_S^+, C_T^+). If the SM

is the UV completion of our EFT, all these Wilson coefficients are zero (ignoring the tiny induced C_S^+), and moreover $C_{FA}^+ = C_A^+$, $C_{FV}^+ = C_V^+$, $C_{E'}^+ = C_E^+$.

Moreover, in appendix B.11 we also quote the results for another class of recoil corrections to the correlations. They appear because the recoil corrections to the phase space and the relativistic normalization of the nuclear states result in the overall factor $1 + \frac{3E_e - E_e^{\max}}{m_{\mathcal{N}}} - 3\frac{\boldsymbol{k}_e \cdot \boldsymbol{k}_\nu}{E_\nu m_{\mathcal{N}}} + \mathcal{O}(m_{\mathcal{N}}^{-2})$ multiplying the differential width. The contributions in appendix B.11 result from multiplying the $\mathcal{O}(m_{\mathcal{N}}^{-1})$ terms in this expression with the zero-th order correlations discussed in section 3.2. These effects are in fact relevant to establish the matching with the results in ref. [16].

B.1 C_P^+ Wilson coefficient

$$\mathcal{L}^{(1)} \supset \frac{iC_P^+}{2m_N}(\psi_p^\dagger \sigma^k \psi_n)\nabla_k(\bar{e}_R \nu_L). \tag{B.1}$$

$$\hat{\xi}\xi_b(E_e) = \frac{r^2}{3}\frac{1}{m_N}\left[\left(\frac{E_e^{\max}}{E_e}-1\right)m_e\mathrm{Re}\left(C_A^+\bar{C}_P^+\right)\pm\left(E_e^{\max}-2E_e+\frac{m_e^2}{E_e}\right)\mathrm{Re}\left(C_T^+\bar{C}_P^+\right)\right],$$

$$\hat{\xi}\Delta a(E_e) = \frac{r^2}{3}\frac{1}{m_N}\left[m_e\mathrm{Re}\left(C_A^+\bar{C}_P^+\right)\pm(2E_e-E_e^{\max})\mathrm{Re}\left(C_T^+\bar{C}_P^+\right)\right],$$

$$\hat{\xi}a'(E_e) = 0,$$

$$\hat{\xi}\Delta A(E_e) = \frac{1}{3m_N}\left[-3m_e r\sqrt{\frac{J}{J+1}}\mathrm{Re}\left(C_V^+\bar{C}_P^+\right)\pm r\sqrt{\frac{J}{J+1}}\left(E_e^{\max}-4E_e\right)\mathrm{Re}\left(C_S^+\bar{C}_P^+\right)\right.$$
$$\left.+(E_e^{\max}-E_e)\frac{r^2}{J+1}\mathrm{Re}\left(C_T^+\bar{C}_P^+\right)\right],$$

$$\hat{\xi}A'(E_e) = \frac{E_e}{2m_N}\left[\pm2r\sqrt{\frac{J}{J+1}}\mathrm{Re}\left(C_S^+\bar{C}_P^+\right)+\frac{r^2}{J+1}\mathrm{Re}\left(C_T^+\bar{C}_P^+\right)\right],$$

$$\hat{\xi}\Delta B(E_e) = \frac{1}{3m_N}\left[-3\left(\frac{E_e^{\max}}{E_e}-1\right)m_e r\sqrt{\frac{J}{J+1}}\mathrm{Re}\left(C_V^+\bar{C}_P^+\right)\right.$$
$$\left.\mp r\sqrt{\frac{J}{J+1}}\left(3E_e^{\max}-4E_e+\frac{m_e^2}{E_e}\right)\mathrm{Re}\left(C_S^+\bar{C}_P^+\right)-\frac{r^2}{J+1}\left(E_e-\frac{m_e^2}{E_e}\right)\mathrm{Re}\left(C_T^+\bar{C}_P^+\right)\right],$$

$$\hat{\xi}B'(E_e) = \frac{E_e^{\max}-E_e}{2m_N}\left[\pm2r\sqrt{\frac{J}{J+1}}\mathrm{Re}\left(C_S^+\bar{C}_P^+\right)-\frac{r^2}{J+1}\mathrm{Re}\left(C_T^+\bar{C}_P^+\right)\right],$$

$$\hat{\xi}\Delta D(E_e) = \frac{r^2}{J+1}\frac{1}{2m_N}\left[\mp m_e\mathrm{Im}\left(C_A^+\bar{C}_P^+\right)-E_e^{\max}\mathrm{Im}\left(C_T^+\bar{C}_P^+\right)\right],$$

$$\hat{\xi}D'(E_e) = 0,$$

$$\hat{\xi}\Delta\hat{c}(E_e) = \frac{r^2}{2}\frac{1}{m_N}\left[m_e\mathrm{Re}\left(C_A^+\bar{C}_P^+\right)\pm(2E_e-E_e^{\max})\mathrm{Re}\left(C_T^+\bar{C}_P^+\right)\right],$$

$$\hat{\xi}c'(E_e) = 0,$$

$$\hat{\xi}c_1(E_e) = \frac{r^2}{6} \frac{E_e^{\max} - E_e}{m_N} \left[\frac{m_e}{E_e} \mathrm{Re}\left(C_A^+ \bar{C}_P^+\right) \pm \mathrm{Re}\left(C_T^+ \bar{C}_P^+\right) \right],$$

$$\hat{\xi}c_2(E_e) = \mp \frac{r^2}{6} \frac{E_e}{m_N} \mathrm{Re}\left(C_T^+ \bar{C}_P^+\right),$$

$$\hat{\xi}c_3(E_e) = \mp \frac{r^2}{2} \frac{E_e^{\max} - E_e}{m_N} \mathrm{Im}\left(C_T^+ \bar{C}_P^+\right),$$

$$\hat{\xi}c_4(E_e) = \mp \frac{r^2}{2} \frac{E_e^{\max} - E_e}{m_N} \mathrm{Im}\left(C_T^+ \bar{C}_P^+\right). \tag{B.2}$$

B.2 C_M^+ Wilson coefficient

$$\mathcal{L}^{(1)} \supset -\frac{C_M^+}{2m_N} \epsilon^{ijk} (\psi_p^\dagger \sigma^j \psi_n) \nabla_i (\bar{e}_L \gamma^k \nu_L). \tag{B.3}$$

$$\hat{\xi}\xi_b(E_e) = \frac{2r^2}{3} \frac{1}{m_N} \left[\pm \left(E_e^{\max} - 2E_e + \frac{m_e^2}{E_e} \right) \mathrm{Re}\left(C_A^+ \bar{C}_M^+\right) + \left(\frac{E_e^{\max}}{E_e} - 1 \right) m_e \mathrm{Re}\left(C_T^+ \bar{C}_M^+\right) \right],$$

$$\hat{\xi}\Delta a(E_e) = \frac{2r^2}{3} \frac{1}{m_N} \left[\pm (2E_e - E_e^{\max}) \mathrm{Re}\left(C_A^+ \bar{C}_M^+\right) + m_e \mathrm{Re}\left(C_T^+ \bar{C}_M^+\right) \right],$$

$$\hat{\xi}a'(E_e) = 0,$$

$$\hat{\xi}\Delta A(E_e) = \frac{1}{m_N} \left[\mp \frac{2}{3} (E_e^{\max} - E_e) r \sqrt{\frac{J}{J+1}} \mathrm{Re}\left(C_V^+ \bar{C}_M^+\right) + \frac{r^2}{J+1} \left(\frac{5}{3} E_e - \frac{2}{3} E_e^{\max} \right) \mathrm{Re}\left(C_A^+ \bar{C}_M^+\right) \right.$$
$$\left. \pm m_e \frac{r^2}{J+1} \mathrm{Re}\left(C_T^+ \bar{C}_M^+\right) \right],$$

$$\hat{\xi}A'(E_e) = \frac{E_e}{m_N} \left[\mp r \sqrt{\frac{J}{J+1}} \mathrm{Re}\left(C_V^+ \bar{C}_M^+\right) - \frac{r^2}{2(J+1)} \mathrm{Re}\left(C_A^+ \bar{C}_M^+\right) \right],$$

$$\hat{\xi}\Delta B(E_e) = \frac{1}{m_N} \left[\pm \frac{2}{3} r \sqrt{\frac{J}{J+1}} \left(E_e - \frac{m_e^2}{E_e} \right) \mathrm{Re}\left(C_V^+ \bar{C}_M^+\right) \pm \frac{r^2}{J+1} \left(\frac{E_e^{\max}}{E_e} - 1 \right) m_e \mathrm{Re}\left(C_T^+ \bar{C}_M^+\right) \right.$$
$$\left. + \frac{r^2}{J+1} \left(E_e^{\max} - \frac{5}{3} E_e + \frac{2m_e^2}{3E_e} \right) \mathrm{Re}\left(C_A^+ \bar{C}_M^+\right) \right],$$

$$\hat{\xi}B'(E_e) = \frac{E_e^{\max} - E_e}{m_N} \left[\pm r \sqrt{\frac{J}{J+1}} \mathrm{Re}\left(C_V^+ \bar{C}_M^+\right) - \frac{r^2}{2(J+1)} \mathrm{Re}\left(C_A^+ \bar{C}_M^+\right) \right],$$

$$\hat{\xi}\Delta D(E_e) = \frac{1}{2m_N} \left[\pm 2r \sqrt{\frac{J}{J+1}} (2E_e - E_e^{\max}) \mathrm{Im}\left(C_V^+ \bar{C}_M^+\right) - \frac{r^2}{J+1} E_e^{\max} \mathrm{Im}\left(C_A^+ \bar{C}_M^+\right) \right.$$
$$\left. + 2m_e r \sqrt{\frac{J}{J+1}} \mathrm{Im}\left(C_S^+ \bar{C}_M^+\right) \mp m_e \frac{r^2}{J+1} \mathrm{Im}\left(C_T^+ \bar{C}_M^+\right) \right],$$

$$\hat{\xi}D'(E_e) = 0,$$

$$\hat{\xi}\Delta \hat{c}(E_e) = \frac{r^2}{2} \frac{1}{m_N} \left[\mp (2E_e - E_e^{\max}) \mathrm{Re}\left(C_A^+ \bar{C}_M^+\right) - m_e \mathrm{Re}\left(C_T^+ \bar{C}_M^+\right) \right],$$

$$\hat{\xi}c'(E_e) = 0,$$

$$\hat{\xi}c_1(E_e) = \frac{r^2}{6}\frac{E_e^{\max}-E_e}{m_N}\left[\mp\mathrm{Re}\left(C_A^+\bar{C}_M^+\right)-\frac{m_e}{E_e}\mathrm{Re}\left(C_T^+\bar{C}_M^+\right)\right],$$

$$\hat{\xi}c_2(E_e) = \pm\frac{r^2}{6}\frac{E_e}{m_N}\mathrm{Re}\left(C_A^+\bar{C}_M^+\right),$$

$$\hat{\xi}c_3(E_e) = \mp\frac{r^2}{2}\frac{E_e^{\max}-E_e}{m_N}\mathrm{Im}\left(C_A^+\bar{C}_M^+\right),$$

$$\hat{\xi}c_4(E_e) = \pm\frac{r^2}{2}\frac{E_e^{\max}-E_e}{m_N}\mathrm{Im}\left(C_A^+\bar{C}_M^+\right). \tag{B.4}$$

The contribution of another Wilson coefficient C_{FV}^+ multiplied by the form factor β_{FV} in eq. (3.4) is exactly the same as that of C_M^+. The joint effect can be described by replacing above $C_M^+ \to C_{WM}^+ \equiv C_M^+ + \beta_{FV}C_{FV}^+$.

B.3 C_E^+ Wilson coefficient

$$\mathcal{L}^{(1)} \supset -\frac{iC_E^+}{2m_N}(\psi_p^\dagger\sigma^k\psi_n)\nabla_k(\bar{e}_L\gamma^0\nu_L). \tag{B.5}$$

$$\hat{\xi}\xi_b(E_e) = \frac{r^2}{3}\frac{1}{m_N}\left[\mp\left(E_e^{\max}-\frac{m_e^2}{E_e}\right)\mathrm{Re}\left(C_A^+\bar{C}_E^+\right)-m_e\left(\frac{E_e^{\max}}{E_e}-1\right)\mathrm{Re}\left(C_T^+\bar{C}_E^+\right)\right],$$

$$\hat{\xi}\Delta a(E_e) = \frac{r^2}{3}\frac{1}{m_N}\left[\mp E_e^{\max}\mathrm{Re}\left(C_A^+\bar{C}_E^+\right)-m_e\mathrm{Re}\left(C_T^+\bar{C}_E^+\right)\right],$$

$$\hat{\xi}a'(E_e) = 0,$$

$$\hat{\xi}\Delta A(E_e) = \frac{1}{3m_N}\left[\pm r\sqrt{\frac{J}{J+1}}\left(E_e^{\max}+2E_e\right)\mathrm{Re}\left(C_V^+\bar{C}_E^+\right)+\left(E_e^{\max}-E_e\right)\frac{r^2}{J+1}\mathrm{Re}\left(C_A^+\bar{C}_E^+\right)\right.$$
$$\left.+3m_e r\sqrt{\frac{J}{J+1}}\mathrm{Re}\left(C_S^+\bar{C}_E^+\right)\right],$$

$$\hat{\xi}A'(E_e) = \frac{E_e}{2m_N}\left[\pm 2r\sqrt{\frac{J}{J+1}}\mathrm{Re}\left(C_V^+\bar{C}_E^+\right)+\frac{r^2}{J+1}\mathrm{Re}\left(C_A^+\bar{C}_E^+\right)\right],$$

$$\hat{\xi}\Delta B(E_e) = \frac{1}{3m_N}\left[\pm r\sqrt{\frac{J}{J+1}}\left(3E_e^{\max}-2E_e-\frac{m_e^2}{E_e}\right)\mathrm{Re}\left(C_V^+\bar{C}_E^+\right)-\frac{r^2}{J+1}\left(E_e-\frac{m_e^2}{E_e}\right)\mathrm{Re}\left(C_A^+\bar{C}_E^+\right)\right.$$
$$\left.+3r\sqrt{\frac{J}{J+1}}\left(\frac{E_e^{\max}}{E_e}-1\right)m_e\mathrm{Re}\left(C_S^+\bar{C}_E^+\right)\right],$$

$$\hat{\xi}B'(E_e) = \frac{E_e^{\max}-E_e}{2m_N}\left[\pm 2r\sqrt{\frac{J}{J+1}}\mathrm{Re}\left(C_V^+\bar{C}_E^+\right)-\frac{r^2}{J+1}\mathrm{Re}\left(C_A^+\bar{C}_E^+\right)\right],$$

$$\hat{\xi}\Delta D(E_e) = \frac{r^2}{J+1}\frac{1}{2m_N}\left[(2E_e-E_e^{\max})\mathrm{Im}\left(C_A^+\bar{C}_E^+\right)\pm m_e\mathrm{Im}\left(C_T^+\bar{C}_E^+\right)\right],$$

$$\hat{\xi}D'(E_e) = 0,$$

$$\hat{\xi}\Delta\hat{c}(E_e)=\frac{r^2}{2}\frac{1}{m_N}\left[\mp E_e^{\max}\mathrm{Re}\left(C_A^+\bar{C}_E^+\right)-m_e\mathrm{Re}\left(C_T^+\bar{C}_E^+\right)\right],$$

$$\hat{\xi}c'(E_e)=0,$$

$$\hat{\xi}c_1(E_e)=\frac{r^2}{6}\frac{E_e^{\max}-E_e}{m_N}\left[\mp\mathrm{Re}\left(C_A^+\bar{C}_E^+\right)-\frac{m_e}{E_e}\mathrm{Re}\left(C_T^+\bar{C}_E^+\right)\right],$$

$$\hat{\xi}c_2(E_e)=\mp\frac{r^2}{6}\frac{E_e}{m_N}\mathrm{Re}\left(C_A^+\bar{C}_E^+\right),$$

$$\hat{\xi}c_3(E_e)=\mp\frac{r^2}{2}\frac{E_e^{\max}-E_e}{m_N}\mathrm{Im}\left(C_A^+\bar{C}_E^+\right),$$

$$\hat{\xi}c_4(E_e)=\mp\frac{r^2}{2}\frac{E_e^{\max}-E_e}{m_N}\mathrm{Im}\left(C_A^+\bar{C}_E^+\right). \tag{B.6}$$

B.4 $C_{E'}^+$ Wilson coefficient

$$\mathcal{L}^{(1)}\supset-\frac{iC_{E'}^+}{2m_N}(\psi_p^\dagger\sigma^k\psi_n)\partial_t(\bar{e}_L\gamma^k\nu_L). \tag{B.7}$$

$$\hat{\xi}\xi_b(E_e)=\frac{E_e^{\max}}{m_N}r^2\left[\pm\mathrm{Re}\left(C_A^+\bar{C}_{E'}^+\right)+\frac{m_e}{E_e}\mathrm{Re}\left(C_T^+\bar{C}_{E'}^+\right)\right],$$

$$\hat{\xi}\Delta a(E_e)=\mp\frac{E_e^{\max}}{3m_N}r^2\mathrm{Re}\left(C_A^+\bar{C}_{E'}^+\right),$$

$$\hat{\xi}a'(E_e)=0,$$

$$\hat{\xi}\Delta A(E_e)=\frac{E_e^{\max}}{m_N}\left[\mp r\sqrt{\frac{J}{J+1}}\mathrm{Re}\left(C_V^+\bar{C}_{E'}^+\right)-\frac{r^2}{J+1}\mathrm{Re}\left(C_A^+\bar{C}_{E'}^+\right)\right],$$

$$\hat{\xi}A'(E_e)=0,$$

$$\hat{\xi}\Delta B(E_e)=\frac{E_e^{\max}}{m_N}\left[\mp r\sqrt{\frac{J}{J+1}}\mathrm{Re}\left(C_V^+\bar{C}_{E'}^+\right)+\frac{r^2}{J+1}\mathrm{Re}\left(C_A^+\bar{C}_{E'}^+\right)-r\sqrt{\frac{J}{J+1}}\frac{m_e}{E_e}\mathrm{Re}\left(C_S^+\bar{C}_{E'}^+\right)\right.$$
$$\left.\pm\frac{r^2}{J+1}\frac{m_e}{E_e}\mathrm{Re}\left(C_T^+\bar{C}_{E'}^+\right)\right],$$

$$\hat{\xi}B'(E_e)=0,$$

$$\hat{\xi}\Delta D(E_e)=\mp\frac{E_e^{\max}}{m_N}r\sqrt{\frac{J}{J+1}}\mathrm{Im}\left(C_V^+\bar{C}_{E'}^+\right),$$

$$D'(E_e)=0,$$

$$\hat{\xi}\Delta\hat{c}(E_e)=\pm\frac{E_e^{\max}}{m_N}r^2\mathrm{Re}\left(C_A^+\bar{C}_{E'}^+\right),$$

$$\hat{\xi}c'(E_e)=0,$$

$$\hat{\xi}c_1(E_e)=0,$$

$$\hat{\xi}c_2(E_e)=0,$$

$$\hat{\xi}c_3(E_e) = 0,$$

$$\hat{\xi}c_4(E_e) = 0. \tag{B.8}$$

B.5 C_{T1}^+ Wilson coefficient

$$\mathcal{L}^{(1)} \supset -\frac{iC_{T1}^+}{2m_N}(\psi_p^\dagger \psi_n)\nabla_k(\bar{e}_R \gamma^0 \gamma^k \nu_L). \tag{B.9}$$

$$\hat{\xi}\xi_b(E_e) = \frac{1}{m_N}\left[\left(\frac{E_e^{\max}}{E_e}-1\right)m_e \mathrm{Re}\left(C_V^+ \bar{C}_{T1}^+\right) \pm \left(E_e^{\max}-2E_e+\frac{m_e^2}{E_e}\right)\mathrm{Re}\left(C_S^+ \bar{C}_{T1}^+\right)\right],$$

$$\hat{\xi}\Delta a(E_e) = \frac{1}{m_N}\left[m_e \mathrm{Re}\left(C_V^+ \bar{C}_{T1}^+\right) \pm (2E_e-E_e^{\max})\mathrm{Re}\left(C_S^+ \bar{C}_{T1}^+\right)\right],$$

$$\hat{\xi}a'(E_e) = 0,$$

$$\hat{\xi}\Delta A(E_e) = -\frac{1}{m_N}r\sqrt{\frac{J}{J+1}}\left[m_e \mathrm{Re}\left(C_A^+ \bar{C}_{T1}^+\right) \pm (2E_e-E_e^{\max})\mathrm{Re}\left(C_T^+ \bar{C}_{T1}^+\right)\right],$$

$$\hat{\xi}A'(E_e) = 0,$$

$$\hat{\xi}\Delta B(E_e) = -\frac{1}{m_N}r\sqrt{\frac{J}{J+1}}\left[\left(\frac{E_e^{\max}}{E_e}-1\right)m_e \mathrm{Re}\left(C_A^+ \bar{C}_{T1}^+\right) \pm \left(E_e^{\max}-2E_e+\frac{m_e^2}{E_e}\right)\mathrm{Re}\left(C_T^+ \bar{C}_{T1}^+\right)\right],$$

$$\hat{\xi}B'(E_e) = 0,$$

$$\hat{\xi}\Delta D(E_e) = \frac{1}{m_N}r\sqrt{\frac{J}{J+1}}\left[m_e \mathrm{Im}\left(C_A^+ \bar{C}_{T1}^+\right) \pm (2E_e-E_e^{\max})\mathrm{Im}\left(C_T^+ \bar{C}_{T1}^+\right)\right],$$

$$\hat{\xi}D'(E_e) = 0,$$

$$\hat{\xi}\Delta\hat{c}(E_e) = 0,$$

$$\hat{\xi}c'(E_e) = 0,$$

$$\hat{\xi}c_1(E_e) = 0,$$

$$\hat{\xi}c_2(E_e) = 0,$$

$$\hat{\xi}c_3(E_e) = 0,$$

$$\hat{\xi}c_4(E_e) = 0. \tag{B.10}$$

The effects proportional to $\alpha_{FT}C_{FT}^+$ entering via the subleading tensor matrix element in eq. (3.4) have the same functional form as in eq. (B.10). They can be obtained via the replacement $C_{T1}^+ \to C_{T1}^+ - \alpha_{FT}C_{FT}^+$ in eq. (B.10).

B.6 C_{T2}^+ Wilson coefficient

$$\mathcal{L}^{(1)} \supset \frac{iC_{T2}^+}{2m_N}(\psi_p^\dagger \psi_n)(\bar{e}_R \overleftrightarrow{\partial_t} \nu_L). \tag{B.11}$$

$$\hat{\xi}\xi_b(E_e) = \frac{E_e^{\max}-2E_e}{m_N}\left[\frac{m_e}{E_e}\mathrm{Re}\left(C_V^+ \bar{C}_{T2}^+\right) \pm \mathrm{Re}\left(C_S^+ \bar{C}_{T2}^+\right)\right],$$

$$\hat{\xi}\Delta a(E_e) = \pm \frac{2E_e - E_e^{\max}}{m_N}\text{Re}\left(C_S^+\bar{C}_{T2}^+\right),$$

$$\hat{\xi}a'(E_e) = 0,$$

$$\hat{\xi}\Delta A(E_e) = \pm r\sqrt{\frac{J}{J+1}}\frac{E_e^{\max} - 2E_e}{m_N}\text{Re}\left(C_T^+\bar{C}_{T2}^+\right),$$

$$\hat{\xi}A'(E_e) = 0,$$

$$\hat{\xi}\Delta B(E_e) = r\sqrt{\frac{J}{J+1}}\frac{2E_e - E_e^{\max}}{m_N}\left[\frac{m_e}{E_e}\text{Re}\left(C_A^+\bar{C}_{T2}^+\right) \pm \text{Re}\left(C_T^+\bar{C}_{T2}^+\right)\right],$$

$$\hat{\xi}B'(E_e) = 0,$$

$$\hat{\xi}\Delta D(E_e) = \pm r\sqrt{\frac{J}{J+1}}\frac{2E_e - E_e^{\max}}{m_N}\text{Im}\left(C_T^+\bar{C}_{T2}^+\right),$$

$$\hat{\xi}D'(E_e) = 0,$$

$$\hat{\xi}\Delta\hat{c}(E_e) = 0,$$

$$\hat{\xi}c'(E_e) = 0,$$

$$\hat{\xi}c_1(E_e) = 0,$$

$$\hat{\xi}c_2(E_e) = 0,$$

$$\hat{\xi}c_3(E_e) = 0,$$

$$\hat{\xi}c_4(E_e) = 0. \tag{B.12}$$

B.7 C_{T3}^+ Wilson coefficient

$$\mathcal{L}^{(1)} \supset \frac{iC_{T3}^+}{m_N}(\psi_p^\dagger\sigma^k\psi_n)(\bar{e}_R \overleftrightarrow{\nabla}_k \nu_L). \tag{B.13}$$

$$\hat{\xi}\xi_b(E_e) = \frac{2r^2}{3}\frac{1}{m_N}\left[m_e\left(\frac{E_e^{\max}}{E_e} - 1\right)\text{Re}\left(C_A^+\bar{C}_{T3}^+\right) \pm \left(E_e^{\max} - \frac{m_e^2}{E_e}\right)\text{Re}\left(C_T^+\bar{C}_{T3}^+\right)\right],$$

$$\hat{\xi}\Delta a(E_e) = -\frac{2r^2}{3}\frac{1}{m_N}\left[m_e\text{Re}\left(C_A^+\bar{C}_{T3}^+\right) \mp E_e^{\max}\text{Re}\left(C_T^+\bar{C}_{T3}^+\right)\right],$$

$$\hat{\xi}a'(E_e) = 0,$$

$$\hat{\xi}\Delta A(E_e) = \frac{1}{m_N}\left[2r\sqrt{\frac{J}{J+1}}m_e\text{Re}\left(C_V^+\bar{C}_{T3}^+\right) \pm \frac{2r}{3}\sqrt{\frac{J}{J+1}}\left(2E_e + E_e^{\max}\right)\text{Re}\left(C_S^+\bar{C}_{T3}^+\right)\right.$$
$$\left. + \frac{2r^2}{3(J+1)}\left(E_e^{\max} - E_e\right)\text{Re}\left(C_T^+\bar{C}_{T3}^+\right)\right],$$

$$\hat{\xi}A'(E_e) = \frac{1}{m_N}\left[\mp 2r\sqrt{\frac{J}{J+1}}E_e\text{Re}\left(C_S^+\bar{C}_{T3}^+\right) - \frac{r^2}{J+1}E_e\text{Re}\left(C_T^+\bar{C}_{T3}^+\right)\right],$$

$$\hat{\xi}\Delta B(E_e) = \frac{1}{m_N}\left[-2r\sqrt{\frac{J}{J+1}}m_e\frac{E_e^{\max}-E_e}{E_e}\mathrm{Re}\left(C_V^+\bar{C}_{T3}^+\right)\right.$$

$$\left.\mp 2r\sqrt{\frac{J}{J+1}}\frac{3E_eE_e^{\max}-2E_e^2-m_e^2}{3E_e}\mathrm{Re}\left(C_S^+\bar{C}_{T3}^+\right)+\frac{2r^2}{3(J+1)}\frac{E_e^2-m_e^2}{E_e}\mathrm{Re}\left(C_T^+\bar{C}_{T3}^+\right)\right],$$

$$\hat{\xi}B'(E_e) = \frac{1}{m_N}\left[\pm 2r\sqrt{\frac{J}{J+1}}(E_e^{\max}-E_e)\mathrm{Re}\left(C_S^+\bar{C}_{T3}^+\right)-\frac{r^2}{J+1}(E_e^{\max}-E_e)\mathrm{Re}\left(C_T^+\bar{C}_{T3}^+\right)\right],$$

$$\hat{\xi}\Delta D(E_e) = \pm\frac{r^2}{J+1}\frac{1}{m_N}\left[m_e\mathrm{Im}\left(C_A^+\bar{C}_{T3}^+\right)+(2E_e-E_e^{\max})\mathrm{Im}\left(C_T^+\bar{C}_{T3}^+\right)\right],$$

$$\hat{\xi}D'(E_e) = 0,$$

$$\hat{\xi}\Delta\hat{c}(E_e) = \frac{r^2}{m_N}\left[-m_e\mathrm{Re}\left(C_A^+\bar{C}_{T3}^+\right)\mp E_e^{\max}\mathrm{Re}\left(C_T^+\bar{C}_{T3}^+\right)\right],$$

$$\hat{\xi}c'(E_e) = 0,$$

$$\hat{\xi}c_1(E_e) = \frac{r^2}{3}\frac{E_e^{\max}-E_e}{m_N}\left[\frac{m_e}{E_e}\mathrm{Re}\left(C_A^+\bar{C}_{T3}^+\right)\pm\mathrm{Re}\left(C_T^+\bar{C}_{T3}^+\right)\right],$$

$$\hat{\xi}c_2(E_e) = \pm\frac{r^2}{3}\frac{E_e}{m_N}\mathrm{Re}\left(C_T^+\bar{C}_{T3}^+\right),$$

$$\hat{\xi}c_3(E_e) = \mp r^2\frac{E_e^{\max}-E_e}{m_N}\mathrm{Im}\left(C_T^+\bar{C}_{T3}^+\right),$$

$$\hat{\xi}c_4(E_e) = \pm r^2\frac{E_e^{\max}-E_e}{m_N}\mathrm{Im}\left(C_T^+\bar{C}_{T3}^+\right). \tag{B.14}$$

B.8 C_{FV}^+ Wilson coefficient

$$\mathcal{L}^{(1)} \supset -\frac{iC_{FV}^+}{2m_N}(\psi_p^\dagger\overleftrightarrow{\nabla}_k\psi_n)(\bar{e}_L\gamma^k\nu_L). \tag{B.15}$$

We start with the contribution due to the first term in the $\langle\psi_p^\dagger\overleftrightarrow{\nabla}_k\psi_n\rangle$ matrix element in eq. (3.4).

$$\hat{\xi}\xi_b(E_e) = \frac{1}{m_{\mathcal{N}}}\left[\left(E_e^{\max}-\frac{m_e^2}{E_e}\right)\mathrm{Re}\left(C_V^+\bar{C}_{FV}^+\right)\pm\left(\frac{E_e^{\max}}{E_e}-1\right)m_e\mathrm{Re}\left(C_S^+\bar{C}_{FV}^+\right)\right],$$

$$\hat{\xi}\Delta a(E_e) = \frac{1}{m_{\mathcal{N}}}\left[E_e^{\max}\mathrm{Re}\left(C_V^+\bar{C}_{FV}^+\right)\pm m_e\mathrm{Re}\left(C_S^+\bar{C}_{FV}^+\right)\right],$$

$$\hat{\xi}a'(E_e) = 0,$$

$$\hat{\xi}\Delta A(E_e) = -r\sqrt{\frac{J}{J+1}}\frac{1}{m_{\mathcal{N}}}\left[E_e^{\max}\mathrm{Re}\left(C_A^+\bar{C}_{FV}^+\right)\pm m_e\mathrm{Re}\left(C_T^+\bar{C}_{FV}^+\right)\right],$$

$$\hat{\xi}A'(E_e) = 0,$$

$$\hat{\xi}\Delta B(E_e) = -r\sqrt{\frac{J}{J+1}}\frac{1}{m_{\mathcal{N}}}\left[\left(E_e^{\max}-\frac{m_e^2}{E_e}\right)\mathrm{Re}\left(C_A^+\bar{C}_{FV}^+\right)\pm\left(\frac{E_e^{\max}}{E_e}-1\right)m_e\mathrm{Re}\left(C_T^+\bar{C}_{FV}^+\right)\right],$$

$$\hat{\xi}B'(E_e) = 0,$$

$$\hat{\xi}\Delta D(E_e) = r\sqrt{\frac{J}{J+1}}\frac{1}{m_\mathcal{N}}\left[E_e^{\max}\mathrm{Im}\left(C_A^+\bar{C}_{FV}^+\right)\pm m_e\mathrm{Im}\left(C_T^+\bar{C}_{FV}^+\right)\right],$$

$$\hat{\xi}D'(E_e) = 0,$$

$$\hat{\xi}\Delta\hat{c}(E_e) = 0,$$

$$\hat{\xi}c'(E_e) = 0,$$

$$\hat{\xi}c_1(E_e) = 0,$$

$$\hat{\xi}c_2(E_e) = 0,$$

$$\hat{\xi}c_3(E_e) = 0,$$

$$\hat{\xi}c_4(E_e) = 0. \tag{B.16}$$

The contribution proportional to $\beta_{FV}C_{FV}^+$ due to the second term in the $\langle\psi_p^\dagger\overleftrightarrow{\nabla}_k\psi_n\rangle$ matrix element in eq. (3.4) can be obtained from eq. (B.4) via the replacement $C_M^+ \to C_M^+ + \beta_{FV}C_{FV}^+$.

B.9 C_{FA}^+ Wilson coefficient

$$\mathcal{L}^{(1)} \supset \frac{iC_{FA}^+}{2m_N}(\psi_p^\dagger\sigma^k\overleftrightarrow{\nabla}_k\psi_n)(\bar{e}_L\gamma^0\nu_L). \tag{B.17}$$

$$\hat{\xi}\xi_b(E_e) = \frac{r^2}{3}\frac{1}{m_\mathcal{N}}\left[\left(E_e^{\max}-\frac{m_e^2}{E_e}\right)\mathrm{Re}\left(C_A^+\bar{C}_{FA}^+\right)\pm m_e\left(\frac{E_e^{\max}}{E_e}-1\right)\mathrm{Re}\left(C_T^+\bar{C}_{FA}^+\right)\right],$$

$$\hat{\xi}\Delta a(E_e) = \frac{r^2}{3}\frac{1}{m_\mathcal{N}}\left[E_e^{\max}\mathrm{Re}\left(C_A^+\bar{C}_{FA}^+\right)\pm m_e\mathrm{Re}\left(C_T^+\bar{C}_{FA}^+\right)\right],$$

$$\hat{\xi}a'(E_e) = 0,$$

$$\hat{\xi}\Delta A(E_e) = \frac{1}{m_\mathcal{N}}\left[-r\sqrt{\frac{J}{J+1}}\frac{2E_e+E_e^{\max}}{3}\mathrm{Re}\left(C_V^+\bar{C}_{FA}^+\right)\mp\frac{r^2}{3(J+1)}(E_e^{\max}-E_e)\mathrm{Re}\left(C_A^+\bar{C}_{FA}^+\right)\right.$$
$$\left.\mp r\sqrt{\frac{J}{J+1}}m_e\mathrm{Re}\left(C_S^+\bar{C}_{FA}^+\right)\right],$$

$$\hat{\xi}A'(E_e) = \frac{E_e}{m_\mathcal{N}}\left[-r\sqrt{\frac{J}{J+1}}\mathrm{Re}\left(C_V^+\bar{C}_{FA}^+\right)\mp\frac{r^2}{2(J+1)}\mathrm{Re}\left(C_A^+\bar{C}_{FA}^+\right)\right],$$

$$\hat{\xi}\Delta B(E_e) = \frac{1}{m_\mathcal{N}}\left[-r\sqrt{\frac{J}{J+1}}\frac{3E_eE_e^{\max}-2E_e^2-m_e^2}{3E_e}\mathrm{Re}\left(C_V^+\bar{C}_{FA}^+\right)\pm\frac{r^2}{3(J+1)}\frac{E_e^2-m_e^2}{E_e}\mathrm{Re}\left(C_A^+\bar{C}_{FA}^+\right)\right.$$
$$\left.\mp r\sqrt{\frac{J}{J+1}}\frac{m_e(E_e^{\max}-E_e)}{E_e}\mathrm{Re}\left(C_S^+\bar{C}_{FA}^+\right)\right],$$

$$\hat{\xi}B'(E_e) = \frac{E_e^{\max}-E_e}{m_\mathcal{N}}\left[-r\sqrt{\frac{J}{J+1}}\mathrm{Re}\left(C_V^+\bar{C}_{FA}^+\right)\pm\frac{r^2}{2(J+1)}\mathrm{Re}\left(C_A^+\bar{C}_{FA}^+\right)\right],$$

$$\hat{\xi}\Delta D(E_e) = \frac{r^2}{2(J+1)}\frac{1}{m_\mathcal{N}}\left[\pm(E_e^{\max}-2E_e)\mathrm{Im}\left(C_A^+\bar{C}_{FA}^+\right)-m_e\mathrm{Im}\left(C_T^+\bar{C}_{FA}^+\right)\right],$$

$$\hat{\xi}D'(E_e) = 0,$$

$$\hat{\xi}\Delta\hat{c}(E_e) = \frac{r^2}{2}\frac{1}{m_\mathcal{N}}\left[E_e^{\max}\mathrm{Re}\left(C_A^+\bar{C}_{FA}^+\right)\pm m_e\mathrm{Re}\left(C_T^+\bar{C}_{FA}^+\right)\right],$$

$$\hat{\xi}c'(E_e) = 0,$$

$$\hat{\xi}c_1(E_e) = \frac{E_e^{\max}-E_e}{m_\mathcal{N}}\frac{r^2}{6}\left[\mathrm{Re}\left(C_A^+\bar{C}_{FA}^+\right)\pm\frac{m_e}{E_e}\mathrm{Re}\left(C_T^+\bar{C}_{FA}^+\right)\right],$$

$$\hat{\xi}c_2(E_e) = \frac{E_e}{m_\mathcal{N}}\frac{r^2}{6}\mathrm{Re}\left(C_A^+\bar{C}_{FA}^+\right),$$

$$\hat{\xi}c_3(E_e) = \frac{E_e^{\max}-E_e}{m_\mathcal{N}}\frac{r^2}{2}\mathrm{Im}\left(C_A^+\bar{C}_{FA}^+\right),$$

$$\hat{\xi}c_4(E_e) = \frac{E_e^{\max}-E_e}{m_\mathcal{N}}\frac{r^2}{2}\mathrm{Im}\left(C_A^+\bar{C}_{FA}^+\right). \tag{B.18}$$

B.10 C_{FT}^+ Wilson coefficient

$$\mathcal{L}^{(1)} \supset \frac{C_{FT}^+}{2m_N}\epsilon^{ijk}(\psi_p^\dagger\sigma^i\overleftrightarrow{\nabla}_j\psi_n)(\bar{e}_R\gamma^0\gamma^k\nu_L). \tag{B.19}$$

We start with the contribution due to the first term in the $\langle\psi_p^\dagger\sigma^i\overleftrightarrow{\nabla}_j\psi_n\rangle$ matrix element in eq. (3.4).

$$\hat{\xi}\xi_b(E_e) = \frac{2r^2}{3}\frac{1}{m_\mathcal{N}}\left[-\left(\frac{E_e^{\max}}{E_e}-1\right)m_e\mathrm{Re}\left(C_A^+\bar{C}_{FT}^+\right)\mp\left(E_e^{\max}-\frac{m_e^2}{E_e}\right)\mathrm{Re}\left(C_T^+\bar{C}_{FT}^+\right)\right],$$

$$\hat{\xi}\Delta a(E_e) = \frac{2r^2}{3}\frac{1}{m_\mathcal{N}}\left[-m_e\mathrm{Re}\left(C_A^+\bar{C}_{FT}^+\right)\mp E_e^{\max}\mathrm{Re}\left(C_T^+\bar{C}_{FT}^+\right)\right],$$

$$\hat{\xi}a'(E_e) = 0,$$

$$\hat{\xi}\Delta A(E_e) = \frac{1}{m_\mathcal{N}}\left[\mp\frac{r^2}{J+1}m_e\mathrm{Re}\left(C_A^+\bar{C}_{FT}^+\right)\mp\frac{2}{3}(E_e^{\max}-E_e)r\sqrt{\frac{J}{J+1}}\mathrm{Re}\left(C_S^+\bar{C}_{FT}^+\right)\right.$$
$$\left.-\frac{r^2}{J+1}\frac{E_e+2E_e^{\max}}{3}\mathrm{Re}\left(C_T^+\bar{C}_{FT}^+\right)\right],$$

$$\hat{\xi}A'(E_e) = \frac{E_e}{m_\mathcal{N}}\left[\mp r\sqrt{\frac{J}{J+1}}\mathrm{Re}\left(C_S^+\bar{C}_{FT}^+\right)-\frac{r^2}{2(J+1)}\mathrm{Re}\left(C_T^+\bar{C}_{FT}^+\right)\right],$$

$$\hat{\xi}\Delta B(E_e) = \frac{1}{m_\mathcal{N}}\left[\mp\frac{r^2}{J+1}\frac{m_e}{E_e}(E_e^{\max}-E_e)\mathrm{Re}\left(C_A^+\bar{C}_{FT}^+\right)\pm\frac{2(E_e^2-m_e^2)}{3E_e}r\sqrt{\frac{J}{J+1}}\mathrm{Re}\left(C_S^+\bar{C}_{FT}^+\right)\right.$$
$$\left.-\frac{3E_eE_e^{\max}-E_e^2-2m_e^2}{3E_e}\frac{r^2}{J+1}\mathrm{Re}\left(C_T^+\bar{C}_{FT}^+\right)\right],$$

$$\hat{\xi}B'(E_e) = \frac{1}{2}\frac{E_e^{\max}-E_e}{m_N}\left[\pm 2r\sqrt{\frac{J}{J+1}}\mathrm{Re}\left(C_S^+\bar{C}_{FT}^+\right)-\frac{r^2}{J+1}\mathrm{Re}\left(C_T^+\bar{C}_{FT}^+\right)\right],$$

$$\hat{\xi}\Delta D(E_e) = \frac{1}{m_{\mathcal{N}}}\left[-m_e r\sqrt{\frac{J}{J+1}}\text{Im}\left(C_V^+\bar{C}_{FT}^+\right) - \frac{E_e^{\max}-2E_e}{2}\frac{r^2}{J+1}\text{Im}\left(C_T^+\bar{C}_{FT}^+\right)\right.$$

$$\left.\pm\frac{m_e}{2}\frac{r^2}{J+1}\text{Im}\left(C_A^+\bar{C}_{FT}^+\right)\mp E_e^{\max}r\sqrt{\frac{J}{J+1}}\text{Im}\left(C_S^+\bar{C}_{FT}^+\right)\right],$$

$$\hat{\xi}D'(E_e) = 0,$$

$$\hat{\xi}\Delta\hat{c}(E_e) = r^2\frac{1}{2m_{\mathcal{N}}}\left[m_e\text{Re}\left(C_A^+\bar{C}_{FT}^+\right)\pm E_e^{\max}\text{Re}\left(C_T^+\bar{C}_{FT}^+\right)\right],$$

$$\hat{\xi}c'(E_e) = 0,$$

$$\hat{\xi}c_1(E_e) = \frac{r^2}{6}\frac{E_e^{\max}-E_e}{m_{\mathcal{N}}}\left[\frac{m_e}{E_e}\text{Re}\left(C_A^+\bar{C}_{FT}^+\right)\pm\text{Re}\left(C_T^+\bar{C}_{FT}^+\right)\right],$$

$$\hat{\xi}c_2(E_e) = \pm\frac{r^2}{6}\frac{E_e}{m_{\mathcal{N}}}\text{Re}\left(C_T^+\bar{C}_{FT}^+\right),$$

$$\hat{\xi}c_3(E_e) = \mp\frac{r^2}{2}\frac{E_e^{\max}-E_e}{m_{\mathcal{N}}}\text{Im}\left(C_T^+\bar{C}_{FT}^+\right),$$

$$\hat{\xi}c_4(E_e) = \pm\frac{r^2}{2}\frac{E_e^{\max}-E_e}{m_{\mathcal{N}}}\text{Im}\left(C_T^+\bar{C}_{FT}^+\right). \tag{B.20}$$

The contributions proportional to α_{FT} due to the second term in the $\langle\psi_p^\dagger\sigma^i\overleftrightarrow{\nabla}_j\psi_n\rangle$ matrix element in eq. (3.4) can be obtained via the replacement $C_{T1}^+ \to C_{T1}^+ - \alpha_{FT}C_{FT}^+$ in eq. (B.10).

We move to the contributions proportional to γ_{FT} due to the last term in the $\langle\psi_p^\dagger\sigma^i\overleftrightarrow{\nabla}_j\psi_n\rangle$ matrix element in eq. (3.4). These have to be treated separately because the resulting correlations do not fit into the template in eq. (3.6). Instead, they induce the following additional correlations in the differential decay distribution:

$$\Delta\frac{d\Gamma}{dE_e d\Omega_e d\Omega_\nu} = M_F^2 F(Z,E_e)(1+\delta_R)\frac{p_e E_e(E_e^{\max}-E_e)^2}{64\pi^5}\hat{\xi}\Bigg\{$$

$$\left(A''(E_e)\frac{\boldsymbol{J}\cdot\boldsymbol{k}_e}{JE_e}+B''(E_e)\frac{\boldsymbol{J}\cdot\boldsymbol{k}_\nu}{JE_\nu}\right)\frac{(\boldsymbol{k}_e\cdot\boldsymbol{j})(\boldsymbol{k}_\nu\cdot\boldsymbol{j})}{E_e E_\nu} - \frac{B''(E_e)}{3}\frac{\boldsymbol{J}\cdot\boldsymbol{k}_e}{JE_e} - \frac{A''(E_e)}{3}\frac{p_e^2}{E_e^2}\frac{\boldsymbol{J}\cdot\boldsymbol{k}_\nu}{JE_\nu}$$

$$+\frac{(\boldsymbol{J}\cdot\boldsymbol{j})^2}{J(J+1)}\left[\frac{\boldsymbol{J}\cdot\boldsymbol{k}_e}{JE_e}\left(\hat{A}(E_e)+\hat{A}'(E_e)\frac{\boldsymbol{k}_e\cdot\boldsymbol{k}_\nu}{E_e E_\nu}+\hat{A}''(E_e)\frac{(\boldsymbol{k}_e\cdot\boldsymbol{j})(\boldsymbol{k}_\nu\cdot\boldsymbol{j})}{E_e E_\nu}\right)\right.$$

$$\left.+\frac{\boldsymbol{J}\cdot\boldsymbol{k}_\nu}{JE_\nu}\left(\hat{B}(E_e)+\hat{B}'(E_e)\frac{\boldsymbol{k}_e\cdot\boldsymbol{k}_\nu}{E_e E_\nu}+\hat{B}''(E_e)\frac{(\boldsymbol{k}_e\cdot\boldsymbol{j})(\boldsymbol{k}_\nu\cdot\boldsymbol{j})}{E_e E_\nu}\right)\right]\Bigg\}, \tag{B.21}$$

with

$$A''(E_e) = 2\gamma_{FT}r^2\frac{3J^2+3J-1}{J(J+1)}\frac{E_e}{m_N}\text{Re}\left(C_T^+\bar{C}_{FT}^+\right),$$

$$B''(E_e) = 2\gamma_{FT}r^2\frac{3J^2+3J-1}{J(J+1)}\frac{E_e^{\max}-E_e}{m_N}\text{Re}\left(C_T^+\bar{C}_{FT}^+\right),$$

$$\hat{A}(E_e) = 2\gamma_{FT}r^2\frac{E_e^{\max}-E_e}{m_N}\text{Re}\left(C_T^+\bar{C}_{FT}^+\right),$$

$$\hat{A}'(E_e) = 4\gamma_{FT}r^2\frac{E_e}{m_N}\text{Re}\left(C_T^+\bar{C}_{FT}^+\right),$$

$$\hat{A}''(E_e) = -10\gamma_{FT}r^2\frac{E_e}{m_N}\text{Re}\left(C_T^+\bar{C}_{FT}^+\right),$$

$$\hat{B}(E_e) = 2\gamma_{FT}r^2\frac{E_e^2 - m_e^2}{E_e m_N}\text{Re}\left(C_T^+\bar{C}_{FT}^+\right),$$

$$\hat{B}'(E_e) = 4\gamma_{FT}r^2\frac{E_e^{\max} - E_e}{m_N}\text{Re}\left(C_T^+\bar{C}_{FT}^+\right),$$

$$\hat{B}''(E_e) = -10\gamma_{FT}r^2\frac{E_e^{\max} - E_e}{m_N}\text{Re}\left(C_T^+\bar{C}_{FT}^+\right). \tag{B.22}$$

On the other hand, the contributions proportional to γ_{FT} to the usual correlations in eq. (3.6) are

$$\hat{\xi}\xi_b(E_e) = 0,$$

$$\hat{\xi}\Delta a(E_e) = 0,$$

$$\hat{\xi}a'(E_e) = 0,$$

$$\hat{\xi}\Delta A(E_e) = \frac{\gamma_{FT}}{m_N}\frac{r^2(2J-1)(2J+3)}{3J(J+1)}\left[\pm m_e\text{Re}\left(C_A^+\bar{C}_{FT}^+\right) + E_e\text{Re}\left(C_T^+\bar{C}_{FT}^+\right)\right],$$

$$\hat{\xi}A'(E_e) = -\frac{\gamma_{FT}}{m_N}\frac{r^2(4J^2+4J-1)}{2J(J+1)}E_e\text{Re}\left(C_T^+\bar{C}_{FT}^+\right),$$

$$\hat{\xi}\Delta B(E_e) = \frac{\gamma_{FT}(E_e^{\max} - E_e)}{m_N}\frac{r^2(2J-1)(2J+3)}{3J(J+1)}\left[\pm\frac{m_e}{E_e}\text{Re}\left(C_A^+\bar{C}_{FT}^+\right) + \text{Re}\left(C_T^+\bar{C}_{FT}^+\right)\right],$$

$$\hat{\xi}B'(E_e) = -\frac{\gamma_{FT}(E_e^{\max} - E_e)}{m_N}\frac{r^2(4J^2+4J-1)}{2J(J+1)}\text{Re}\left(C_T^+\bar{C}_{FT}^+\right),$$

$$\hat{\xi}\Delta D(E_e) = \frac{\gamma_{FT}}{m_N}\frac{r^2(2J-1)(2J+3)}{6J(J+1)}\left[\pm m_e\text{Im}\left(C_A^+\bar{C}_{FT}^+\right) + (E_e^{\max} - 2E_e)\text{Im}\left(C_T^+\bar{C}_{FT}^+\right)\right],$$

$$\hat{\xi}D'(E_e) = 0,$$

$$\hat{\xi}\Delta\hat{c}(E_e) = \frac{\gamma_{FT}}{m_N}\left[\mp m_e r\sqrt{\frac{J+1}{J}}\text{Re}\left(C_V^+\bar{C}_{FT}^+\right) + \frac{3m_e}{2}\frac{r^2}{J}\text{Re}\left(C_A^+\bar{C}_{FT}^+\right)\right.$$
$$\left. + (E_e^{\max} - 2E_e)r\sqrt{\frac{J+1}{J}}\text{Re}\left(C_S^+\bar{C}_{FT}^+\right) \pm \frac{3E_e^{\max}}{2}\frac{r^2}{J}\text{Re}\left(C_T^+\bar{C}_{FT}^+\right)\right],$$

$$\hat{\xi}c'(E_e) = 0,$$

$$\hat{\xi}c_1(E_e) = \frac{\gamma_{FT}(E_e^{\max} - E_e)}{m_N}\left[\mp\frac{m_e}{3E_e}r\sqrt{\frac{J+1}{J}}\text{Re}\left(C_V^+\bar{C}_{FT}^+\right) + \frac{m_e}{2E_e}\frac{r^2}{J}\text{Re}\left(C_A^+\bar{C}_{FT}^+\right)\right.$$
$$\left. - \frac{1}{3}r\sqrt{\frac{J+1}{J}}\text{Re}\left(C_S^+\bar{C}_{FT}^+\right) \pm \frac{1}{2}\frac{r^2}{J}\text{Re}\left(C_T^+\bar{C}_{FT}^+\right)\right],$$

$$\hat{\xi}c_2(E_e) = \frac{\gamma_{FT}E_e}{m_N}\left[\frac{1}{3}r\sqrt{\frac{J+1}{J}}\text{Re}\left(C_S^+\bar{C}_{FT}^+\right) \pm \frac{1}{2}\frac{r^2}{J}\text{Re}\left(C_T^+\bar{C}_{FT}^+\right)\right],$$

$$\hat{\xi}c_3(E_e) = \frac{\gamma_{FT}(E_e^{\max} - E_e)}{m_N}\left[-r\sqrt{\frac{J+1}{J}}\text{Im}\left(C_S^+\bar{C}_{FT}^+\right) \pm \frac{1}{2}\frac{r^2}{J}\text{Im}\left(C_T^+\bar{C}_{FT}^+\right)\right],$$

$$\hat{\xi}c_4(E_e) = \frac{\gamma_{FT}(E_e^{\max} - E_e)}{m_N}\left[-r\sqrt{\frac{J+1}{J}}\text{Im}\left(C_S^+\bar{C}_{FT}^+\right) \mp \frac{1}{2}\frac{r^2}{J}\text{Im}\left(C_T^+\bar{C}_{FT}^+\right)\right]. \tag{B.23}$$

B.11 Phase space and normalization

$$\hat{\xi}\xi_b(E_e) = \frac{1}{m_{\mathcal{N}}}\left[\left(2E_e - E_e^{\max} + \frac{m_e^2}{E_e}\right)|C_V^+|^2 + \left(\frac{10}{3}E_e - E_e^{\max} - \frac{m_e^2}{3E_e}\right)r^2|C_A^+|^2\right.$$

$$+\left(4E_e - E_e^{\max} - \frac{m_e^2}{E_e}\right)|C_S^+|^2 + \left(\frac{8}{3}E_e - E_e^{\max} + \frac{m_e^2}{3E_e}\right)r^2|C_T^+|^2$$

$$\left.\pm 2m_e\left(3 - \frac{E_e^{\max}}{E_e}\right)\mathrm{Re}\left(C_V^+\bar{C}_S^+ + r^2 C_A^+\bar{C}_T^+\right)\right],$$

$$\hat{\xi}\Delta a(E_e) = \frac{1}{m_{\mathcal{N}}}\left[-E_e^{\max}|C_V^+|^2 + \left(\frac{1}{3}E_e^{\max} - 4E_e\right)r^2|C_A^+|^2\right.$$

$$\left.+(E_e^{\max} - 6E_e)|C_S^+|^2 - \left(\frac{1}{3}E_e^{\max} + 2E_e\right)r^2|C_T^+|^2 \mp 6m_e\mathrm{Re}\left(C_V^+\bar{C}_S^+ + r^2 C_A^+\bar{C}_T^+\right)\right],$$

$$\hat{\xi}a'(E_e) = \frac{E_e}{m_{\mathcal{N}}}\left[-3\left(|C_V^+|^2 - |C_S^+|^2\right) + r^2\left(|C_A^+|^2 - |C_T^+|^2\right)\right],$$

$$\hat{\xi}\Delta A(E_e) = 2r\sqrt{\frac{J}{J+1}}\left[\frac{E_e^{\max} - 2E_e}{m_{\mathcal{N}}}\mathrm{Re}\left(C_V^+\bar{C}_A^+\right) - \frac{E_e^{\max} - 4E_e}{m_{\mathcal{N}}}\mathrm{Re}\left(C_S^+\bar{C}_T^+\right) \pm \frac{m_e}{m_{\mathcal{N}}}\mathrm{Re}\left(C_V^+\bar{C}_T^+ + C_A^+\bar{C}_S^+\right)\right]$$

$$\pm \frac{r^2}{J+1}\frac{1}{m_{\mathcal{N}}}\left[(E_e^{\max} - 4E_e)|C_A^+|^2 - \left(E_e^{\max} - 2E_e\right)|C_T^+|^2 \mp 2m_e\mathrm{Re}\left(\bar{C}_A^+ C_T^+\right)\right],$$

$$\hat{\xi}A'(E_e) = 6r\sqrt{\frac{J}{J+1}}\frac{E_e}{m_{\mathcal{N}}}\mathrm{Re}\left(C_V^+\bar{C}_A^+ - C_S^+\bar{C}_T^+\right) \pm \frac{3r^2}{J+1}\frac{E_e}{m_{\mathcal{N}}}\left(|C_A^+|^2 - |C_T^+|^2\right),$$

$$\hat{\xi}\Delta B(E_e) = 2r\sqrt{\frac{J}{J+1}}\frac{1}{m_{\mathcal{N}}}\left[(E_e^{\max} - 2E_e)\mathrm{Re}\left(C_V^+\bar{C}_A^+\right) + (E_e^{\max} - 4E_e)\mathrm{Re}\left(C_S^+\bar{C}_T^+\right)\right.$$

$$\left.\pm m_e\frac{E_e^{\max}}{E_e}\mathrm{Re}\left(C_V^+\bar{C}_T^+ + C_A^+\bar{C}_S^+\right) \mp 3m_e\mathrm{Re}\left(C_V^+\bar{C}_T^+ + C_A^+\bar{C}_S^+\right) - \frac{m_e^2}{E_e}\mathrm{Re}\left(C_V^+\bar{C}_A^+ - C_S^+\bar{C}_T^+\right)\right]$$

$$\pm \frac{r^2}{J+1}\frac{1}{m_{\mathcal{N}}}\left[-E_e^{\max}(|C_A^+|^2 + |C_T^+|^2) + 2E_e(2|C_A^+|^2 + |C_T^+|^2)\right.$$

$$\left.\mp 2m_e\frac{E_e^{\max}}{E_e}\mathrm{Re}\left(C_A^+\bar{C}_T^+\right) \pm 6m_e\mathrm{Re}\left(C_A^+\bar{C}_T^+\right) - \frac{m_e^2}{E_e}\left(|C_A^+|^2 - |C_T^+|^2\right)\right],$$

$$\hat{\xi}B'(E_e) = 6r\sqrt{\frac{J}{J+1}}\frac{1}{m_{\mathcal{N}}}\left[E_e\mathrm{Re}\left(C_V^+\bar{C}_A^+ + C_S^+\bar{C}_T^+\right) \pm m_e\mathrm{Re}\left(C_V^+\bar{C}_T^+ + C_A^+\bar{C}_S^+\right)\right]$$

$$\mp \frac{3r^2}{J+1}\frac{1}{m_{\mathcal{N}}}\left[E_e\left(|C_A^+|^2 + |C_T^+|^2\right) \pm 2m_e\mathrm{Re}\left(C_A^+\bar{C}_T^+\right)\right],$$

$$\hat{\xi}\Delta D(E_e) = 2r\sqrt{\frac{J}{J+1}}\frac{E_e^{\max} - 3E_e}{m_{\mathcal{N}}}\mathrm{Im}\left(C_V^+\bar{C}_A^+ - C_S^+\bar{C}_T^+\right),$$

$$\hat{\xi}D'(E_e) = 6r\sqrt{\frac{J}{J+1}}\frac{E_e}{m_{\mathcal{N}}}\mathrm{Im}\left(C_V^+\bar{C}_A^+ - C_S^+\bar{C}_T^+\right),$$

$$\hat{\xi}\Delta\hat{c}(E_e) = \frac{3E_e - E_e^{\max}}{m_{\mathcal{N}}}r^2\left(|C_A^+|^2 - |C_T^+|^2\right),$$

$$\hat{\xi}c'(E_e) = -\frac{3E_e}{m_{\mathcal{N}}}r^2\left(|C_A^+|^2 - |C_T^+|^2\right),$$

$$\hat{\xi}c_1(E_e) = \hat{\xi}c_2(E_e) = \hat{\xi}c_3(E_e) = \hat{\xi}c_4(E_e) = 0.$$

Parent	$\mathcal{F}t$ [s]	$\langle m_e/E_e \rangle$
^{10}C	3075.7 ± 4.4	0.619
^{14}O	3070.2 ± 1.9	0.438
^{22}Mg	3076.2 ± 7.0	0.308
^{26m}Al	3072.4 ± 1.1	0.300
^{26}Si	3075.4 ± 5.7	0.264
^{34}Cl	3071.6 ± 1.8	0.234
^{34}Ar	3075.1 ± 3.1	0.212
^{38m}K	3072.9 ± 2.0	0.213
^{38}Ca	3077.8 ± 6.2	0.195
^{42}Sc	3071.7 ± 2.0	0.201
^{46}V	3074.3 ± 2.0	0.183
^{50}Mn	3071.1 ± 1.6	0.169
^{54}Co	3070.4 ± 2.5	0.157
^{62}Ga	3072.4 ± 6.7	0.142
^{74}Rb	3077 ± 11	0.125

Table 5. Input from superallowed $0^+ \to 0^+$ beta transitions [9] used in our analysis.

Observable	Value	S factor	$\langle m_e/E_e \rangle$	References
τ_n (s)	878.64(59)	2.2	0.655	[49, 60–69]
$\tilde{A}_n$	−0.11958(21)	1.2	0.569	[70–76]
$\tilde{B}_n$	0.9805(30)		0.591	[77–80]
λ_{AB}	−1.2686(47)		0.581	[81]
a_n	−0.10426(82)			[58, 82, 83]
$\tilde{a}_n$	−0.1078(18)		0.695	[48]

Table 6. Input from neutron decay used in our analysis.

C Data used in the analysis

In our numerical analysis we use the input from superallowed $0^+ \to 0^+$ beta transitions (table 5), neutron decay (table 6), mirror decays (table 7), and correlation measurements in pure Fermi decays (table 8).

D On the many-body currents

In this appendix we briefly discuss how the many-body currents affect our analysis. At the leading order in recoil, we can calculate the amplitudes for nuclear beta transitions in two different ways, corresponding to distinct effective theory expansions. One way involves matrix elements of *quark* operators in eq. (2.1) between the initial and final nuclear states. The other involves matrix elements of *nucleon* operators in eq. (2.8). These two ways will in general yield different results, because the latter misses the contribution of operators quartic and higher in the nucleon field (and still bi-linear in the lepton fields), which are neglected

Parent	$J = J'$	Δ [MeV]	$\langle m_e/E_e \rangle$	f_A/f_V	$\mathcal{F}t$ [s]	Correlation
^{17}F	5/2	2.24947(25)	0.447	1.0007(1)	2292.4(2.7) [84]	$\tilde{A} = 0.960(82)$ [85, 86]
^{19}Ne	1/2	2.72849(16)	0.386	1.0012(2)	1721.44(92) [56]	$\tilde{A}_0 = -0.0391(14)$ [87]
						$\tilde{A}_0 = -0.03871(91)$ [57]
^{21}Na	3/2	3.035920(18)	0.355	1.0019(4)	4071(4) [88]	$\tilde{a} = 0.5502(60)$ [89]
^{29}P	1/2	4.4312(4)	0.258	0.9992(1)	4764.6(7.9) [90]	$\tilde{A} = 0.681(86)$ [91]
^{35}Ar	3/2	5.4552(7)	0.215	0.9930(14)	5688.6(7.2) [92]	$\tilde{A} = 0.430(22)$ [93–95]
^{37}K	3/2	5.63647(23)	0.209	0.9957(9)	4605.4(8.2) [96]	$\tilde{A} = -0.5707(19)$ [97]
						$\tilde{B} = -0.755(24)$ [98]

Table 7. Input from mirror beta decays used in our analysis.

Parent	$J = J'$	Type	Observable	Value	$\langle m_e/E_e \rangle$	Ref.
^{32}Ar	0	F/β^+	$\tilde{a}$	0.9989(65)	0.210	[99]
^{38m}K	0	F/β^+	$\tilde{a}$	0.9981(48)	0.161	[100]

Table 8. Input from correlation measurements in pure Fermi decays used in our analysis.

in our pionless EFT Lagrangian. The contributions of these operators are referred to as *many-body currents* in the nuclear literature [101–108]; two-body currents corresponding to quartic nucleon operators, etc. The difference between the two ways of calculating matrix elements therefore gives us an insight into the structure and magnitude of many-body effects.

For simplicity, let us restrict to β_- transitions with parent and daughter nucleus of spin $J = 1/2$; the general case is qualitatively similar and will be discussed in a separate future publication. In analogy to eq. (2.2), Lorentz symmetry and parity determines the matrix elements of the quark bi-linears occurring in eq. (2.1) to be

$$
\begin{aligned}
\langle \mathcal{N}'| \, \bar{u}\gamma_\mu d \, |\mathcal{N}\rangle &= g_V^i \bar{u}_{\mathcal{N}'} \gamma_\mu u_{\mathcal{N}} \; (1 + \mathcal{O}(q/m_{\mathcal{N}}))\,, \\
\langle \mathcal{N}'| \, \bar{u}\gamma_\mu\gamma_5 d \, |\mathcal{N}\rangle &= g_A^i \bar{u}_{\mathcal{N}'} \gamma_\mu \gamma_5 u_{\mathcal{N}} \; (1 + \mathcal{O}(q/m_{\mathcal{N}}))\,, \\
\langle \mathcal{N}'| \, \bar{u} d \, |\mathcal{N}\rangle &= g_S^i \bar{u}_{\mathcal{N}'} u_{\mathcal{N}} \; (1 + \mathcal{O}(q/m_{\mathcal{N}}))\,, \\
\langle \mathcal{N}'| \, \bar{u}\gamma_5 d \, |\mathcal{N}\rangle &= g_P^i \bar{u}_{\mathcal{N}'} \gamma_5 u_{\mathcal{N}} \; (1 + \mathcal{O}(q/m_{\mathcal{N}}))\,, \\
\langle \mathcal{N}'| \, \bar{u}\sigma_{\mu\nu} d \, |\mathcal{N}\rangle &= g_T^i \bar{u}_{\mathcal{N}'} \sigma_{\mu\nu} u_{\mathcal{N}} \; (1 + \mathcal{O}(q/m_{\mathcal{N}}))\,.
\end{aligned} \tag{D.1}
$$

Here, $u_{\mathcal{N}} = u(p, J_z, m_{\mathcal{N}})$ $(u_{\mathcal{N}'} = u(k', J_z', m_{\mathcal{N}'}))$ is the spinor wave function of the mother (daughter) nucleus, $p \approx k'$ is the momentum of the mother and daughter nucleus, J_z, J_z' are the projection of their polarizations on the z axis, and $q = p - k'$ corrections are neglected. The nuclear charges g_X^i are numerical parameters depending on the strong nuclear dynamics, and a priori they are transition dependent, which is indicated by the index i. However, for some of the charges one can determine the transition dependence from symmetry arguments.

In particular, if $\mathcal{N}$ and $\mathcal{N}'$ reside within the same isospin multiplet then $g_V^i = M_F g_V$ in the limit of unbroken isospin symmetry. For the scalar charges, we can relate them to the vector ones using the equations of motion in the limit $e \to 0$ where QED is decoupled, $i\partial^\mu[\bar{u}\gamma^\mu d] = (m_d - m_u)\bar{u}d$. Then, along the lines of ref. [31],

$$
\begin{aligned}
\langle \mathcal{N}'| \bar{u}d |\mathcal{N}\rangle &= \frac{\langle \mathcal{N}'| i\partial_\mu[\bar{u}\gamma_\mu d] |\mathcal{N}\rangle}{m_d - m_u} = \frac{[m_\mathcal{N} - m_{\mathcal{N}'}]_{\mathrm{QCD}}}{m_d - m_u} g_V^i \bar{u}_{\mathcal{N}'} u_\mathcal{N} \\
&= \frac{[m_n - m_p]_{\mathrm{QCD}}}{m_d - m_u} g_V^i \bar{u}_{\mathcal{N}'} u_\mathcal{N},
\end{aligned}
\tag{D.2}
$$

where the QCD subscript denotes the mass difference in the limit $e \to 0$. The last step relies on the fact that in this limit the isospin breaking interactions are negligible. Thus, $g_S^i = \frac{[m_n - m_p]_{\mathrm{QCD}}}{m_d - m_u} M_F g_V = M_F\, g_S$, where we used $g_S = \frac{[m_n - m_p]_{\mathrm{QCD}}}{(m_d - m_u)}$ [31]. Similar discussion applies to the pseudoscalar charges. The equation of motion $i\partial^\mu[\bar{u}\gamma^\mu\gamma_5 d] = -(m_d + m_u)\bar{u}\gamma_5 d$ implies

$$
\begin{aligned}
\langle \mathcal{N}'| \bar{u}\gamma_5 d |\mathcal{N}\rangle &= -\frac{\langle \mathcal{N}'| i\partial_\mu[\bar{u}\gamma_\mu\gamma_5 d] |\mathcal{N}\rangle}{m_d + m_u} = \frac{[m_\mathcal{N} + m_{\mathcal{N}'}]_{\mathrm{QCD}}}{m_d + m_u} g_A^i \bar{u}_{\mathcal{N}'}\gamma_5 u_\mathcal{N} \\
&\approx \frac{2A g_A^i m_N}{m_d + m_u} \bar{u}_{\mathcal{N}'}\gamma_5 u_\mathcal{N},
\end{aligned}
\tag{D.3}
$$

that is, $g_P^i = A\, g_P\, g_A^i / g_A$. All in all, for the vector and scalar charges the transition dependence is fixed by the isospin quantum numbers, while for the pseudoscalar charges it can be related to the transition dependence of the axial charges. On the other hand, for the tensor charges the transition dependence cannot be established from simple arguments. The beta decay amplitude in the quark level EFT, at leading order in recoil for each coupling, takes the form

$$
\begin{aligned}
\mathcal{M}_{\mathrm{QEFT}} = -\frac{V_{ud}}{v^2}\Big\{ & M_F g_V (1 + \epsilon_L + \epsilon_R) L^\mu(\bar{u}_{\mathcal{N}'}\gamma_\mu u_\mathcal{N}) - g_A^i(1 + \epsilon_L - \epsilon_R)L^\mu(\bar{u}_{\mathcal{N}'}\gamma_\mu\gamma_5 u_\mathcal{N}) \\
& + M_F g_S \epsilon_S L(\bar{u}_{\mathcal{N}'} u_\mathcal{N}) - g_P \epsilon_P A \frac{g_A^i}{g_A} L(\bar{u}_{\mathcal{N}'}\gamma_5 u_\mathcal{N}) + g_T^i \frac{\epsilon_T}{2} i L^{\mu\nu}(\bar{u}_{\mathcal{N}'}\sigma_{\mu\nu} u_\mathcal{N}) \Big\} \\
& \times \{1 + \mathcal{O}(q/m_\mathcal{N})\},
\end{aligned}
\tag{D.4}
$$

where the leptonic currents L^μ, L, and $L^{\mu\nu}$ are defined under eq. (3.1). Taking the non-relativistic limit

$$
\begin{aligned}
\mathcal{M}_{\mathrm{QEFT}} = -\frac{2\sqrt{m_\mathcal{N} m_{\mathcal{N}'}} V_{ud}}{v^2}\Big\{ & M_F g_V(1 + \epsilon_L + \epsilon_R)L^0[\mathbf{1}]_{J_z'}{}^{J_z} + g_A^i(1 + \epsilon_L - \epsilon_R)L^k[\sigma^k]_{J_z'}{}^{J_z} \\
& + M_F g_S L[\mathbf{1}]_{J_z'}{}^{J_z} - g_T^i \epsilon_T L^{0k}[\sigma^k]_{J_z'}{}^{J_z} \Big\} \; (1 + \mathcal{O}(q/m_\mathcal{N})).
\end{aligned}
\tag{D.5}
$$

Using the $\mathcal{O}(m_\mathcal{N}^0)$ part of the matching equations in eq. (2.9),

$$
\begin{aligned}
\mathcal{M}_{\mathrm{QEFT}} = -2\sqrt{m_\mathcal{N} m_{\mathcal{N}'}}\Big\{ & M_F[\mathbf{1}]_{J_z'}{}^{J_z}\Big[C_V^+ L^0 + C_S^+ L\Big] \\
& - [\sigma^k]_{J_z'}{}^{J_z}\Big[\frac{g_A^i}{g_A} C_A^+ L^k + C_T^+ \frac{g_T^i}{g_T} L^{0k}\Big] \Big\} \; (1 + \mathcal{O}(q/m_\mathcal{N})).
\end{aligned}
\tag{D.6}
$$

Comparing this result with the one obtained in the non-relativistic nucleon-level EFT, cf. eqs. (3.1) and (3.2), which we refer to as $\mathcal{M}_{\mathrm{NEFT}}$, we can determine the leading contribution

of the many-body currents to the beta decay amplitude. Defining $\mathcal{M}_{\text{MB}} \equiv \mathcal{M}_{\text{QEFT}} - \mathcal{M}_{\text{NEFT}}$ we find

$$\mathcal{M}_{\text{MB}} = 2\sqrt{m_{\mathcal{N}} m_{\mathcal{N}'}} [\sigma^k]_{J'_z}{}^{J_z} \left[\left(\frac{g_A^i}{g_A} - \frac{M_F r_i}{\sqrt{3}} \right) C_A^+ L^k + \left(\frac{g_T^i}{g_T} - \frac{M_F r_i}{\sqrt{3}} \right) C_T^+ L^{0k} \right] (1 + \mathcal{O}(q/m_{\mathcal{N}})).$$
(D.7)

The first observation is that many-body currents do not affect the vector (as is well known) and scalar contributions, up to effects suppressed by the ratio of typical beta decay momenta and the nuclear masses. On the other hand, many-body currents do affect the axial and tensor contributions. For the axial ones, however, this does not have any practical consequences for our analysis. The reason is that the parameter r_i in the nucleon EFT, defined by eq. (3.2) is not known accurately from first principles (except for neutron decay), and is thus fixed by beta decay data. From the phenomenological point of view it does not matter whether r_i or g_A^i is fitted — the constraints on the parameters of interest remain the same. From the theoretical perspective one concludes that the global fit effectively constrains $r_i^{\text{eff}} \equiv \frac{\sqrt{3}}{g_A M_F} g_A^i$ (which include many-body effects) rather than r_i (which is the parameter defined in the nucleon EFT where many-body effects are neglected). Finally, many-body currents also affect tensor contributions, and the effect is physical except for neutron decay (where $g_T^i = g_T$ and many-body effects are absent by definition) and for pure Fermi transitions (which are only sensitive to vector and scalar contributions and thus are free of many-body effects at the discussed order). In order to precisely determine the sensitivity of mirror decays to C_T^+ one would have to know the parameters g_T^i for each given transition. Currently, no such calculations exist. In our analysis we effectively used $g_T^i = \frac{g_T g_A^i}{g_A}$, which assumes that tensor and axial many body corrections are the same. The difference between g_T^i and $g_T^{i,1\text{B}}$ might not be a small effect.[20] This introduces an uncertainty to our fit. Its practical consequence are however not important at this point, because the constraints on the tensor Wilson coefficient C_T^+ are dominated by neutron data, where many-body effects are absent by definition. On the other hand, the many-body contributions entering through the tensor currents are estimated to be larger than the recoil effects. Therefore, any future fit including the subleading tensor parameters will require precise determinations of the parameters g_T^i, perhaps from ab-initio calculations.

Open Access. This article is distributed under the terms of the Creative Commons Attribution License (CC-BY4.0), which permits any use, distribution and reproduction in any medium, provided the original author(s) and source are credited.

References

[1] W. Pauli, *Dear radioactive ladies and gentlemen*, *Phys. Today* **31N9** (1978) 27 [INSPIRE].

[2] E. Fermi, *An attempt of a theory of beta radiation. I*, *Z. Phys.* **88** (1934) 161 [INSPIRE].

[3] C.L. Cowan et al., *Detection of the free neutrino: A Confirmation*, *Science* **124** (1956) 103 [INSPIRE].

---

[20]For the axial case, the many body corrections are estimated to be $\mathcal{O}(10\%)$ for light nuclei [101], and are expected to grow as $\sim A$ for heavier nuclei [102].

[4] T.D. Lee and C.-N. Yang, *Question of Parity Conservation in Weak Interactions*, *Phys. Rev.* **104** (1956) 254 [INSPIRE].

[5] C.S. Wu et al., *Experimental Test of Parity Conservation in β Decay*, *Phys. Rev.* **105** (1957) 1413 [INSPIRE].

[6] S. Weinberg, *V-A was the key*, *J. Phys. Conf. Ser.* **196** (2009) 012002 [INSPIRE].

[7] H. Abele, *The neutron. Its properties and basic interactions*, *Prog. Part. Nucl. Phys.* **60** (2008) 1 [INSPIRE].

[8] M. González-Alonso, O. Naviliat-Cuncic and N. Severijns, *New physics searches in nuclear and neutron β decay*, *Prog. Part. Nucl. Phys.* **104** (2019) 165 [arXiv:1803.08732] [INSPIRE].

[9] J.C. Hardy and I.S. Towner, *Superallowed $0^+ \to 0^+$ nuclear β decays: 2020 critical survey, with implications for V_{ud} and CKM unitarity*, *Phys. Rev. C* **102** (2020) 045501 [INSPIRE].

[10] D. Dubbers and B. Märkisch, *Precise Measurements of the Decay of Free Neutrons*, *Ann. Rev. Nucl. Part. Sci.* **71** (2021) 139 [arXiv:2106.02345] [INSPIRE].

[11] A. Falkowski, M. González-Alonso and O. Naviliat-Cuncic, *Comprehensive analysis of beta decays within and beyond the Standard Model*, *JHEP* **04** (2021) 126 [arXiv:2010.13797] [INSPIRE].

[12] P. Herczeg, *Beta decay beyond the standard model*, *Prog. Part. Nucl. Phys.* **46** (2001) 413 [INSPIRE].

[13] J.D. Jackson, S.B. Treiman and H.W. Wyld, *Possible tests of time reversal invariance in Beta decay*, *Phys. Rev.* **106** (1957) 517 [INSPIRE].

[14] S. Weinberg, *Charge symmetry of weak interactions*, *Phys. Rev.* **112** (1958) 1375 [INSPIRE].

[15] U. van Kolck, *Effective field theory of nuclear forces*, *Prog. Part. Nucl. Phys.* **43** (1999) 337 [nucl-th/9902015] [INSPIRE].

[16] B.R. Holstein, *Recoil Effects in Allowed beta Decay: The Elementary Particle Approach*, *Rev. Mod. Phys.* **46** (1974) 789 [INSPIRE].

[17] N. Severijns et al., *Ft values of the mirror β transitions and the weak-magnetism-induced current in allowed nuclear β decay*, *Phys. Rev. C* **107** (2023) 015502 [arXiv:2109.08895] [INSPIRE].

[18] T. Bhattacharya et al., *Probing Novel Scalar and Tensor Interactions from (Ultra)Cold Neutrons to the LHC*, *Phys. Rev. D* **85** (2012) 054512 [arXiv:1110.6448] [INSPIRE].

[19] I. Doršner et al., *Physics of leptoquarks in precision experiments and at particle colliders*, *Phys. Rept.* **641** (2016) 1 [arXiv:1603.04993] [INSPIRE].

[20] A. Angelescu et al., *Single leptoquark solutions to the B-physics anomalies*, *Phys. Rev. D* **104** (2021) 055017 [arXiv:2103.12504] [INSPIRE].

[21] A. Falkowski, M. González-Alonso and Z. Tabrizi, *Reactor neutrino oscillations as constraints on Effective Field Theory*, *JHEP* **05** (2019) 173 [arXiv:1901.04553] [INSPIRE].

[22] J. de Blas, J.C. Criado, M. Perez-Victoria and J. Santiago, *Effective description of general extensions of the Standard Model: the complete tree-level dictionary*, *JHEP* **03** (2018) 109 [arXiv:1711.10391] [INSPIRE].

[23] M. Ademollo and R. Gatto, *Nonrenormalization Theorem for the Strangeness Violating Vector Currents*, *Phys. Rev. Lett.* **13** (1964) 264 [INSPIRE].

[24] J.F. Donoghue and D. Wyler, *Isospin Breaking and the Precise Determination of V(ud)*, *Phys. Lett. B* **241** (1990) 243 [INSPIRE].

[25] M. Gell-Mann, *The symmetry group of vector and axial vector currents*, *Physics Physique Fizika* **1** (1964) 63 [INSPIRE].

[26] V. Cirigliano et al., *Pion-Induced Radiative Corrections to Neutron β Decay*, *Phys. Rev. Lett.* **129** (2022) 121801 [arXiv:2202.10439] [INSPIRE].

[27] FLAVOUR LATTICE AVERAGING GROUP (FLAG) collaboration, *FLAG Review 2021*, *Eur. Phys. J. C* **82** (2022) 869 [arXiv:2111.09849] [INSPIRE].

[28] R. Gupta et al., *Isovector Charges of the Nucleon from 2+1+1-flavor Lattice QCD*, *Phys. Rev. D* **98** (2018) 034503 [arXiv:1806.09006] [INSPIRE].

[29] C.C. Chang et al., *A per-cent-level determination of the nucleon axial coupling from quantum chromodynamics*, *Nature* **558** (2018) 91 [arXiv:1805.12130] [INSPIRE].

[30] A. Walker-Loud et al., *Lattice QCD Determination of g_A*, *PoS* **CD2018** (2020) 020 [arXiv:1912.08321] [INSPIRE].

[31] M. González-Alonso and J. Martin Camalich, *Isospin breaking in the nucleon mass and the sensitivity of β decays to new physics*, *Phys. Rev. Lett.* **112** (2014) 042501 [arXiv:1309.4434] [INSPIRE].

[32] J.F. Donoghue, E. Golowich and B.R. Holstein, *Dynamics of the standard model*, CUP (2014) [DOI:10.1017/CBO9780511524370] [INSPIRE].

[33] C. Chen, C.S. Fischer, C.D. Roberts and J. Segovia, *Nucleon axial-vector and pseudoscalar form factors and PCAC relations*, *Phys. Rev. D* **105** (2022) 094022 [arXiv:2103.02054] [INSPIRE].

[34] RBC and UKQCD collaborations, *Domain wall QCD with physical quark masses*, *Phys. Rev. D* **93** (2016) 074505 [arXiv:1411.7017] [INSPIRE].

[35] BMW collaboration, *Lattice QCD at the physical point: light quark masses*, *Phys. Lett. B* **701** (2011) 265 [arXiv:1011.2403] [INSPIRE].

[36] BMW collaboration, *Lattice QCD at the physical point: Simulation and analysis details*, *JHEP* **08** (2011) 148 [arXiv:1011.2711] [INSPIRE].

[37] C. McNeile et al., *High-Precision c and b Masses, and QCD Coupling from Current-Current Correlators in Lattice and Continuum QCD*, *Phys. Rev. D* **82** (2010) 034512 [arXiv:1004.4285] [INSPIRE].

[38] A. Bazavov et al., *Staggered chiral perturbation theory in the two-flavor case and SU(2) analysis of the MILC data*, *PoS* **LATTICE2010** (2010) 083 [arXiv:1011.1792] [INSPIRE].

[39] FERMILAB LATTICE et al. collaborations, *Up-, down-, strange-, charm-, and bottom-quark masses from four-flavor lattice QCD*, *Phys. Rev. D* **98** (2018) 054517 [arXiv:1802.04248] [INSPIRE].

[40] EUROPEAN TWISTED MASS collaboration, *Up, down, strange and charm quark masses with N_f = 2+1+1 twisted mass lattice QCD*, *Nucl. Phys. B* **887** (2014) 19 [arXiv:1403.4504] [INSPIRE].

[41] M. Gorchtein, *γW Box Inside Out: Nuclear Polarizabilities Distort the Beta Decay Spectrum*, *Phys. Rev. Lett.* **123** (2019) 042503 [arXiv:1812.04229] [INSPIRE].

[42] M. Gorchtein and C.-Y. Seng, *Dispersion relation analysis of the radiative corrections to g_A in the neutron β-decay*, *JHEP* **10** (2021) 053 [arXiv:2106.09185] [INSPIRE].

[43] S. Ando et al., *Neutron beta decay in effective field theory*, *Phys. Lett. B* **595** (2004) 250 [nucl-th/0402100] [InSPIRE].

[44] D.H. Wilkinson, *Analysis of neutron beta decay*, *Nucl. Phys. A* **377** (1982) 474 [InSPIRE].

[45] J.D. Jackson, S.B. Treiman and H.W. Wyld, *Coulomb corrections in allowed beta transitions*, *Nucl. Phys.* **4** (1957) 206 [InSPIRE].

[46] M. González-Alonso and O. Naviliat-Cuncic, *Kinematic sensitivity to the Fierz term of β-decay differential spectra*, *Phys. Rev. C* **94** (2016) 035503 [arXiv:1607.08347] [InSPIRE].

[47] G. Darius et al., *Measurement of the Electron-Antineutrino Angular Correlation in Neutron β Decay*, *Phys. Rev. Lett.* **119** (2017) 042502 [InSPIRE].

[48] M.T. Hassan et al., *Measurement of the neutron decay electron-antineutrino angular correlation by the aCORN experiment*, *Phys. Rev. C* **103** (2021) 045502 [arXiv:2012.14379] [InSPIRE].

[49] UCNτ collaboration, *Improved neutron lifetime measurement with UCNτ*, *Phys. Rev. Lett.* **127** (2021) 162501 [arXiv:2106.10375] [InSPIRE].

[50] T.E. Chupp et al., *Search for a T-odd, P-even Triple Correlation in Neutron Decay*, *Phys. Rev. C* **86** (2012) 035505 [arXiv:1205.6588] [InSPIRE].

[51] A. Kozela et al., *Measurement of transverse polarization of electrons emitted in free neutron decay*, *Phys. Rev. C* **85** (2012) 045501 [arXiv:1111.4695] [InSPIRE].

[52] J. Ng and S. Tulin, *D versus d: CP Violation in Beta Decay and Electric Dipole Moments*, *Phys. Rev. D* **85** (2012) 033001 [arXiv:1111.0649] [InSPIRE].

[53] K.K. Vos, H.W. Wilschut and R.G.E. Timmermans, *Symmetry violations in nuclear and neutron β decay*, *Rev. Mod. Phys.* **87** (2015) 1483 [arXiv:1509.04007] [InSPIRE].

[54] S. Alioli et al., *Right-handed charged currents in the era of the Large Hadron Collider*, *JHEP* **05** (2017) 086 [arXiv:1703.04751] [InSPIRE].

[55] V. Cirigliano et al., *Semileptonic tau decays beyond the Standard Model*, *JHEP* **04** (2022) 152 [arXiv:2112.02087] [InSPIRE].

[56] B.M. Rebeiro et al., *Precise branching ratio measurements in $^{19}Ne\beta$ decay and fundamental tests of the weak interaction*, *Phys. Rev. C* **99** (2019) 065502 [arXiv:1810.02331] [InSPIRE].

[57] D. Combs et al., *A look into mirrors: A measurement of the β-asymmetry in ^{19}Ne decay and searches for new physics*, arXiv:2009.13700 [InSPIRE].

[58] M. Beck et al., *Improved determination of the β-$\overline{\nu}_e$ angular correlation coefficient a in free neutron decay with the aSPECT spectrometer*, *Phys. Rev. C* **101** (2020) 055506 [arXiv:1908.04785] [InSPIRE].

[59] N. Arkani-Hamed, T.-C. Huang and Y.-T. Huang, *Scattering amplitudes for all masses and spins*, *JHEP* **11** (2021) 070 [arXiv:1709.04891] [InSPIRE].

[60] W. Mampe et al., *Measuring neutron lifetime by storing ultracold neutrons and detecting inelastically scattered neutrons*, *JETP Lett.* **57** (1993) 82.

[61] J. Byrne and P.G. Dawber, *A revised Value for the Neutron Lifetime Measured Using a Penning Trap*, *EPL* **33** (1996) 187 [InSPIRE].

[62] A. Serebrov et al., *Measurement of the neutron lifetime using a gravitational trap and a low-temperature Fomblin coating*, *Phys. Lett. B* **605** (2005) 72 [nucl-ex/0408009] [InSPIRE].

[63] A. Pichlmaier, V. Varlamov, K. Schreckenbach and P. Geltenbort, *Neutron lifetime measurement with the UCN trap-in-trap MAMBO II*, *Phys. Lett. B* **693** (2010) 221 [InSPIRE].

[64] A. Steyerl et al., *Quasielastic scattering in the interaction of ultracold neutrons with a liquid wall and application in a reanalysis of the Mambo I neutron-lifetime experiment*, *Phys. Rev. C* **85** (2012) 065503 [INSPIRE].

[65] A.T. Yue et al., *Improved Determination of the Neutron Lifetime*, *Phys. Rev. Lett.* **111** (2013) 222501 [arXiv:1309.2623] [INSPIRE].

[66] V.F. Ezhov et al., *Measurement of the neutron lifetime with ultra-cold neutrons stored in a magneto-gravitational trap*, *JETP Lett.* **107** (2018) 671 [arXiv:1412.7434] [INSPIRE].

[67] S. Arzumanov et al., *A measurement of the neutron lifetime using the method of storage of ultracold neutrons and detection of inelastically up-scattered neutrons*, *Phys. Lett. B* **745** (2015) 79 [INSPIRE].

[68] R.W. Pattie Jr. et al., *Measurement of the neutron lifetime using a magneto-gravitational trap and in situ detection*, *Science* **360** (2018) 627 [arXiv:1707.01817] [INSPIRE].

[69] A.P. Serebrov et al., *Neutron lifetime measurements with a large gravitational trap for ultracold neutrons*, *Phys. Rev. C* **97** (2018) 055503 [arXiv:1712.05663] [INSPIRE].

[70] P. Bopp et al., *The Beta Decay Asymmetry of the Neutron and g_A/g_V*, *Phys. Rev. Lett.* **56** (1986) 919 [*Erratum ibid.* **57** (1986) 1192] [INSPIRE].

[71] P. Liaud et al., *The measurement of the beta asymmetry in the decay of polarized neutrons*, *Nucl. Phys. A* **612** (1997) 53 [INSPIRE].

[72] B. Erozolimsky, I. Kuznetsov, I. Stepanenko and Y.A. Mostovoi, *Corrigendum: Corrected value of the beta-emission asymmetry in the decay of polarized neutrons measured in 1990* [DOI:10.1016/S0370-2693(97)01004-6] [INSPIRE].

[73] D. Mund et al., *Determination of the Weak Axial Vector Coupling from a Measurement of the Beta-Asymmetry Parameter A in Neutron Beta Decay*, *Phys. Rev. Lett.* **110** (2013) 172502 [arXiv:1204.0013] [INSPIRE].

[74] UCNA collaboration, *New result for the neutron β-asymmetry parameter A_0 from UCNA*, *Phys. Rev. C* **97** (2018) 035505 [arXiv:1712.00884] [INSPIRE].

[75] B. Märkisch et al., *Measurement of the Weak Axial-Vector Coupling Constant in the Decay of Free Neutrons Using a Pulsed Cold Neutron Beam*, *Phys. Rev. Lett.* **122** (2019) 242501 [arXiv:1812.04666] [INSPIRE].

[76] PARTICLE DATA GROUP collaboration, *Review of Particle Physics*, *PTEP* **2020** (2020) 083C01 [INSPIRE].

[77] I.A. Kuznetsov et al., *Measurements of the anti-neutrino spin asymmetry in beta decay of the neutron and restrictions on the mass of a right-handed gauge boson*, *Phys. Rev. Lett.* **75** (1995) 794 [INSPIRE].

[78] A.P. Serebrov et al., *Measurement of the anti-neutrino escape asymmetry with respect to the spin of the decaying neutron*, *J. Exp. Theor. Phys.* **86** (1998) 1074 [INSPIRE].

[79] M. Kreuz et al., *A measurement of the antineutrino asymmetry B in free neutron decay*, *Phys. Lett. B* **619** (2005) 263 [INSPIRE].

[80] M. Schumann et al., *Measurement of the neutrino asymmetry parameter B in neutron decay*, *Phys. Rev. Lett.* **99** (2007) 191803 [arXiv:0706.3788] [INSPIRE].

[81] Y.A. Mostovoi et al., *Experimental value of G_A/G_V from a measurement of both P-odd correlations in free-neutron decay*, *Phys. Atom. Nucl.* **64** (2001) 1955 [INSPIRE].

[82] C. Stratowa, R. Dobrozemsky and P. Weinzierl, *Ratio G_a/G_v Derived from the Proton Spectrum in Free Neutron Decay*, *Phys. Rev. D* **18** (1978) 3970 [INSPIRE].

[83] J. Byrne et al., *Determination of the electron$\bar{n}$eutrino angular correlation coefficient a0 and the parameter $|\lambda| = |G_A/G_V|$ in free neutron beta decay from measurements of the integrated energy spectrum of recoil protons stored in an ion trap*, *J. Phys. G* **28** (2002) 1325 [INSPIRE].

[84] M. Brodeur et al., *Precision half-life measurement of ^{17}F*, *Phys. Rev. C* **93** (2016) 025503 [INSPIRE].

[85] N. Severijns, J. Wouters, J. Vanhaverbeke and L. Vanneste, *β-decay anisotropies of the mirror nuclei ^{15}O and ^{17}F*, *Phys. Rev. Lett.* **63** (1989) 1050.

[86] N. Severijns, M. Beck and O. Naviliat-Cuncic, *Tests of the standard electroweak model in beta decay*, *Rev. Mod. Phys.* **78** (2006) 991 [nucl-ex/0605029] [INSPIRE].

[87] F.P. Calaprice, S.J. Freedman, W.C. Mead and H.C. Vantine, *Experimental Study of Weak Magnetism and Second-Class Interaction Effects in the beta Decay of Polarized Ne-19*, *Phys. Rev. Lett.* **35** (1975) 1566 [INSPIRE].

[88] J. Karthein et al., *QEC -value determination for $^{21}Na\rightarrow^{21}Ne$ and $^{23}Mg\rightarrow^{23}Na$ mirror-nuclei decays using high-precision mass spectrometry with ISOLTRAP at the CERN ISOLDE facility*, *Phys. Rev. C* **100** (2019) 015502 [*Erratum ibid.* **101** (2020) 049901] [arXiv:1906.01538] [INSPIRE].

[89] P.A. Vetter, J.R. Abo-Shaeer, S.J. Freedman and R. Maruyama, *Measurement of the $\beta - \nu$ correlation of ^{21}Na using shakeoff electrons*, *Phys. Rev. C* **77** (2008) 035502 [arXiv:0805.1212] [INSPIRE].

[90] J. Long et al., *Precision half-life measurement of ^{29}P*, *Phys. Rev. C* **101** (2020) 015501 [INSPIRE].

[91] G.S. Masson and P.A. Quin, *Measurement of the asymmetry parameter for ^{29}P beta decay*, *Phys. Rev. C* **42** (1990) 1110 [INSPIRE].

[92] N. Severijns, M. Tandecki, T. Phalet and I.S. Towner, *Ft values of the $T = 1/2$ mirror β transitions*, *Phys. Rev. C* **78** (2008) 055501 [arXiv:0807.2201] [INSPIRE].

[93] J.D. Garnett, E.D. Commins, K.T. Lesko and E.B. Norman, *The Beta Decay Asymmetry Parameter for ^{35}Ar: An Anomaly Resolved*, *Phys. Rev. Lett.* **60** (1988) 499 [INSPIRE].

[94] A. Converse et al., *Measurement of the asymmetry parameter for ^{35}Ar β-decay as a test of the CVC hypothesis*, *Phys. Lett. B* **304** (1993) 60 [INSPIRE].

[95] O. Naviliat-Cuncic and N. Severijns, *Test of the Conserved Vector Current Hypothesis in $T = 1/2$ Mirror Transitions and New Determination of $|V_{ud}|$*, *Phys. Rev. Lett.* **102** (2009) 142302 [arXiv:0809.0994] [INSPIRE].

[96] P.D. Shidling et al., *Precision half-life measurement of the β^+ decay of ^{37}K*, *Phys. Rev. C* **90** (2014) 032501 [arXiv:1407.1742] [INSPIRE].

[97] B. Fenker et al., *Precision measurement of the β-asymmetry in spin-polarized ^{37}K decay*, *Phys. Rev. Lett.* **120** (2018) 062502 [arXiv:1706.00414] [INSPIRE].

[98] D. Melconian et al., *Measurement of the neutrino asymmetry in the beta decay of laser-cooled polarized ^{37}K*, *Phys. Lett. B* **649** (2007) 370 [INSPIRE].

[99] ISOLDE collaboration, *Positron neutrino correlation in the $0^+ \rightarrow 0^+$ decay of ^{32}Ar*, *Phys. Rev. Lett.* **83** (1999) 1299 [*Erratum ibid.* **83** (1999) 3101] [nucl-ex/9903002] [INSPIRE].

[100] A. Gorelov et al., *Scalar interaction limits from the $\beta - \nu$ correlation of trapped radioactive atoms*, *Phys. Rev. Lett.* **94** (2005) 142501 [`nucl-ex/0412032`] [InSPIRE].

[101] M. Butler and J.-W. Chen, *Proton proton fusion in effective field theory to fifth order*, *Phys. Lett. B* **520** (2001) 87 [`nucl-th/0101017`] [InSPIRE].

[102] V. Cirigliano, M.L. Graesser and G. Ovanesyan, *WIMP-nucleus scattering in chiral effective theory*, *JHEP* **10** (2012) 025 [`arXiv:1205.2695`] [InSPIRE].

[103] M. Hoferichter, P. Klos and A. Schwenk, *Chiral power counting of one- and two-body currents in direct detection of dark matter*, *Phys. Lett. B* **746** (2015) 410 [`arXiv:1503.04811`] [InSPIRE].

[104] M.J. Savage et al., *Proton-Proton Fusion and Tritium β Decay from Lattice Quantum Chromodynamics*, *Phys. Rev. Lett.* **119** (2017) 062002 [`arXiv:1610.04545`] [InSPIRE].

[105] H. De-Leon, L. Platter and D. Gazit, *Tritium β-decay in pionless effective field theory*, *Phys. Rev. C* **100** (2019) 055502 [`arXiv:1611.10004`] [InSPIRE].

[106] C. Körber, A. Nogga and J. de Vries, *First-principle calculations of Dark Matter scattering off light nuclei*, *Phys. Rev. C* **96** (2017) 035805 [`arXiv:1704.01150`] [InSPIRE].

[107] NPLQCD collaboration, *Axial charge of the triton from lattice QCD*, *Phys. Rev. D* **103** (2021) 074511 [`arXiv:2102.03805`] [InSPIRE].

[108] W. Detmold and P.E. Shanahan, *Few-nucleon matrix elements in pionless effective field theory in a finite volume*, *Phys. Rev. D* **103** (2021) 074503 [`arXiv:2102.04329`] [InSPIRE].